Comparative Analysis of Signaling Pathways Triggered by Different Pattern-recognition Receptor-types

Dissertation

der Mathematisch-Naturwissenschaftlichen Fakultät

der Eberhard Karls Universität Tübingen

zur Erlangung des Grades eines

Doktors der Naturwissenschaften

(Dr. rer. nat.)

vorgelegt von

Wei-Lin Wan

aus Taipei, Taiwan

Tübingen

2017

Tag der mündlichen Qualifikation: 01.12.2017

Dekan: Prof. Dr. Wolfgang Rosenstiel

1. Berichterstatter: Prof. Dr. Thorsten Nürnberger

2. Berichterstatter: Dr. Andrea Gust

Contents

Figures

Tables

1. Introduction

1.1 Plant defense system against pathogens

Being sessile, plants need to employ a prompt and effective defense strategy to confront constant threats from diverse pathogens. Phytopathogens are referred to as biotrophic (e.g. the oomycete *Hyaloperonospora arabidopsidis*), hemibiotrophic (e.g. the bacterium *Pseudomonas syringae*), or necrotrophic (e.g. the fungus *Botrytis cinerea*), depending on their infection and feeding strategy. Pathogen strategies range from feeding on living host cells to killing plant cells to get nutrients [1]. Phytopathogens can severely damage plants, causing reduction of biomass, decrease of fertility, or even death. Pathogen disease is of great concern because it can decrease the quantity and quality of crop production.

Plants are generally resistant to the majority of potential pathogens. This phenomenon is termed non-host resistance. The first line of defense against plant pathogens comprises physical barriers including the cuticle and the cell wall. The cuticle is present on the external surface of the epidermis of all land plants and is mainly composed of cutin and wax [2]. The cuticle reduces water loss, protects against UV radiation and blocks phytopathogens and pests. In order to infect a plant cell, fungal pathogens must penetrate the cuticle by mechanical rupture and secretion of cutinases that hydrolyze the cutin polyester [3, 4].

The plant cell wall is like an exoskeleton surrounding the plant cell and consists of cellulose microfibrils, pectin, hemicelluloses, proteins, and, in certain cases, lignin [5]. It provides both structural support and protection against biotic and abiotic stresses, and the cell wall adjusts its' structure and composition upon

pathogen infection [6]. Some fungal pathogens are capable of penetrating both the cuticle and plant cell wall. Bacteria, on the other hand, cannot directly penetrate the plant epidermis. Instead, bacteria often enter the plant via natural openings including: hydathodes, nectarthodes, lenticels, and, most importantly, stomata [7]. In addition, plant wounds, caused by pests, herbivores, or mechanical damage, constitute other routes of plant infection.

In addition to physical barriers, plants also repel potential pathogens by secretion of antimicrobial compounds (generically called phytoanticipins), which inhibit pathogen growth [8]. Several proteins have antimicrobial activity as well as some metabolites, such as glucosinolates and their derivatives, which are secondary metabolites produced in Brassicaceae [8].

The few successful pathogens breaking the preformed barriers then have to face the plant immune system, which employs sophisticated mechanisms of pathogen recognition and defense. The first layer of inducible defense is activated by pattern recognition receptors (PRRs) that recognize conserved molecules of microbes (microbe-associated or pathogen-associated molecular patterns; MAMPs/PAMPs), and this defense is termed MAMP/PAMP-triggered immunity (MTI/PTI). PRR activation induces a complex set of responses including activation of mitogen-associated and calcium-dependent protein kinases (MAPKs and CDPKs), as well as bursts of calcium and reactive oxygen species (ROS), followed by massive transcriptional reprogramming [9-11]. MTI effectively repels most non-adapted pathogens, while contributing to basal immunity during infection. The plant is also able to detect damage-associated molecular patterns (DAMPs), which are plant degradation products resulting from the action of invading pathogens, or endogenous peptides, constitutively present or newly synthesized, which are released by the

plants following pathogen attacks [12]. Recognition of DAMPs also triggers immune responses similar to the MTI response [13].

Pathogen perception can also occur via the recognition of pathogen effectors, which are molecules synthesized by the pathogens and delivered to the extracellular matrix or into the plant cell to enhance pathogen fitness. Some microbial effectors counteract MTI or block its activation, resulting in effector-triggered susceptibility. These pathogen-secreted effectors can be recognized by another group of receptors: Intracellular nucleotide-binding domain leucine-rich repeat-containing receptors/ nucleotide-binding site leucine-rich repeat (NLR/NBS-LRR) [14, 15]. NLRs implement the second layer of inducible defense called effector-triggered immunity (ETI). Effector recognition may occur through direct binding or by sensing the perturbing activity of an effector on host components [15]. According to the guard hypothesis proposed by Van der Biezen and Jones [16], crucial immune components can be guarded by NLRs, which become activated upon effector-triggered modification of their 'guardees'. The decoy model suggests that plant NLRs can also guard structural mimics (or 'decoys') of key immune components that are normally targeted by effectors [17]. In addition, domains targeted by effectors may be fused to NLRs to form 'integrated decoys' or 'integrated sensors' which directly trigger NLR activation upon effector-mediated modification [18-21]. The evolutionary arms race between plants and pathogens and notably their repertoire of effectors and disease resistance proteins led to the so-called zigzag model [22].

1.2 PRRs: Receptor Kinases and Receptor Proteins

Plants have evolved an expanded collection of cell surface receptor kinases (RKs) and receptor proteins (RPs), many of which have been implicated in sensing external or internal signals, activating signaling cascades. The various downstream outputs are central to plant growth, development, immunity, and stress adaptation [23, 24]. RKs comprise a unique extracellular domain, a single transmembrane domain, and an intracellular kinase domain, while RPs have an extracellular domain, a transmembrane domain, and a relatively short cytoplasmic region without a kinase domain [24, 25]. The *Arabidopsis thaliana* genome encodes more than 600 RKs and RPs. With more than 200 members in Arabidopsis, the largest group of RKs and RPs contains an extracellular leucine-rich repeat (LRR) domain [24].

Plant PRRs can be subdivided based on the nature of their ligand-binding ectodomain. LRR-containing PRRs preferentially bind proteins or peptides, such as bacterial flagellin or elongation factor Tu (EF-Tu), or endogenous AtPep peptides [25, 26]. PRRs containing lysine motifs (LysM), on the other hand, bind carbohydrate-based ligands such as fungal chitin or bacterial peptidoglycan [25, 26]. Furthermore, lectin-type PRRs bind extracellular ATP or bacterial lipopolysaccharides (LPS) [27], whereas PRRs with epidermal growth factor (EGF)-like ectodomains recognize plant cell-wall derived oligogalacturonides (OGs) [28].

Several LRR-RKs and LRR-RPs function as receptors of plant growth hormones, pathogen signatures, or endogenous peptides. For instance, BRASSINOSTEROID INSENSITIVE 1 (BRI1) perceives brassinosteroid hormones (BRs) which regulate plant growth. FLAGELLIN-SENSING 2 (FLS2) and ELONGATION FACTOR-TU RECEPTOR (EFR) perceive bacterial flagellin and EF-

Tu, respectively, and are involved in regulating plant immunity [26, 29, 30]. The roles of LRR-RPs in the developmental program of Arabidopsis was demonstrated with TOO MANY MOUTHS (TMM; RLP17), regulating stomata distribution and initiation of stomatal precursor cells [31, 32], and CLAVATA 2 (CLV2; RLP10), being required for proper meristem and organ development [33, 34].

LRR-RPs display high conservation of the four LRRs preceding the Cys–Cys pair that delimits the LRR domains and a short apoplastic juxtamembrane domain rich in acidic residues. Lacking a signaling kinase domain, LRR-RPs constitutively associate with SUPPRESSOR OF BRI1-ASSOCIATED RECEPTOR KINASE 1-INTERACTING RECEPTOR-LIKE KINASE1‑1 (SOBIR1) or SOBIR1‑like LRR-receptor kinases to form a bimolecular equivalent of a genuine receptor kinase [29, 35]. The single transmembrane spanning domains of LRR-RPs commonly have one or several GxxxG motifs in a series for transmembrane helix–helix interactions [36]. SOBIR1 and RPs exhibit complementary characteristics that could allow physical interaction via their LRR domains, opposite charges in their apoplastic juxtamembrane domains and helix–helix interaction of their transmembrane domains [36].

BRI1-ASSOCIATED RECEPTOR KINASE 1 (BAK1), also known as SOMATIC EMBRYOGENESIS RECEPTOR KINASE 3 (SERK3), and other SERK members bind LRR-RKs or LRR-RP/SOBIR complexes upon cognate ligand perception [37-41]. BAK1 or other SERKs seem to be only recruited to the RP–SOBIR1 complex upon ligand binding, as recently shown for Arabidopsis RLP23 and tomato Cf4 [42, 43]. SERKs complex with several RP immune receptors, including RLP23, which perceives NECROSIS- AND ETHYLENE-INDUCING PEPTIDE 1 (NEP1)-LIKE PROTEINS (NLPs) secreted by various plant-associated

microorganisms [42]; tomato Cf9 required for *Cladosporium fulvum* avirulence (Avr) 9-triggered responses [43]; potato ELICITIN RESPONSE (ELR) required for oomycete *Phytophthora* elicitin-triggered responses [44]; and tobacco COLD-SHOCK PROTEIN 22 (CSP22) RESPONSIVENESS (CSPR) required for csp22-triggered responses [45]. Thus, SERKs appear to function as a shared signaling node that connects complex signaling networks via association with various RKs and RPs and modulates distinct cellular responses in plant immunity [46-48].

BOTRYTIS-INDUCED KINASE 1 (BIK1) is the best-studied example of Arabidopsis receptor-like cytoplasmic kinase (RLCK) subfamily VII. Under resting conditions, BIK1 associates with FLS2 and is likely to associate with BAK1 [49, 50]. Upon flagellin elicitation, BAK1 associates with FLS2 and phosphorylates BIK1 [49, 50]. In turn, BIK1 phosphorylates both BAK1 and FLS2 before dissociating from the PRR complex to activate downstream signaling components [49, 50]. BIK1 and the closely related AVRPPHB SUSCEPTIBLE 1 (PBS1)‑LIKE KINASE (PBL) proteins are also required to activate immune responses triggered by elf18, AtPep1 and chitin [49-51], thus representing an early convergence for distinct PRR-mediated pathways.

1.2.1 LRR-RKs and S-lectin-RK for MAMP Recognition

1.2.1.1 FLS2 & Flagellin

Flagellin is a principal component of bacterial flagellae and can be recognized by the innate immune system in organisms as diverse as flies, plants and mammals [26, 52-57]. A 22 amino acid sequence from the most conserved part of the N-terminal region of flagellin, an immunogenic epitope named flg22, is recognized by the LRR-RK FLS2 [58]. The sequence of the classically and often used flg22 is based on that

of flagellin from *Pseudomonas aeruginosa*. In Arabidopsis, flg22 perception can induce multiple defense responses including the production of ROS, activation of MAPKs, callose deposition, expression of defense-related genes and strong inhibition of seedling root growth [59-64]. Perception of flg22 also initiates the closure of stomata in order to prevent entry of the pathogen [65].

*At*FLS2 homologues have been identified in rice (*Oryza sativa*), *Nicotiana benthamina* and tomato [66-68], indicating that the PRR for flagellin is evolutionarily conserved. Arabidopsis plants mutated in FLS2 are more susceptible to infections by the pathogenic bacteria *Pseudomonas syringae* pv. tomato DC3000 (*Pto* DC3000) and allow more growth of the non-adapted bacteria *P. syringae* pv. *phaseolicola* (*Pph*, a bean pathogen) [69]. Furthermore, silencing *Nb*FLS2 in *N. benthamiana* causes plants to become more susceptible to a range of adapted and non-adapted bacteria [70].

Investigation of binding sites of flg22 in the LRR domain of *At*FLS2 reveal that LRR9 to LRR15 seem to be important for flagellin responsiveness [71]. A comparison of *At*FLS2 and the orthologous tomato (*Solanum lycopersicum*) receptor (*Sl*FLS2) by mapping the species-specific sites in the recognition of shortened or sequence-modified flg22 provide further knowledge of the relation of LRR and flg22 perception [72]. LRRs 7 to 10 of *Sl*FLS2 confer high affinity binding of *Sl*FLS2 to the core peptide RINSAKDD of flg22. In addition, the LRRs 19 to 24 also play an important role for the responsiveness to C-terminally modified flagellin peptides [72]. The crystal structure of FLS2 and BAK1 ectodomains complexed with flg22 shows that flg22 binds to the concave surface of FLS2 LRR from LRR3 to LRR16 [73].

Upon ligand-binding, the interaction between FLS2 and BAK1 occurs almost instantaneously (<15s) [74], a study using multi-parameter fluorescence imaging

spectrometry showed that flg22 first triggered RLK heterodimerization and later assembly into larger complexes through homomerization [75], which in the latter case could be detected by co-immunoprecipitation [76]. The biological relevance of these larger complexes is not yet understood.

Strict regulation of PRR signaling is essential since exaggerated and prolonged immune responses would be harmful and influence development [77]. Receptor internalization and subsequent degradation is a major mechanism to control receptor abundance and influence the intensity and duration of receptor signaling [78]. Analysis of FLS2-GFP-expressing plants by confocal microscopy revealed that FLS2-GFP was rapidly and specifically internalized from cell surfaces upon flg22 stimulation [79]. It has also been shown that flg22-triggered signaling can be attenuated by ubiquitination-dependent degradation [80]. This process depends on two partially redundant E3 ligases, PLANT U-BOX 12 (PUB12) and PUB13. Upon flg22 perception, BAK1 phosphorylates PUB12 and PUB13, promoting their transfer to FLS2, which is then ubiqutinated [80]. Reticulon-like protein B1 (RTNLB1) and RTNLB2 were also identified as FLS2 interactors and regulate FLS2 immune activity by controlling transport of newly synthesized FLS2 to the plasma membrane [81].

Other mechanisms are also employed to regulate flg22-triggered plant immunity. FLS2 and BIK1 associate with heterotrimeric G proteins, which contribute to the regulation of BIK1 steady-state levels and potentially to RESPIRATORY BURST OXIDASE-D (RBOHD) activation [82]. BAK1-interacting receptor-like kinase 2 (BIR2) negatively regulates BAK1–FLS2 complex formation and it can be phosphorylated by BAK1 kinase domain *in vitro* [83, 84]. BIR2 associates with BAK1 to prevent unintended interaction between BAK1 and FLS2. Whether phosphorylation by BAK1, or other kinases, accounts for BIR2 dissociation from BAK1 remains to be shown.

Arabidopsis PROTEIN PHOSPHATASE 2C (PP2C) KINASE-ASSOCIATED PROTEIN PHOSPHATASE (KAPP), interacts with the FLS2 cytoplasmic domain in yeast two-hybrid assays, and its overexpression inhibits flg22 responsiveness [85]. However, KAPP also interacts with a number of unrelated receptor kinases [86]. A specific Arabidopsis protein phosphatase type 2A (PP2A) holoenzyme, composed of subunits A1, C4, and B′η, constitutively associates with BAK1 and controls BAK1 phosphorylation status, negatively regulate immune response [87]. Recently, MAP3K MKKK7 was identified as part of the FLS2 complex [77]. MKKK7 becomes rapidly phosphorylated in response to flg22 and attenuates MPK6 activation, as well as ROS production, suggesting that it acts as a negative regulator in flg-22 triggered signaling [77].

1.2.1.2 EFR & EF-Tu

Another well-known bacterial PAMP is EF-Tu, one of the most abundant and most conserved proteins of bacteria [88]. Screening Arabidopsis T-DNA insertion lines of various *RKs* revealed that EFR is the receptor for EF-Tu. EFR directly recognizes the conserved N-acetylated epitope elf18, comprising the first 18 amino acids of EF-Tu [89, 90]. EF-Tu can be recognized by Arabidopsis and other members of the Brassicaceae family. *N. benthamiana*, from the Solanaceae family, lacks endogenous EF-Tu receptors but acquires the ability to perceive to elf18 upon transient expression of EFR. This reveals that interfamily transfer of plant PRRs can be used to engineer disease resistance in crops [89].

Chimeric receptors were used to map sub-domains of EFR ligand binding and receptor activation [91]. Replacement of LRRs of EFR with the corresponding LRRs of FLS2 revealed that the first six LRRs and/or the last two LRRs play a critical role in

elf18 binding and EFR activation [92]. The results also indicate that modular assembly of chimeras from different receptors can be used to form functional receptors [91].

FLS2 and EFR-signaling induce many of the same immune responses and share many common features including the requirement of BAK1 for signal transduction. Microarray analysis also reveals highly overlap of transcriptome profiling after flg22 and elf26 treatments [89]. However, different regulatory systems exist for these two receptors. For instance, forward genetic screens for elf18 insensitive mutants revealed that components in the endoplasmic reticulum control the EFR receptor quality [93-96]. Intriguingly, although these mutants were affected in elf18 triggered immune responses, they still responded normally to flg22 [93-96] .

1.2.1.3 CORE & csp22

Many plant species of the Solanaceae family detect the highly conserved nucleic acid binding motif RNP-1 of bacterial CSPs, represented by the peptide csp22, as a MAMP [97]. Cold shock protein receptor (CORE) of tomato is a LRR-RK that specifically recognizes csp22 with high affinity. Heterologous expression of CORE in *Arabidopsis thaliana* conferred full sensitivity to csp22 and, importantly, it also rendered these plants more resistant to bacterial pathogen *Pto* DC3000 [98].

*Nb*BAK1 associates with *Nb*CSPR, a LRR-RLP, and both proteins are required for csp22-triggered defense responses. Although *Nb*SOBIR1 associates with *Nb*CSPR, it appears that *Nb*SOBIR1 is not required for csp22-triggered responses [45]. It is possible that additional components with functional redundancy of *Nb*SOBIR1 participate in csp22-triggered signaling.

1.2.1.4 XA21 & RaxX

The LRR-RK XA21 confers resistance against the rice blight pathogen *Xanthomonas oryzae* [99]. As with other PRRs, XA21 localizes at the plasma membrane but is subsequently cleaved to release the intracellular kinase domain. This domain localizes in the nucleus and interacts with *Os*WRKY62 [100]. Intriguingly, mutation of the XA21 predicted NLS does not affect XA21-mediated immunity [101]. RaxX is highly conserved in many plant pathogenic *Xanthomonas* species and it is required for activation of XA21-mediated immunity. A sulfated, 21–amino acid synthetic RaxX peptide (RaxX21-sY) is sufficient for triggering immune response [102]. The evidence of interaction between RaxX and XA21 [102], however, is still missing. The Arabidopsis BAK1 orthologue *Os*SERK2 consistently associates with XA21 in a ligand independent manner, and *Os*SERK2 is required XA21-mediated resistance [103]. The rice PP2C XA21-BINDING PROTEIN 15 (XB15) dephosphorylates XA21 *in vitro* and negatively regulates XA21-mediated immune responses [104]. ATPase XB24 promotes autophosphorylation of specific XA21 phosphorylation sites to inhibit its kinase activity [105].

1.2.1.5 LORE & LPS

LIPOOLIGOSACCHARIDE-SPECIFIC REDUCED ELICITATION (LORE) is an S-lectin-receptor kinase which was recently identified as the Arabidopsis receptor for bacterial LPS. Remarkably, neither BAK1 nor CERK1 are required to mediate signaling by LORE [27].

1.2.2 LRR-RP in plant immunity

1.2.2.1 RLP23 & nlp20

NLPs are phytotoxins and microbial virulence factors secreted by bacteria, fungi and oomycetes. Approximately 1,100 NLP sequences from 262 microbial species are currently deposited in public databases [106-108]. NLPs trigger necrosis and immune responses only in dicotyledonous plants. Initially, the immunogenic activity was linked to cytotoxicity, supposedly through toxin-triggered release of endogenous DAMPs. Analysis of the immunogenic activities of NLPs other than *Pcc*NLP (*Phytopthora parasitica Pp*NLP, *Phytophthora infestans Pi*NLP) revealed that mutant proteins impaired in cytotoxic activity retained the ability to trigger plant defense in Arabidopsis. A conserved 20-mer fragment harbored in both cytotoxic and non-cytotoxic NLPs is sufficient for immune activation. This fragment is designated as nlp20 [109]. Orthologous immunogenic sequences can be found in NLPs of bacteria, fungi and oomycetes, an unusual broad taxonomic distribution not observed in other known MAMPs.

Nlp20 is perceived directly by Arabidopsis RLP23 [42]. SOBIR1 and BAK1/BKK1 are required as co-receptors for transducing nlp20-induced signaling [42, 110]. RLP23 interacts constitutively with SOBIR1, whereas BAK1 is recruited into the receptor complex in an nlp20-dependent manner. All three receptors are in close physical proximity, likely forming a tripartite receptor complex. Synthetic nlp20 triggers various plant immunity-associated responses such as ROS production, MAPK activation, callose deposition, PR gene expression, ethylene production, and defense priming [42]. Transgenic potato carrying RLP23 displays broad-spectrum disease resistance against fungi and oomycetes, revealing RLP23 as a potential

candidate for engineering durable disease resistance against a wide range of pathogens [42].

1.2.2.2 RLP42 & PG

RESPONSIVENESS TO BOTRYTIS POLYGALACTURONASES 1 (RBPG1) can recognize several fungal endopolygalacturonases (PGs) from the plant pathogen *B. cinerea* as well as one from the saprotroph *Aspergillus niger*. PGs can induce resistance to *H. arabidopsidis* [111]. RBPG1 was identified as *At*RLP42. *At*RLP42 and PGs form a complex in *N. benthamiana*, which also involves SOBIR1. Infiltration of *B. cinerea* PGs into Arabidopsis Col-0 induced a necrotic response, which was abolished in *sobir1* mutant plants [111].

1.2.2.3 RLP30 & SCFE1

A partially purified proteinaceous elicitor called sclerotinia culture filtrate elicitor 1 (SCFE1) was isolated from the necrotrophic fungal pathogen *Sclerotinia sclerotiorum* [112]. SCFE1 can induce immune responses in *Arabidopsis thaliana*. From a forward genetics approach, RLP30 was identified to be responsible for the sensitivity to SCFE1 [112]. Induction of SCFE1-triggered immune responses is dependent on BAK1 and SOBIR1. Mutants of RLP30, BAK1, and SOBIR1 are more susceptible to *S. sclerotiorum* and the related fungus *B. cinerea* [112].

1.2.2.4 ReMAX & eMAX

Proteinaceous MAMP called eMax (enigmatic MAMP of *Xanthomonas*) derives from *Xanthomonas* and is recognized by ReMAX (RECEPTOR OF eMax) of *A. thaliana*. ReMAX was mapped to RLP1 [113]. Functionality of ReMAX depends on

the presence of the SOBIR [114].

1.2.2.5 Ave1 & Ve1

Verticillium dahliae is a soil-borne fungus which causes vascular wilt and is characterized in over 200 plant species [115]. A LRR-RP named Ve1 in tomato provide resistance against race 1 strains of *V. dahliae*. A race 1-specific effector, named AVE1, was identified through comparative population genomics of race 1 and race 2 strains [116]. Ave1 is characterized as a small, secreted protein that is recognized by the Ve1 immune receptor. Ve1-mediated defense responses in tomato require both BAK1 and SOBIR1 [117, 118].

Intriguingly, Ave1 is conserved in fungal pathogens such as *Fusarium oxysporum f.* sp. *lycopersici*, *Colletotrichum higginsianum* and *Cercospora beticola* and bacterial pathogens such as *Xanthomonas axonopodis pv. citri.* Ave1 is homologous to a widespread family of plant peptides, which may have been acquired through horizontal gene transfer from plants [119].

1.2.2.6 *Le*Eix1/2 & Xylanase

ETHYLENE-INDUCING XYLANASE (EIX), originating from the fungus *Trichoderma viride* [120, 121], EIX is a potent MAMP which induces hypersensitive response (HR) in tomato and tobacco [122]. The immunogenic portion of the EIX was identified as the pentapeptide , which maps to an exposed β-strand of the EIX protein [123].

The two LRR-RPs *Le*Eix1 and *Le*Eix2 can bind EIX independently, but only *Le*EIX2 confers signaling when expressed heterologously in tobacco. Upon application of EIX, *Le*Eix2 can form heterodimers with *Le*Eix1, and *Le*Eix1 attenuates

defense responses activated by *Le*EIX2. BAK1 interacts with *Le*Eix1 but not *Le*Eix2, and negatively regulates *Le*Eix2-mediated signaling. Here BAK1 does not serve as a positive regulator as in many other signaling pathways. [122].

1.2.2.7 Cf and Avr

The LRR-RP Cf proteins confer resistance to *Cladisporium fulvum* in tomato. However, there is an open debate whether to classify Cf proteins as PRR [124]. Cf proteins recognize *C. fulvum* race-specific secreted effectors and Cf9 was the first identified RP [125]. Several potential interactors of the cytoplasmic C terminus of Cf9 were isolated by yeast two-hybrid [126-128]. For instance, ER-resident chaperones were identified as *in planta* interactors of Cf proteins that are required for Cf protein biogenesis [129]. The tomato ortholog of the Arabidopsis SOBIR1 [130, 131] and its close homolog SOBIR1-like were also identified as Cf interactors. Cf4 and Cf9 recruit SERK1 or SERK3a upon Avr4 or Avr9 perception. Avr4 triggers endocytosis of the Cf4/SOBIR1 complex, and SERKs are required for ligand-triggered HR and resistance to *C. fulvum* [43].

1.2.3 LYM-RK and LYM-RP for MAMPs

1.2.3.1 LYM3/LYM1/CERK1 & Peptidoglycan

Peptidoglycan (PGN) is a major constituent of bacterial cell walls which consists of heteropolymeric chains of N-acetylglucosamine (GlcNAc) and N-acetylmuramic acid (MurNAc) crosslinked with a short peptide. Virtually all bacteria contain a layer of PGN, but differ in amount, location and specific composition [132, 133]. PGN is a classical MAMP which can trigger defense responses in plants like Arabidopsis and

rice [134, 135].

In Arabidopsis, Lysin-motif proteins LysM-DOMAIN CONTAINING GPI-ANCHORED PROTEIN 1 (LYM1), LYM3 and CHITIN ELICITOR RECEPTOR KINASE 1 (CERK1) are proven to have a critical role in the perception of bacterial peptidoglycan and in innate immunity to bacterial infection [136]. LYM1 and LYM3 are plasma membrane proteins that directly interact with structurally different PGNs [136]. CERK1, previously identified as chitin receptor, is a LysM receptor kinase that does not bind PGN, but is required for PGN sensitivity and immunity to bacterial infection [136, 137]. It is likely that the three proteins form a heterotrimeric receptor complex for recognizing PGNs and relaying the extracellular signal into the cell [136]. The *in vivo* interaction between LYM1/LYM3 and CERK1, however, still needs to be demonstrated. Intriguingly, LYM1 and LYM3 do not seem to have a role in chitin-induced responses [138], but the paralogous LYM2 protein contributes to chitin-triggered plasmodesmata closure in a CERK1-independent manner [139]. The PGN sensing system in rice is similar, involving the LysM-RK *Os*CERK1 and [140] LysM-containing RPs, *Os*LYP4 and *Os*LYP6, which are homologs of LYM1 and LYM3 [135, 141, 142].

1.2.3.2 CEBiP/CERK1 & Chitin

Chitin is a major constituent of fungal cell walls which triggers immune response in plants including Arabidopsis, rice, tomato and wheat [143-148]. The first PRR shown to be involved in chitin perception was the rice CHITIN ELICITOR-BINDING PROTEIN (*Os*CEBiP). *Os*CEBiP is an RP which contains two extracellular LysMs for chitin-binding, a transmembrane domain and a short cytoplasmic tail [149]. The lack of an intracellular kinase domain of *Os*CEBiP suggested the requirement of additional

components for chitin-induced signaling pathway. A second LysM domain containing protein, *Os*CERK1, the rice ortholog of *At*CERK1, was revealed as an important component in chitin perception of rice [150]. *Os*CEBiP homodimerizes upon chitin binding and forms a heterooligomeric complex with *Os*CERK1 [150]. *Os*RLCK176 and *Os*RLCK185, which are members of the rice RLCK family VII, both interact with *Os*CERK1 and positively regulate responses to chitin as well as PGNs [135, 140].

The role of CERK1 in chitin perception was first identified in Arabidopsis [143, 147]. *At*CERK1 (also named LysM-RLK1) is a membrane protein with three extracellular LysMs, a transmembrane domain and an intracellular kinase domain [143, 151]. The crystal structure of the ectodomain of *At*CERK1 show that the three LysM domains of AtCERK1 are tightly packed in a globular structure, and LysM domain 2 binds N-acetylglucosamine pentamers [152]. A chitin octamer acts as a bivalent ligand to induce *At*CERK1 dimerization. Shorter chitin fragments inhibit dimerization. Ligand-induced *At*CERK1 homodimerization is essential for receptor activation and immune signal transduction [152, 153]. CERK1 was thought to be the unique chitin receptor [154-156]. However, a recent study demonstrated that LysM-CONTAINING RECEPTOR-LIKE KINASE 5 (LYK5) displays higher chitin-binding affinity than CERK1 [140]. Furthermore, LYK5 is required for chitin responsiveness, and forms a complex with CERK1 in a chitin-dependent manner [140, 157]. Whether LYK5 and CERK1 organize into a receptor system similar to *Os*CEBiP and *Os*CERK1 in rice remains to be shown.

Studies also investigated the role of the three homologs of *Os*CEBiP in Arabidopsis, LYM1, LYM2 and LYM3, in chitin perception [158]. Only one member of the *At*LYM family, *At*LYM2/*At*CEBiP, displayed a high-affinity binding for chitin similar to rice CEBiP [158]. However, the single/triple knockout mutants of *At*LYM1, *At*LYM2

and *At*LYM3 and the overexpression line of *At*LYM2/*At*CEBiP showed the same chitin-induced defense responses as the wild type, indicating that *At*LYM2/AtCEBiP does not contribute to chitin signaling [158]. Arabidopsis mutants for LysM RLK1-INTERACTING KINASE 1 (LIK1), an LRR-RLK, show higher ROS production in response to chitin than the wild type [159], and CERK1 phosphorylates LIK1 in a chitin-independent manner [159], but the relevance of this activity has not been clarified. PBL27, an Arabidopsis ortholog of OsRLCK185, regulates chitin-induced defense responses in Arabidopsis [160] .

1.2.4 PRR & DAMPs

Plants can also sense DAMPs which are generated upon wounding or pathogen recognition. The first plant DAMP/PRR pairs have been identified in Arabidopsis. LRR-RLKs PEP RECEPTOR 1 (PEPR1) and PEPR2 perceive AtPep peptides. These peptides are derived from PRECURSOR OF PEPTIDEs (PROPEPs), which are encoded by a seven-member multigenic family whose expression is induced by wounding or MAMP perception [161-164]. AtPep perception is involved in MTI amplification and is important for the induction of systemic immunity [51, 165-169]. BAK1 and BIK1 interact with PEPR1 and PEPR2 upon AtPep perception, which triggers responses such as ROS burst and ethylene production [51, 170]. Precursors of PAMP-induced secreted peptide1 (PIP1) are secreted into extracellular spaces and cleaved at the C-terminus. Mature peptide PIP1 can be perceived by receptor-like kinase 7 (RLK7) and triggers immune response [171]. Several other plant-derived peptides have also been shown to activate immune responses in plants, via unknown PRRs [13].

During infection, pathogens produce enzymes to degrade cell wall. This

process releases active molecules that are normally embedded in the plant cell wall matrix. Some of these host-derived molecules can be recognized by PRRs. OGs, for example, are perceived by the EGF motif-containing RLK WALL-ASSOCIATED KINASE1 (WAK1) in Arabidopsis [28]. Extracellular ATP (eATP) can be released on cell rupture during pathogen attack or wounding and thus serves as a DAMP, and a novel class of plant receptor for eATP was identified as the Arabidopsis DORN1/LecRK-I.9 (Does not Respond to Nucleotides 1/ lectin receptor kinase-I.9) [172].

1.3 Aim of the project

Although many studies focused individually on the signal pathways triggered by different receptor types during the establishment of immunity to microbial infection, the relation between these pathways remains unknown. Furthermore, small variations in growing conditions and handling of plants can cause significant differences in phenotypes [173]. It is important to compare these receptors side-by-side by the same person, and to let plants grow under identical conditions in order to get reliable results. The purpose of this project is to thoroughly compare signaling pathways triggered by LRR-RK, LRR-RP or LysM-RKs. By systematic analyses of these signaling pathways, putative differences or key regulators will be studied. In this project, Arabidopsis plants were treated with water (control), flg22 (LRR-RK), nlp20 (LRR-RP), or chitin (LysM-RK). Various typical immune responses were analyzed including MAPK activation, ROS production, callose deposition and camalexin accumulation. Moreover, using Next-generation RNA-sequencing (RNA-Seq) we unraveled regulatory components or defense genes of the different signaling pathways. There are many proteins known to be involved in immune pathway triggered by flg22. We compared responses of mutant lines to flg22 and nlp20 to establish the knowledge of the pathway following LRR-RP. In this work, we draw a comprehensive picture of MAMP-triggered immunity and discover candidates playing different roles in pathways following FLS2 and RLP23.

2. Materials and Methods

2.1 Materials

2.1.1 Chemicals

All used standard chemicals were of standard purity and purchased from Sigma-Aldrich (Taufkirchen), Carl Roth (Karlsruhe), Merck (Darmstadt), Qiagen (Hilden), Invitrogen (Karlsruhe), Duchefa (Haarlem, The Netherlands), Molecular Probes (Leiden, The Netherlands), Fluka (Buchs, Switzerland) and BD Diagnostics (Sparks, USA), unless noted otherwise in the text. Restriction enzymes, ligase and DNA modification enzymes were purchased from Thermo Fisher Scientific (St. Leon-Rot) and New England Biolabs (Beverly, USA). Primary antibodies were purchased from Cell Signaling Technology (Phospho p44/42 MAPK (Erk1/2)), Sigma-Aldrich (α-Myc, α-HA), Sicgen (α-GFP) and Agrisera (α-BAK). Alkaline phosphatase conjugated secondary antibodies α-rabbit IgG, α-goat IgG and α-mouse IgG were purchased from Sigma-Aldrich. Synthetic nlp20 peptide, flg22 peptide are from GenScript (New Jersey, USA) and chitin (C6) were purchased from Seikagaku (Tokyo, Japan). For stock solution, flg22, nlp20 and chitin were dissolved in water and were stored at -20 °C. For low concentration short-term storage of flg22 (10 µM), 1 mg/mL BSA and 0.1 M NaCl were used.

2.1.2 Primers

Oligonucleotides were received from Eurofins MWG Operon (Ebersberg). The primers used in this study are listed in Table 2.1.

Table 2-1: Primers used in this study

Name	Target	sequence 5´-3´
FRK1-F	At2g19190	AAG AGT TTC GAG CAG AGG TTG AC
FRK1-R		CCA ACA AGA GAA GTC AGG TTC GTG
At_eF1a_qF	At1g07920, At1g07930 At1g07940,At5g60390	GAG GCA GAC TGT TGC AGT CG
At_eF1a_qR		TCA CTT CGC ACC CTT CTT GA
eF1a-s		TCA CAT CAA CAT TGT GGT CAT TGG-3'
eF1a-as		TTG ATC TGG TCA AGA GCC TAC AG-3'
oligo-dT		TTT TTT TTT TTT TTT TTT TT(AGC)

2.1.3 Antbiotics

Antbiotics used in this study are listed in Table 2.2

Table 2-2: Antibiotics used in this study

Antibiotics	Concentration µg/ml	Solvent
Carbenicillin	100	Water
Spectinomycin	100	Water
Kanamycin	50	Water
Rifampicin	50	Methanol
Hygromycin	20 (for Arabidopsis)	

2.1.4 Vectors

Vectors used in this study are listed in Table 2.3.

Table 2-3: Vectors used in this study

Vectors	Characteristics	Reference
pCR8/GW/TOPO	Ori Puc, rrnB, T2, rrnB,T1, attP1, attP2, ccdB, Sm/Sp$_r$	Thermo Fisher Scientific
pGWB5	p35S, t35S, attR1, attR2, ccdB, Kan$_r$, Hyg$_r$, GFP	[174]
pGWB14	p35S, t35S, attR1, attR2, ccdB, Kan$_r$, Hyg$_r$, 3x-HA	[174]

2.2 Organisms

2.2.1 *Arabidopsis thaliana* lines

All experiments were conducted using the *Arabidopsis thaliana* ecotype Columbia-0 (Col-0) and transgenic lines generated in this ecotype. The T-DNA insertion lines mainly used in this study are listed in Table 2.4. These lines were purchased from the Nottingham Arabidopsis Stock Centre (NASC) or received from the lab of Dr. Cyril Zipfel, lab of Dr. Yuelin Zhang, lab of Dr. Jian-Min Zhou, or lab of Dr. Birgit Kemmerling.

Table 2-4: Arabidopsis thaliana lines used in this study

Name	Description
fls2 (SALK_062054)	T-DNA in At5g46330 exon
rlp23-1 (SALK_034225)	T-DNA in At2g32680 exon [42]
cerk1-2 (GK_096F09)	T-DNA insertion in At3g21630 exon [175]
bak1-5	point mutation in At4g33430 (Y408C) [176, 177]
bir2-1 (GK-793F12)	T-DNA insertion in At3g28450 exon [84]
amiR-*BIR2*#1	artificial microRNA targeting At3g28450 [84]
cpk28-1 (GK_523B08)	T-DNA insertion in At5g66210 exon
CPK28-OE	35S:CPK28-YFP in *cpk28-1* [178]
pp2a-a1 (SALK_059903)	T-DNA insertion in At1g25490 intron [87]
pp2a-c4 (SALK_035009)	T-DNA insertion in At3g58500 exon [87]
bik1 (SALK_005291)	T-DNA insertion in At2g39660 exon [50]
pbl1 (SAIL_1236_D07)	T-DNA insertion in At3g55450 intron [49]
pbl2 (SALK_149140)	T-DNA insertion in At1g14370 intron [49]

pbl3 (SALK_039503)	T-DNA insertion in At2g02800 300-5'UTR
pbl4 (SALK_097999)	T-DNA insertion in At1g26970 300-5'UTR
pbl5 (SALK_045613)	T-DNA insertion in At1g07870 exon
pbl7 (SALK_114130)	T-DNA insertion in At5g02800 exon
pbl8 (GK_625H05)	T-DNA insertion in At5g01020 exon
pbl9 (GK_430_G06)	T-DNA insertion in At1g07570 exon
pbl10 (SALK_001115)	T-DNA insertion in At2g28930 exon
pbl11 (SALK_046795)	T-DNA insertion in At5g02290 exon
pbl12 (SALK_017105)	T-DNA insertion in At2g26290 exon
pbl13_1 (GK_586B09)	T-DNA insertion in At5g35580 exon [179]
pbl15 (SALK_055095)	T-DNA insertion in At1g61590 exon
pbl16 (SALK_201102)	T-DNA insertion in At5g56460 exon
pbl18 (SALK_097486)	T-DNA insertion in At1g69790 exon
pbl19 (SALK_021064)	T-DNA insertion in At5g47070
pbl20 (SALK_049965)	T-DNA insertion in At4g17660 exon
pbl21 (SALK_025049)	T-DNA insertion in At1g20650 exon
pbl22 (SALK_045159)	T-DNA insertion in At1g76370 exon
pbl23 (SALK_112111)	T-DNA insertion in At3g20530 exon
pbl24 (SALK_072589)	T-DNA insertion in At4g13190 exon
pbl26 (SALK_023374)	T-DNA insertion in At3g07070 exon
pbl27_2 (GK_088H03)	T-DNA insertion in At5g18610 exon [160]
pbl28 (SALK_120599)	T-DNA insertion in At1g24030
pbl29 (SALK_050111)	T-DNA insertion in At1g74490 exon
pbl31 (SAIL_273_C01)	T-DNA insertion in At1g76360 exon

pbl32 (SALK_113804)	T-DNA insertion in At2g17220 exon
pbl35 (SALK_039402)	T-DNA insertion in At3g01300 exon
pbl36 (SAIL_885_B03)	T-DNA insertion in At3g28690 exon
pbl37 (GK_090A05)	T-DNA insertion in At2g28940 exon
pbl38 (SALK_140489)	T-DNA insertion in AT2G39110 exon
pbl39 (*pcrk1-2*) (SALK_145629)	T-DNA insertion in At3g09830 exon [180]
pbl40 (*pcrk2-1*) (SAIL_129_D02)	T-DNA insertion in At5g03320 exon [180]
pbl41 (SALK_150918)	T-DNA insertion in At1g61860 exon
pbl42 (SALK_000019)	T-DNA insertion in At3g02810 exon [181]
pbl43 (SALK_055909)	T-DNA insertion in At5g16500 exon [181]
bik1 pbl1	[49]
pbl39 pbl40 (pcrk1 pcrk2)	At3g09830 At5g03320 [180]
xlg2-1 (SALK_062645)	T-DNA insertion in At4g34390 exon [182, 183]
agb1-2 (SALK_061896)	T-DNA insertion in At4g34460 exon [183, 184]
agg1agg2	AT3G63420 AT3G22942 [183, 185]
bak1-4 (SALK_116202)	T-DNA insertion in At4g33430 [38]
bak1-4/BAK1	*pBAK1:BAK* in *bak1-4* [38]
bak1-4/BAK1(Y403F)	*pBAK1:BAK(Y403F)* in *bak1-4*
bak1-4/BAK1 (S602A/T603A/S604A)	*pBAK1:BAK(S602A/T603A/S604A)* in *bak1-4*
bak1-4/BAK1(S612A)	*pBAK1:BAK(S612A)* in *bak1-4*
BIK1-HA	*pBIK1:BIK1-HA* in *rps5* [49]

2.2.2 Cultivation conditions of Arabidopsis thaliana

A. thaliana seeds were sown on steam-sterilized GS90-soil (Gebr. Patzer GmbH) mixed with vermiculite or on sterile ½ Murashige and Skoog medium plate after surface-sterilization with chlorine gas. For ½ MS medium, 2.2 g MS (Duchefa) was resolved in deionized water and adjusted to pH 5.7 by KOH, for solid MS plates 10 g/L phyto agar (Duchefa) was added to the medium. Medium was sterilized by autoclaving for 20 minutes at 121 °C. After stratification of the seeds for two days at 4 °C in the dark the plants were grown in environmental chambers either in long-day (16 hr light, 8 hr darkness) or short-day (8 hr light, 16 hr darkness) under standard conditions (150 µmol/cm^{2}s light, 40-60 % humidity, 22 °C).

2.2.3 Bacterial strains

Table 2-5 Bacterial strains used in this study

Strains	Genotype	Reference
E. coli DH5α	fhuA2 lac(del)U169 phoA glnV44 Φ80' lacZ(del)M15 gyrA96 recA1 relA1 endA1 thi-1 hsdR17	Invitrogen
Agrobacterium C58C1	T-DNA- vir+ rifr	[186]

2.3 Methods

2.3.1 General molecular biology methods

Standard protocols were used for PCR, agarose gel electrophoresis, restriction digestion, ligation, and transformation of bacteria [187]. The enzymes were used according to the manufacturer's protocol (Thermo Fisher Sientific, Fermentas and NEB). For the generation of PCR fragments either the *Taq* DNA-Polymerase or *pfu* DNA-Polymerase was used. Agarose gel electrophoresis to separate DNA fragments was performed with a 1 % agarose gel containing 0.01 µL/mL pegGREEN (Peqlab) in 1 x TAE buffer (4 mM Tris/acetate, 1 mM EDTA pH 8.0). Samples were mixed with loading dye (6 x loading dye: 10 mM Tris-HCl (pH 7.6), 0.15% orange G, 60% glycerol, 60 mM EDTA) and GeneRuler™ DNA Ladder Mix (Fermentas) was used as size marker for the agarose gel electrophoresis. Electrophoresis was performed in an electric field strength of 5 V/cm. DNA fragments were visualized in a UV-transilluminator (Infinity-3026 WL/26 Mx, Peqlab) with the software InfinityCapt 14.2 (Peqlab). DNA purification from agarose gels was performed with the HiYield PCR Clean-up/Gel Extraction Kit (HiYield). Nucleic acid concentrations were determined with a NanoDrop 2000 spectrophotometer (Thermo Fisher Scientific) at 220-340 nm and evaluated with the NanDrop Software. One Shot® TOP10 Competent *E. coli* were acquired from Thermo Fisher Scientific. Plasmid isolation was performed using the GeneJET Plasmid Miniprep Kit (Thermo Fisher Scientific). Sequencing of plasmid DNA was performed by GATC (Konstanz) and prepared according to the company's instructions. Sequences were analyzed using the CLC Main Workbench 7 (Qiagen).

2.3.2 RNA isolation

Total RNA from leaves or seedlings was isolated using the Trizol method according to the standard protocol [188]. Plant material was harvest in 2 mL reaction tubes and grinded into a fine powder using liquid nitrogen and a plastic pestle (Sigma-Aldrich, Z359947-100EA), 1 mL of the TRIzol reagent was used to suspend the plant material by vigorous vortexing. After 10 minutes incubation at room temperature and centrifugation (16,000 g, 10 min, 4 °C), supernatant was transferred to a new 1.5 mL reaction tube. 500 µL chloroform was added to the supernatant, and each sample was mixed by vigorous vortexing (15 s). The organic (lower phase) and the aqueous (upper phase) phase were separated by centrifugation (16,000 g, 5 min, 4 °C). The aqueous phase which contains total RNA was carefully transferred to a new tube without disturbing the interphase. The steps from adding chloroform were repeated once, 1 volume of isopropanol was added to the aqueous phase in the new tube and the samples were mixed by inverting several times. Samples were incubated overnight at −20 °C. After that, RNA was precipitated by centrifugation (16,000 g, 30 min, 4 °C). The supernatant was carefully removed by pipetting. 500 µL 80 % EtOH was added to each sample, samples were centrifuged (16,000 g, 10 min, 4 °C) and supernatant was carefully remove by pipetting. The samples were air-dried for approximately 3 minutes at room temperature. 50 µL pre-heated nuclease-free water or DEPC-treated water was used to suspend the pellet. Samples were incubated on ice (up to 1 hr). If the pellet had not completely dissolved, the samples were heated to 65 °C for 1–5 minutes. RNA concentration was determined by using Nanodrop. RNA samples were stored at −20 °C.

2.3.3 Reverse Transcription (RT)

RevertAid First Strand cDNA Synthesis Kit (Thermo Scientific) was applied for cDNA synthesis. For cDNA synthesis 1 µg total RNA was used, 2 µL of 50 mM oligo-dT was added to the RNA sample and H_2O was added to total volume of 12.5 µL. The samples were denatured for 5 minutes at 72 °C. Samples were placed on ice immediately. The RT reaction mixture was completed by adding 4 µL 5 x RT buffer, 2 µL10 mM dNTPs, 0.5 µL Ribo-LOCK and 1 µL RevertAid. The RT reaction mixture was mixed well and incubated in a thermocycler at 42 °C for 1.5 hr, then at 72 °C for 10 min.

2.3.4 Semi-quantitative RT-PCR

1 µL cDNA was used for a standard PCR reaction with primers specific for the analyzed transcript. In a control PCR primers specific for the house-keeping gene elongation factor 1α (EF1α) were used.

2.3.5 Quantitative Real-time PCR

For RT-qPCR experiments, cDNA was diluted 16 fold. RT-qPCR amplifications and measurements were performed with the iQ5 Multicolour Real Time PCR detection system (Bio-Rad). RT-qPCR amplifications were monitored using the ABsolute SYBR Green Fluorescein Mix (Thermo Scientific). The gene expression data was quantified using the $2^{-\Delta\Delta CT}$ method [189]. The normalization of the expression levels was done using the CT values obtained for the EF1α gene. The presence of a single PCR product was further verified by dissociation analysis in all amplifications. All quantifications were made in RNA samples obtained from three

independent experiments.

Standard qRT-PCR reaction mixture contains 10 µL Maxima SYBR Green qPCR Master Mix (2X), 1 µL Forward oligonucleotide (10 µM), 1 µL Forward oligonucleotide (10 µM), 1 µL Reverse oligonucleotide (10 µM) and 8 µL template. First the master mix was distributed into the PCR plate, and then template DNA was added. The PCR plate was sealed with an optical adhesive seal. The PCR plate was centrifuged (short spin) and incubated in a qRT-PCR thermocycler. The program in Table 2.6 was used. The melting curves should peak homogenously at one temperature. More than one peak suggests formation of oligonucleotide dimers or production of unspecific PCR products during amplification.

Table 2-6: PCR conditions used for quantitative RT-PCR

(a)	95 °C	5 min
(b)	95 °C	10 s
(c)	55 °C	30 s
(d)	72 °C	20 s
	Photometric measurement at 530 nm	
	Repeat steps b–d 39 times	
	Melting curve:	
(e)	95 °C	30 s
(f)	55–95 °C: Each step + 1 °C; 5 s Photometric measurement at 530 nm	

2.3.6 Protein extraction from plant tissue

Total protein was extracted from plant tissue using extraction buffer containing detergents for solubilization of membrane-bound proteins (50 mM Tris-HCl, pH 7.5, 150 mM NaCl, 1 % (v/v) Nonidet P40 and 1 protease inhibitor cocktail tablet/10 mL from Roche). The plant tissue was first homogenized in liquid nitrogen and after addition of the extraction buffer the sample was incubated for 30 min at 4 °C. Afterwards the soluble proteins were separated from the insoluble ones in a centrifugation step (15 min, 20,800 g, 4 °C) and used for further analysis.

2.3.7 Determination of protein concentration

The protein concentration was measured using the Bradford method [190] and Roti-Quant solution (Carl Roth). Standard curves were prepared using bovine serum albumin (BSA).

2.3.8 SDS-PAGE

SDS polyacrylamide gel electrophoresis was performed according to a standard protocol [187]. Denaturing SDS polyacrylamide gel electrophoresis (SDS-PAGE) was carried out by using the Mini–PROTEAN® 3 system (Biorad) and discontinuous polyacrylamide gels [191]. Separating gels were poured between two glass plates and overlaid with isopropanol. After gels had polymerized for 30 - 45 min, the isopropanol was removed and the gel surface was carefully dried with filter paper. The stacking gel was poured on top of the separating gel. A comb was inserted and the gel was allowed to polymerize for 30 min. In this study, a 9 % separating gel was used and the concentration of the overlaid stacking gel was 4 %.

Gels were 1.0 mm in thickness. Protein extracts prepared from plant samples were mixed with 3 x SDS sample buffer (10 mL: 3 mL Glycerol, 2.4 mL 5 % (w/v) SDS, 0.15 mg Bromphenol blue, 3.75 mL 0.5 M (pH 6.8) Tris-HCl). Then, the samples were heated for 5 minutes in 95 °C, and centrifuged for 1 minute. The samples were loaded on the gels and SDS-PAGE was performed using 1x SDS-running buffer (25 mM Tris base, 192 mM Glycine, 0.1% (w/v) SDS). The Prestained Protein Ladder Mix (Fermentas) was used as a protein marker.

2.3.9 Western blot analysis

For the western blot analysis the proteins were transferred after SDS-PAGE onto a Hybond nitrocellulose membrane (GE Healthcare) using a Mini Trans-Blot® Electrophoretic Transfer Cell (BioRad) for 1 hr at 100 V. The protein transfer was controlled by Ponceau S red stain (0.1 % (w/v) Ponceau S red and 5 % (v/v) acetic acid). Unspecific binding sites were blocked by incubation of the membrane for 1 hr at room temperature with 5 % (w/v) milk in 1 x PBST (140 mM NaCl, 2.7 mM KCl, 10 mM Na_2HPO_4, 1.8 mM KH_2PO_4, 0.1 % (v/v) Tween 20). Afterwards the membrane was incubated with a primary antibody overnight at 4°C. Then the membrane was washed 3 times with 1 x PBST, 5 min each time and incubated for 1.5 hr with a secondary antibody. The signal of a peroxidase-coupled secondary antibody was detected using the Enhanced Chemiluminescence Kit (GE Healthcare) according to the manufacturers' instructions. For the detection of an alkaline phosphatase-coupled secondary antibody the membrane was washed with 1 x PBST for 3 x 5 min and then equilibrated for 2 min with a Tris 9.5 buffer (150 mM Tris-HCl; pH 9.5, 5 mM $MgCl_2$ and 100 mM NaCl). The staining reaction was performed with 1 x BCIP/NBT in Tris 9.5 buffer (5-bromo-4- chloro-3-indolylphosphate; 200 x stock solution 50 mg/ml in 70

% (v/v) dimethylformamide; Nitro-blue tetrazolium chloride; 200 x stock solution 50 mg/mL in 100 % (v/v) dimethylformamide). After the staining the membrane was washed with water.

Table 2-7: Antibodies used for immunoblot detection

Primary antibodies

Antibody	Source	Dilution	Reference
α-p44/42 MAPK	rabbit	1:2000	Cell Signaling Technology
α-HA	rabbit	1:3000	Sigma-Aldrich
α-myc	mouse	1:6000	Sigma-Aldrich
α-GFP	goat	1:4000	Acris Antibodies

Secondary antibodies

Antibody	Feature	Dilution	Reference
α-mouse IgG	HRP conjugated	1:10000	Sigma-Aldrich
α-goat IgG	HRP conjugated	1:10000	Sigma-Aldrich
α-rabbit IgG	HRP conjugated	1:10000	Sigma-Aldrich

2.3.10 Coomassie blue staining

For non-specific staining of proteins after SDS-PAGE, Coomassie Brilliant Blue R-250 staining (0.125 % (w/v) Coomassie blue R-250, 50 % (v/v) MeOH, 10 % (v/v) acetic acid) was performed. After incubation for 30 min at room temperature, the superfluous stain was removed by 10 % (v/v) acetic acid.

2.3.11 ROS burst assay

Leaves of Arabidopsis at the age of 4-6 weeks were cut into about 10 mm^2 square pieces and floated on water overnight. 90 uL of water and 10 µL of the luminol-master mix (9.86 µL H$_2$O, 0.1 µL luminol (20 mM) and 0.04 µL of peroxidase (5 mg / mL)) was added per well in a 96-sample plate. Leaf pieces were distributed individually to the wells. The light emission from the leaf pieces was evaluated over a pre-determined period of time using a Berthold Centro LB 960 luminometer.

2.3.12 Ethylene measurement

Leaves from 4-6 weeks old Arabidopsis plants were cut into approximately 10 mm^2 pieces, and floated on water at room temperature overnight. Four leaf pieces were transferred to 6 mL glass tubes containing 0.5 mL 20 mM MES, pH 5.6. The appropriate elicitors were added to the tubes and mixed thoroughly. Vials were closed with rubber septa. 1 mL ethylene accumulating in the free air space was measured by gas chromatography (GC-14A, Shimadzu, Japan) after incubation.

2.3.13 Salicylic acid and camalexin measurement

6-week-old Arabidopsis leaves were infiltrated with elicitors, for each sample, 200 mg of leaves were collected. The amount of salicylic acid and camalexin were measured by HPLC (High Performance Liquid Chromatography system Agilent 1200) in the analytical laboratories of Mark Stahl (ZMBP, Tübingen).

2.3.14 RNA-sequencing library preparation

10-day-old Arabidopsis seedlings grown on half strength MS plates were

treated with water, 500 nM flg22, 500nM nlp20 or 10 µM chitin (C6). Samples were collected at 0 hr, 1 hr, 6 hr and 24 hr after treatment. RNA was extracted using the RNeasy Plant mini kit (QIAGEN) and RNase-Free DNase set (QIAGEN) was used to eliminate DNA contamination. RNA quantity and quality was checked with ABI 3730xl DNA Analyzer (Applied Biosystems) and Qubit® 2.0 Fluorometer (Invitrogen). 2 µg of total RNA were used for library preparation. The cDNA library was prepared using Illumina® TruSeq® RNA Sample Preparation Kits. The library was sequenced using the Hiseq2000 with cBot (Illumina) at the Max Planck Institute for Developmental Biology, Tübingen.

2.3.14.1 RNA extraction by RNeasy Plant mini kit (QIAGEN)

Plant material was collected in an RNase-free, liquid-nitrogen–cooled, 2 mL tube in liquid nitrogen and grinded thoroughly with a pestle. 450 µL Buffer RLT was add to tissue powder and vortexed vigorously. The lysate was transferred to a QIA shredder spin column (lilac) placed in a 2 mL collection tube, and centrifuged for 2 minutes at full speed. Supernatant of the flow-through was carefully transferred to a new tube without disturbing the cell-debris pellet in the collection tube. This supernatant was used in subsequent steps. 0.5 volume of EtOH (96–100%) was added to the cleared lysate, and mixed immediately by pipetting. The sample (usually 650 µL), including any precipitate that may have formed, was transferred to an RNeasy spin column placed in a 2 mL collection tube. The sample was centrifuged for 15 seconds at ≥8000 g (≥10,000 rpm) and the flow-through was discarded. 700 µL Buffer RW1 was added to the RNeasy spin column. The spin column membrane was washed for 15 seconds at ≥8000 x g (≥10,000 rpm) centrifugation. The flow-through was discarded. 500 µL Buffer RPE was added to the RNeasy spin column. The spin column

membrane was washed through 15 seconds centrifugation at ≥8000 g (≥10,000 rpm). The flow-through was discarded. The spin column was centrifuged again for 2 minutes. The RNeasy spin column was placed in a new 1.5 ml collection tube. 30 μL RNase-free water was added directly to the spin column membrane and centrifuged for 1 minutes at ≥8000 x g (≥10,000 rpm) to elute the RNA. The Step was repeated again. The final volume of RNA sample is 60 μL.

2.3.14.2 Purification of mRNA fragments

Make RNA Bead Plate (RBP)

The total RNA was diluted with nuclease-free ultra pure water to a final volume of 50 μL in the new 96-well MIDI plate (RBP).The room temperature RNA Purification Beads tube was vortexed vigorously to resuspend the oligo-dT beads. 50 μL RNA Purification Beads were added to each well of the RBP plate to bind the polyA RNA to the oligo-dT beads. RBP plate was sealed and mixed thoroughly on a microplate shaker continuously at 1000 rpm for 1 minute. The sealed RBP plate was placed on the pre-heated microheating system and incubated at 65 ℃ for 5 minutes to denature the RNA and facilitate binding of the polyA RNA to the beads. The RBP plate was placed on ice for 1 minute, then 5 minutes at room temperature to allow the RNA to bind to the beads. The adhesive seal was removed and the RBP plate was placed on the magnetic stand at room temperature for 5 minutes to separate the polyA RNA bound beads from the solution. All of the supernatant from each well of the RBP plate was removed and discarded. The RBP plate was removed from the magnetic stand. The beads were washed by adding 200 μL Bead Washing Buffer to remove unbound RNA. The RBP plate was sealed and mixed thoroughly on a microplate shaker continuously at 1000 rpm for 1 minute. The adhesive seal was removed and the RBP

plate was placed on the magnetic stand at room temperature for 5 minutes. The thawed Elution Buffer was centrifuged at 600 g for 5 seconds and all of the supernatant was discarded. The RBP plate was removed from the magnetic stand and 50 µL Elution Buffer was added in each well of the RBP plate. The RBP plate was sealed and mixed thoroughly on a microplate shaker continuously at 1000 rpm for 1 minutes. The Elution Buffer tube was stored at 4 °C. The sealed RBP plate was placed on the pre-heated microheating system and incubated at 80 °C for 2 minutes to elute the mRNA from the beads. RBP plate was placed on ice for 1 minutes then on the bench at room temperature, the adhesive seal was removed from the RBP plate.

Make RNA Fragmentation Plate (RFP)

The thawed Bead Binding Buffer was centrifuged at 600 g for 5 seconds. 50 µL Bead Binding Buffer was added to each well. This allows mRNA to specifically rebind the beads, while reducing the amount of rRNA that non-specifically binds. The RBP plate was sealed and mixed thoroughly on a microplate shaker continuously at 1000 rpm for 1 minute. The RBP plate was incubated at room temperature for 5 minutes. The Bead Binding Buffer tube was stored at 2 °C to 8 °C. The adhesive seal was removed from the RBP plate and the RBP plate was placed on the magnetic stand at room temperature for 5 minutes. All of the supernatant from each well of the RBP plate was removed and discarded. The RBP plate from the magnetic stand was removed and the beads were washed by adding 200 µL Bead Washing Buffer in each well of the RBP plate. The RBP plate was sealed and mixed thoroughly on a microplate shaker continuously at 1000 rpm for 1 minute. The adhesive seal was removed from the RBP plate and the RBP plate was removed on the magnetic stand at room temperature for 5 minutes. All of the supernatant from each well of the RBP

plate was removed and discarded. The supernatant contained residual rRNA and other contaminants that were released in the first elution and did not rebind the beads. The RBP plate was removed from the magnetic stand and 19.5 µL Elute, Prime, Fragment Mix was added to each well of the RBP plate. The Elute, Prime, Fragment Mix contained random hexamers for room temperature priming and serves as the first strand cDNA synthesis reaction buffer. The RBP plate was sealed and mixed thoroughly on a microplate shaker continuously at 1000 rpm for 1 minute. The sealed RFP plate was placed on the pre-programmed thermal cycler. Elution 2 - Frag - Prime (94 °C for 8 min, 4 °C hold) was elected to elute, fragment, and prime the RNA. The RFP plate was removed from the thermal cycler when it reached 4 °C and centrifuged briefly.

2.3.14.3 Synthesis of the first strand cDNA

Make cDNA plate (CDP)

The RFP plate was placed on the magnetic stand at room temperature for 5 minutes. The plate was kept on the magnetic stand. The adhesive seal was removed from the RFP plate and 17 µL of the supernatant (fragmented and primed mRNA) was transferred from each well of the RFP plate to the corresponding well of the new HSP plate (CDP). The thawed First Strand Master Mix tube was centrifuged at 600 g for 5 seconds. 50 µL SuperScript II was added to the First Strand Master Mix tube and mixed gently, but thoroughly, then centrifuged briefly. The First Strand Master Mix tube was labeled to indicate that the SuperScript II had been added. 8 µL First Strand Master Mix and SuperScript II mix was added to each well of the CDP plate. The CDP plate was sealed and mixed thoroughly on a microplate shaker continuously at 1600 rpm for 20 seconds. The sealed CDP plate was placed on the

pre-programmed thermal cycler, and then the 1st Strand program was selected and run.

    a. Choose the pre-heat lid option and set to 100 °C

    b. 25 °C for 10 min

    c. 42 °C for 15 min

    d. 70 °C for 15 min

    e. Hold at 4 °C

2.3.14.4 Synthesis of the second strand cDNA

The thawed Second Strand Master Mix was centrifuged at 600 g for 5 seconds. The adhesive seal was removed from the CDP plate and 25 µL thawed Second Strand Master Mix were added to each well of the CDP plate and mixed thoroughly on a microplate shaker continuously at 1000 rpm for 1 minute. The sealed CDP plate was placed on the pre-heated thermal cycler and incubated at 16°C for 1 hr. The CDP plate was removed from the thermal cycler and placed on the bench. The adhesive seal was removed; the CDP plate was stood to bring it to room temperature. The AMPure XP beads were vortexed and 90 µL well-mixed AMPure XP beads were added to each well of the new MIDI plate (CCP). The entire contents from each well were transferred to the corresponding well of the CCP plate containing AMPure XP beads. The CCP plate was sealed and mixed thoroughly on a microplate shaker continuously at 1800 rpm for 2 minutes. The CCP plate was incubated at room temperature for 15 minutes then centrifuged at 280 g for 1 minute. The adhesive seal was removed from the CCP plate and the CCP plate was placed on the magnetic stand at room temperature for 5 minutes to make sure that all of the beads are bound to the side of the wells. 135 µL of supernatant from each well of the

CCP plate was removed and discarded. With the CCP plate on the magnetic stand, two times EtOH washes were performed, for each time, 200 μL freshly prepared 80% EtOH was added to each well without disturbing the beads, the CCP plate was incubated at room temperature for 30 seconds, and then all of the supernatant from each well was removed and discarded. The CCP plate was stood at room temperature for 15 minutes to dry, and then the plate was removed from the magnetic stand. The thawed, room temperature Resuspension Buffer was centrifuged at 600 g for 5 seconds. 52.5 μL Resuspension Buffer was added to each well of the CCP plate. The CCP plate was sealed and mixed thoroughly on a microplate shaker continuously at 1800 rpm for 2 minutes. The CCP plate was incubated at room temperature for 2 minutes and centrifuged to 280 g for 1 minute. The adhesive seal was removed from the CCP plate. The CCP plate was placed on the magnetic stand at room temperature for 5 minutes. 50 μL supernatant (ds cDNA) was transferred from the CCP plate to the new MIDI plate (IMP).

2.3.14.5 Repair of cDNA ends

10 μL diluted End Repair Control was added to each well of the IMP plate that contains 50 μL ds cDNA. 40 μL End Repair Mix was added to each well of the IMP plate containing the ds cDNA. The IMP plate was sealed and mixed thoroughly on a microplate shaker continuously at 1800 rpm for 2 min. The IMP plate was centrifuged at 280 g for 1 minute. The sealed IMP plate was placed on the pre-heated microheating system and incubated at 30°C for 30 minutes. The IMP plate was removed from the microheating system and placed on ice. The AMPure XP beads were vortexed and 160 μL well-mixed AMPure XP beads were added to each well of the IMP plate containing 100 μL End Repair Mix. The IMP plate was sealed and

mixed thoroughly on a microplate shaker continuously at 1800 rpm for 2 minutes. The IMP plate was incubated at room temperature for 15 minutes. The IMP plate was placed on the magnetic stand at room temperature for 5 minutes or until the liquid was clear. The adhesive seal was removed from the IMP plate and 127.5 µL of supernatant from each well of the IMP plate was removed and discarded. This step was repeated one time. With the IMP plate on the magnetic stand, two times EtOH washes were performed, for each time, 200 µL freshly prepared 80% EtOH was added to each well with a sample without disturbing the beads. The IMP plate was incubated at room temperature for 30 seconds, and then all of the supernatant from each was removed and discarded. The IMP plate was stood at room temperature for 15 minutes to dry, and then the plate was removed from the magnetic stand. 17.5 µL Resuspension Buffer was added to resuspend the dried pellet in each well. The RBP plate was sealed and mixed thoroughly on a microplate shaker continuously at 1800 rpm for 2 minutes. The IMP plate was centrifuged at 280 g for 1 minute. The adhesive seal was removed from the IMP plate and the IMP plate was incubated at room temperature for 2 minutes. The IMP plate was placed on the magnetic stand at room temperature for 5 minutes or until the liquid was clear. 15 µL of supernatant was transferred from each well of the IMP plate to the corresponding well of the new MIDI plate (ALP).

2.3.14.6 Adenylating of 3' ends

2.5 µL Resuspension Buffer was added to each well of the ALP plate. 12.5 µL thawed A-Tailing Mix was added to each well of the ALP plate. The ALP plate was sealed and mixed thoroughly on a microplate shaker continuously at 1800 rpm for 2 minutes. The ALP plate was centrifuged at 280 g for 1 minute. The sealed ALP plate

was placed on the pre-heated microheating system 1 and incubated at 37 °C for 30 minutes. After the 37 °C incubation, The ALP plate was removed from system 1 and plated on the pre-heated microheating system 2 immediately and incubated at 70°C for 5 minutes. The microheating system 1 was set to 30 °C in preparation for Ligate Adapters. The ALP plate was removed from the microheating system 2 and placed on ice for 1 minute. The steps of ligate adapters were proceeded immediately.

2.3.14.7 Ligation of adapters

The thawed RNA Adapter Index tubes, Ligation Control (if using Ligation Control), and Stop Ligation Buffer tubes were centrifuged at 600 g for 5 seconds. The adhesive seal was removed from the ALP plate; 2.5 µL Resuspension Buffer and 2.5 µL Ligation Mix were added to each well of the ALP plate. 2.5 µL thawed RNA Adapter Index was added to each well of the ALP plate. The ALP plate was sealed and mixed thoroughly on a microplate shaker continuously at 1800 rpm for 2 minutes. The ALP plate was centrifuged at 280 g for 1 minute. The sealed ALP plate was placed on the pre-heated microheating system and incubated at 30°C for 10 minutes. The ALP plate was removed from the microheating system and the adhesive seal was removed, 5 µL Stop Ligation Buffer was added to each well of the ALP plate to inactivate the ligation mix. The plate was shaken on a microplate shaker continuously at 1800 rpm for 2 minutes. The ALP plate was centrifuged at 280 g for 1 minute and the adhesive seal was removed from the ALP plate. The AMPure XP beads were vortexed for at least 1 minute or until they were well dispersed. 42 µL mixed AMPure XP beads were added to each well of the ALP plate The ALP plate was sealed and mixed thoroughly on a microplate shaker continuously at 1800 rpm for 2 minutes. The ALP plate was incubated at room temperature for 15 minutes. The ALP plate was

centrifuged at 280 g for 1 minute. The adhesive seal was removed from the ALP plate and the ALP plate was placed on the magnetic stand at room temperature for 5 minutes or until the liquid was clear. 79.5 µL of supernatant was removed and discarded from each well of the ALP plate, the beads should not be disturbed. With the ALP plate on the magnetic stand, two times EtOH washes were performed, for each wash, 200 µL freshly prepared 80% EtOH was added to each well without disturbing the beads. The ALP plate was incubated at room temperature for 30 seconds, and then all of the supernatant from each well was removed and discarded. The beads should not be disturbed. With the ALP plate on the magnetic stand, the samples were air-dried at room temperature for 15 minutes and the ALP plate was removed from the magnetic stand. 52.5 µL Resuspension Buffer was added to each well of the ALP plate. The ALP plate was sealed and mixed thoroughly on a microplate shaker continuously at 1800 rpm for 2 minutes. The ALP plate was incubated at room temperature for 2 minutes and centrifuged at 280 g for 1 minutes. The adhesive seal was removed from the ALP plate and the ALP plate was placed on the magnetic stand at room temperature for 5 minutes or until the liquid was clear. 50 µL of supernatant from each well of the ALP plate was transferred to the corresponding well of the new MIDI plate (CAP). The beads should not be interrupted. The AMPure XP beads were vortexed and 50 µL mixed AMPure XP beads were added to each well of the CAP plate for a second cleanup. The CAP plate was sealed and mixed thoroughly on a microplate shaker continuously at 1800 rpm for 2 minutes. The CAP plate was incubated at room temperature for 15 minutes and centrifuged at 280 g for 1 minute. The adhesive seal was removed from the CAP plate, the CAP plate was placed on the magnetic stand at room temperature for 5 minutes or until the liquid was clear. 95 µL of supernatant from each well of the CAP

plate was removed and discarded. The beads should not be disturbed. With the CAP plate on the magnetic stand, two times EtOH washes were performed, for each wash, 200 µL freshly prepared 80% EtOH was added to each well without disturbing the beads, the CAP plate was incubated at room temperature for 30 seconds, and then all of the supernatant from each well was removed and discarded. The beads should not be disturbed. With the CAP plate on the magnetic stand, the samples were air-dried at room temperature for 15 minutes. The CAP plate was removed from the magnetic stand, 22.5 µL Resuspension Buffer was added to each well of the CAP plate. The plate was sealed and mixed thoroughly on a microplate shaker continuously at 1800 rpm for 2 minutes. The CAP plate was incubated at room temperature for 2 minutes, and then centrifuged at 280 g for 1 minute; the adhesive seal was removed from the CAP plate. The CAP plate was placed on the magnetic stand at room temperature for 5 minutes or until the liquid was clear. 20 µL of supernatant from each well of the CAP plate was transferred to the corresponding well of the new HSP plate (PCR). The beads should not be disturbed.

2.3.14.8 Enrichment of DNA Fragments

5 µL thawed PCR Primer Cocktail and 25 µL thawed PCR Master Mix was added to each well of the PCR plate; the PCR plate was sealed with a Microseal 'A' film. The PCR plate was shaken on a microplate shaker at 1600 rpm for 20 seconds, then centrifuged at 280 g for 1 minute. The sealed PCR plate was placed on the pre-programmed thermal cycler. PCR program was selected and run to amplify the DNA fragments.

a. Choose the pre-heat lid option and set to 100°C

b. 98 °C for 30 s

c. 15 cycles of:

— 98 °C for 10 s

— 60 °C for 30 s

— 72 °C for 30 s

d. 72 °C for 5 min

e Hold at 10 °C

The adhesive seal was removed from the PCR plate. The AMPure XP Beads were vortexed and 50 µL mixed AMPure XP Beads were added to each well of the new MIDI plate labeled (CPP). The entire contents from each well of the PCR plate were transferred to the corresponding well of the CPP plate containing 50 µL mixed AMPure XP Beads. The CPP plate was sealed and mixed thoroughly on a microplate shaker continuously at 1800 rpm for 2 minutes. The CPP plate was incubated at room temperature for 15 minutes then placed on the magnetic stand at room temperature for 5 minutes or until the liquid was clear. The adhesive seal was removed from the CPP plate and 95 µL of supernatant from each well of the CPP plate was discarded. With the CPP plate on the magnetic stand, two times EtOH washes were performed, for each wash, 200 µL freshly prepared 80% EtOH was added to each well without disturbing the beads, the CPP plate was incubated at room temperature for 30 seconds, and then all of the supernatant from each well was removed and discarded. While keeping the CPP plate on the magnetic stand, the samples were air-dried at room temperature for 15 minutes. 32.5 µL Resuspension Buffer was added to resuspend the dried pellet in each well. The CPP plate was sealed and mixed thoroughly on a microplate shaker continuously at 1800 rpm for 2 minutes. The CPP plate was incubated at room temperature for 2 minutes, then the CPP plate was placed on the magnetic stand at room temperature for 5 minutes or

until the liquid was clear. The adhesive seal was removed from the CPP plate and 30 µL of clear supernatant from each well of the CPP plate was transferred to the corresponding well of the new HSP plate (TSP1).

2.3.14.9 Library validation

1 µL of resuspended construct was loaded on an Agilent Technologies 2100 Bioanalyzer using a DNA-specific chip such as the Agilent DNA 1000. The size and purity of the samples were checked. The final product should be a band at approximately 260 bp.

2.3.14.10 Normalization and pooling of libraries

10 µL of sample library from each well of the TSP1 plate was transferred to the corresponding well of the new MIDI plate (DCT plate). The concentration of sample library in each well of the DCT plate to was normalized to 10 nM using 10 mM Tris-HCl, pH 8.5 with 0.1% Tween 20. The DCT plate was sealed and mixed thoroughly on a microplate shaker continuously at 1800 rpm for 2 minutes and centrifuged at 280 g for 1 minute. The adhesive seal was removed from the DCT plate and 10 µL of each normalized sample library was transferred to be pooled from the DCT plate to one well of the new HSP plate (PDP). The total volume in each well of the PDP plate was 10X the number of combined sample libraries, 20 – 240 µL (2 – 24 libraries). The PDP plate was sealed and mixed thoroughly on a microplate shaker continuously at 1800 rpm for 2 minutes. The PDP plate was sealed and stored at -15 °C to -25 °C.

2.3.15 RNA-Seq Experiment and Gene Expression Analysis

Sequencing were performed by the staff of Genome Center of Max Planck Institute for Developmental Biology. RNA-seq reads were aligned to the TAIR10 Col-0 reference genome using Bowtie [192] and BWA [193]. Uniquely mapped reads were counted per representative gene model (excluding introns) according to the TAIR10 annotation using Custom R Scripts. Only genes with reads per kilobase per million >2 in at least two replicates were used for differential expression analysis using EdgeR [194, 195]. This package internally estimates size factors for each sample, calculates dispersion for each gene, and then fits a negative binomial GLM to detect differentially expressed genes taking into account the size factors and dispersion values.

2.4 Statistical analysis

Data sets were analyzed using Microsoft Office Excel or JMP® 12.2.0. The data represent the average of 3 or more replicates with ± SD of the mean. Comparisons between two groups were made using Student's t test. Comparisons between multiple groups were made using one-way or two-way ANOVA tests depending whether one or two different variables were considered, respectively.

3. Results

3.1 Comparative analyses of responses upon different MAMP treatments

Many studies have shown that after pathogen infection or MAMP perception, signaling events such as MAPK activation, ROS burst, and ethylene production are triggered. Defense genes are expressed in response to the threatening pathogen. However, whether different receptor-types lead to the same signaling events and the same immune responses still needs to be investigated. We compared the immune responses mediated by three distinct types of MTI receptors. We treated Arabidopsis Col-0 with different MAMPs: flg22, nlp20 and chitin (C6). Flg22 is perceived by the LRR-RK *At*FLS2; nlp20 is perceived by the LRR-RP RLP23; and C6 is perceived by the LyM-RKs *At*CERK1 and *At*LYK5 [138, 140, 196]. From comprehensively comparing responses which are downstream of these MAMP-receptor pairs, we aimed to clarify the proposed identity of early signaling events and downstream outputs.

3.1.1 ROS burst and MAPK activation showed differences in early responses to MAMPs

The rapid generation of ROS is induced early during pathogen invasion or elicitor treatment [197]. Research studies have shown that flg22, nlp20 and chitin can induce ROS burst in Arabidopsis Col-0 [42, 85, 156]. However, the data cannot be directly compared due to variations in the plant conditions and experimental designs. Research has shown that variances in growing conditions and handling of plants may

affect phenotypes and physiological responses [173]. To determine whether MAMP perception via different receptor-types induces different ROS burst responses, we treated Col-0 leaves with flg22, nlp20 or C6 in parallel. ROS generation following MAMP treatment was monitored over one hour using a luminol-based assay. All three elicitors triggered ROS burst (Figure 3-1). However, the flg22 triggered ROS burst was more than 10 fold higher than the nlp20-triggered ROS burst in maximum value. The magnitude of ROS burst remained the same when we used 0.1 µM or 1 µM flg22/nlp20 (data not shown). 1 µM C6 only induced slight increase of ROS (data not shown). However, the ROS response to 10 µM C6 was comparable to the response to 1 µM flg22. Compared with chitin heptamer (C7) and chitin octamer (C8), C6 has lower affinity to CERK1 [198]. Perhaps, these larger oligomers might be more potent inducers of ROS.

It is interesting to note that the ROS responses to nlp20, flg22 and chitin differ not only in the magnitude of the response, but also in the timing. For flg22 treatment, ROS production was observed in 2 minutes and peaked within 12 minutes before quickly decreasing. There was an obvious delay of ROS burst when Col-0 leaves were treated with nlp20 as compared to flg22. ROS production began to increase after 4 minutes and reached a peak within 20 minutes. ROS accumulated rapidly upon C6 treatment, but it took 20 minutes to reach the peak and the response decreased slowly.

The MAPK cascades represent one of the most important signal transduction systems in eukaryotes. Several MAPK cascades were shown to be associated with the induction of plant defense responses [199]. Like ROS burst, MAPK phosphorylation is an early signaling event in MTI. However, ROS production and MAPK activation lead to different downstream responses.

Col-0 leaves were infiltrated with different concentrations of elicitors and harvested at different time points. MAPK phosphorylation was observed in samples treated with flg22 and C6 after 5 minutes (Figure 3-2A), and the signals were strong up to 10 minutes (Figure 3-2B). In contrast, MAPK phosphorylation triggered by nlp20 was first observed after 10 minutes (Figure 3-2B) and did not get stronger afterward (Figure 3-2C). Higher concentration of MAMPs triggered stronger MAPK phosphorylation; but, in general, MAPK phosphorylation triggered by nlp20 was slower and weaker than phosphorylation triggered by the other two elicitors. All phosphorylation signals decreased within 30 minutes (Figure 3-2D).

The results of ROS burst and MAPK phosphorylation showed that the early signaling events triggered by nlp20 are slow and weak relative to flg22 and chitin.
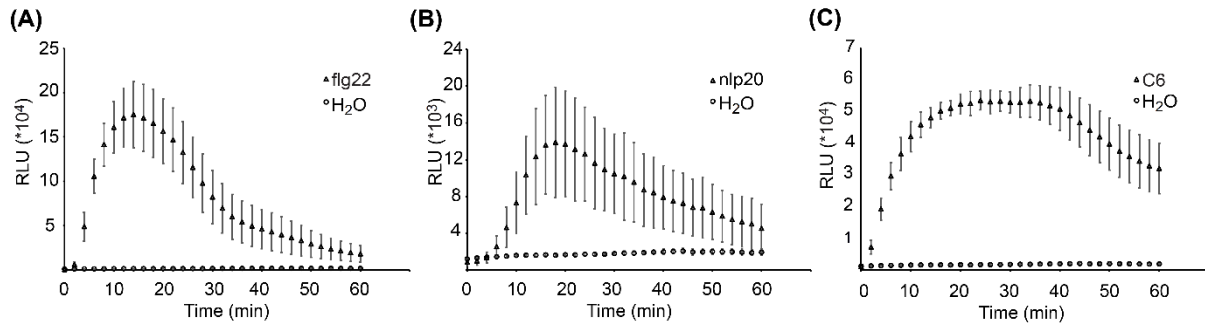
Figure 3-1. ROS burst triggered by different elicitors. 5-week-old *Arabidopsis thaliana* Col-0 leaf discs were treated with 0.5 µM flg22 (A), 0.5 µM nlp20 (B) or 10 µM C6 (C) and ROS production was monitored over time. Bars present means ±s.d. (n≥6). The experiments were performed three times with similar results.
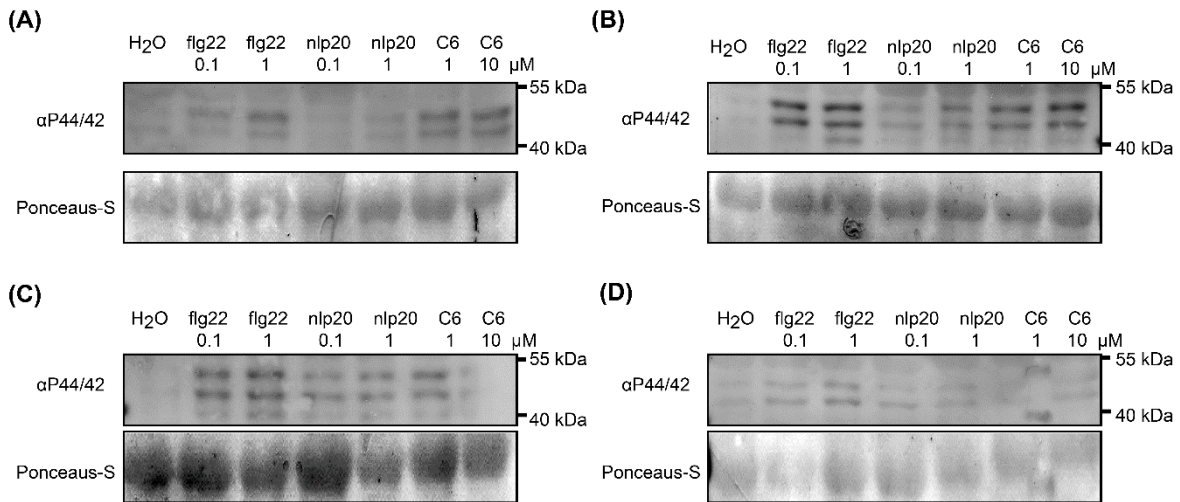
Figure 3-2. MAPK-immunoblot after elicitor treatment. 5-week-old *Arabidopsis thaliana* Col-0 leaves were infiltrated with flg22 (0.1 µM, 1 µM), nlp20 (0.1 µM, 1 µM), C6 (1 µM, 10 µM) or H_2O and harvested in 5 minutes (A), 10 minutes (B), 20 minutes (C) and 30 minutes (D). The activation of the MAPKs was visualized by Western blot with a phospho-p44/42 MAP kinase antibody. Ponceau S staining of the membrane served as a loading control. The experiments were performed three times with similar results.

3.1.2 Hormones participate in MAMP signaling

To further investigate whether the patterns we observed in MAPK phosphorylation and ROS burst influence the subsequent responses, we monitored production of the phytohormones ethylene (ET) and salicylic acid (SA). SA and ET are important regulators of defense gene expression [200]. ET and jasmonic acid (JA) are usually associated with defense against necrotrophic pathogens and herbivorous insects. ET production was observed in Arabidopsis Col-0 leaf discs treated with flg22, nlp20 and C6 (Figure 3-3A). C6 triggered only a small amount of ET production. The accumulation of ET increased significantly with C6 concentration but not with incubation time. In contrast, flg22-triggered ethylene accumulation increased with time, but the difference between 0.5 µM and 1 µM flg22 treatment was not significant. It is possible that the response to flg22 was saturated at 0.5 µM and therefore higher concentration of flg22 does not significantly increase ET formation. ET production induced by nlp20 was highly dose dependent. With increasing of nlp20 concentration, leaf pieces produced more ethylene. ET accumulation after 3 hours and after 6 hours was similar when leaves were treated with 0.1 µM or 0.5 µM nlp20. However, leaves treated with 1 µM nlp20 continued to accumulate ET after 3 hours of treatment. In addition, at high concentrations nlp20 induced high levels of ET which cannot be reached by flg22 treatment.

SA is generally involved in the activation of defense responses against biotrophic and hemi-biotrophic pathogens, and it is required for the establishment of systemic acquired resistance (SAR) [201]. Previous studies have shown that flg22 triggers SA accumulation [202]. We treated 6-week-old Arabidopsis Col-0 leaves with elicitors by infiltration. In our study, flg22-induced SA accumulation can be detected

after 24-hour treatment, but there was no significant increase of SA after 48 hours. Salicylic acid accumulation can be induced significantly by nlp20 (Figure 3-3B). With 1 µM nlp20 treatment, SA constitutively accumulated; more SA was measured after 48 hours than 24 hours. SA accumulation can also be induced by 0.1 µM nlp20. C6 did not cause SA production.

From measuring ET and SA, more differences were found between signaling events following different receptor-types. Both flg22 and nlp20 induced ET and SA production. However, in high concentrations, flg22 was not able to induce such high levels of ET and SA as nlp20. Moreover, SA accumulation persisted in nlp20-treated Col-0, up to 48 hours, but SA accumulation induced by flg22 had been scavenged in 48 hours. C6 induced a low amount of ET production but it did not cause SA production.

(A)

(B)
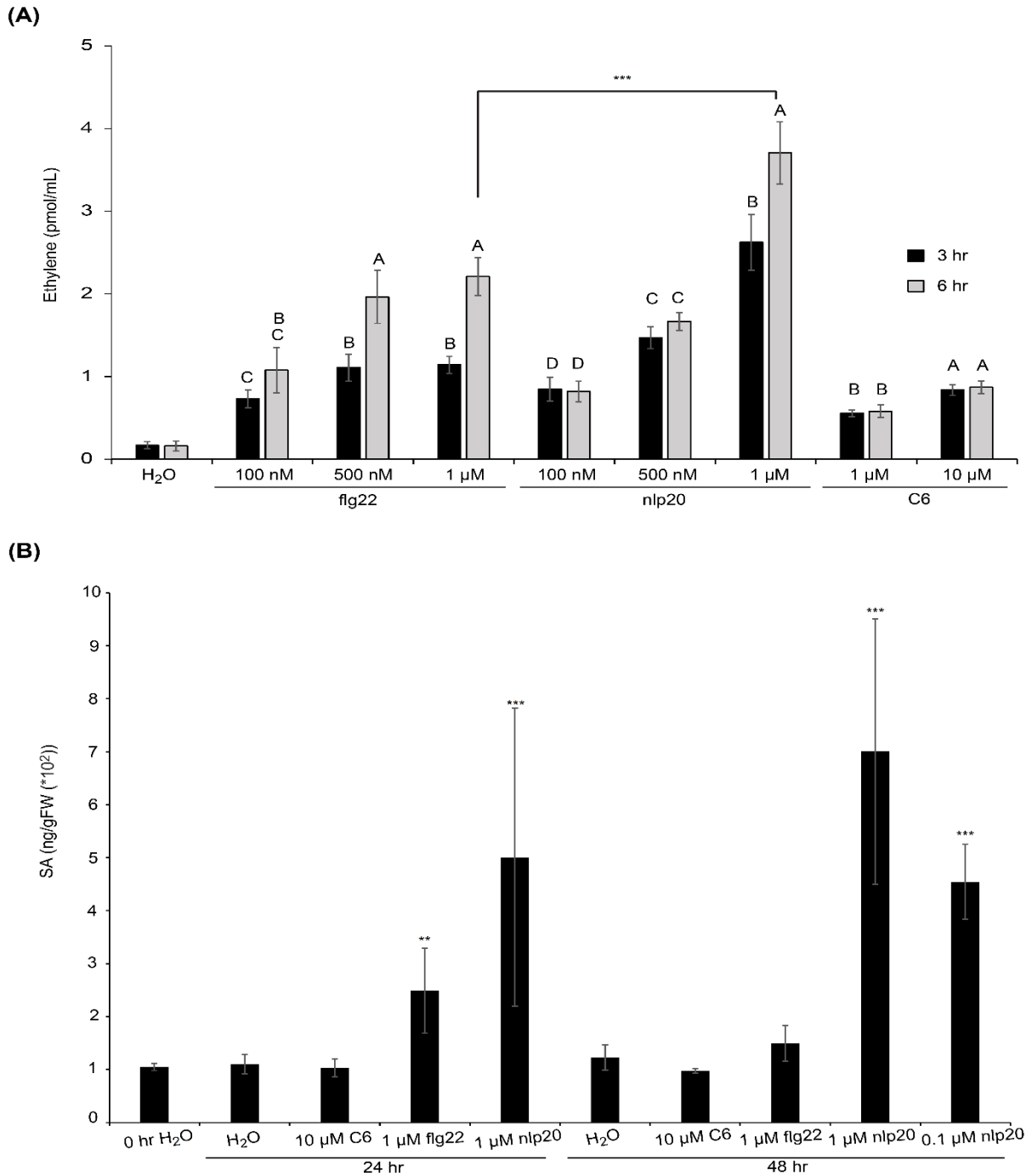
Figure 3-3. Hormone accumulation in response to different elicitors. Ethylene accumulation after treatment of flg22 (0.1 µM, 500nM, 1 µM), nlp20 (0.1 µM, 500nM, 1 µM), C6 (1 µM, 10 µM) and H_2O for 3 hours and 6 hours. Bars present means ±s.d. of replicates (n≥4). Within one elicitor, different letter means significant difference ($P<0.001$) (A). SA accumulation after 24 hours and 48 hours of treatment of 1 µM flg22, 1 µM nlp20 (also 0.1 µM after 48 hours), 10 µM C6 or H_2O. Bars present means ±s.d. of 4 replicates. Asterisks mark significant differences relative to H_2O control treatment as determined by Student's t test (** $P<0.01$, *** $P<0.001$) (B).

3.1.3 RNA-seq to compare MAMP-triggered transcriptome reprogramming

Transcriptional reprogramming determines the strategy for plants facing pathogen infection. A comprehensive comparison of transcriptome changes upon MAMP-treatment may give us an insight into the different responses to different MAMPs. We applied RNA-seq, a powerful tool to analyze transcriptome changes, to monitor the differential response of Arabidopsis seedlings to nlp20, flg22, and C6. Col-0 seedlings were treated with H_2O, 10 µM C6, 0.5 µM nlp20 and 0.5 µM flg22, concentrations which were high enough to trigger immune responses in our previous experiments. We did not use higher concentrations because we wanted to avoid unpredicted side effects. The time points were chosen as 1, 6, and 24 hours to cover early and late responses; one sample was collected before treatment. Thus, a total of 13 samples were processed for each replicate, and four biological replicates were used for cDNA library generation. After sequencing and quality check, 48 cDNA libraries had reads of more than 10 Mb and were suitable for further analyses. For every experimental condition, at least three libraries were available. Reads were mapped to the reference genome, *Arabidopsis thaliana* TAIR10, for corresponding tags. After mapping, 35541 unique tags were found in our dataset. Tags which were not presented in at least two libraries with an expression cut off of 2 counts per million were filtered out. After filtering, the dataset was reduced to 22842 tags. Genes differentially expressed (false discovery rate [FDR] ≤0.01 and fold change ≥2) were defined using the edgeR software package [194]. Gene expression analyses were done only between elicitor and mock treatments at the same time point to avoid temporal effects.

After treatment for 1 hour, flg22 caused dramatic transcriptome changes. A great number of transcripts increased (3130) or decreased (2031) (Figure 3-4A, 3-4B). Nlp20 and C6 caused large numbers (1514 and 1833, respectively) of increased transcripts but, unlike flg22, few decreased transcripts (159 and 365, respectively) (Figure 3-4A, 3-4B). 97% (1631/1673) and 91% (2005/2198) of transcripts which changed after nlp20 and C6 treatment, respectively, were also changed by flg22. A group of transcripts (1221) was induced by all three MAMPs (Figure 3-4A. 3-4B).

After a 6-hour treatment with C6, only 2 genes showed differential expression (Figure 3-4C). One of them is AT2G15220, a member of the plant basic secretory protein (BSP) family, which is involved in plant defense. AT2G15220 was up-regulated in all MAMP-treated samples at 1 and 6 hours. In contrast to C6, flg22 and nlp20 showed extensive transcriptional changes after 6 hours, similar to the 1 hour time point (2883 increased, 2791 decreased for flg22; 1300 increased, 157 decreased for nlp20). 91% of the transcripts (1324/1457) which were up- or down-regulated by nlp20 were similarly regulated by flg22 (Figure 3-4C. 3-4D). After 24-hour treatment, only a few genes showed expressional change in response to any MAMP (Figure 3-4E. 3-4F).

Considering that C6 caused no transcriptome reprogramming after 6 hours and the similar PRR complex of LRR-RP and LRR-RK, we focused on transcripts that were influenced by flg22 or nlp20 treatment. Singular Enrichment Analysis was performed by agriGO [203] to identify the enrichment of Gene Ontology (GO) terms. All the GO terms mentioned here have false discovery rate [FDR] ≤0.01, and complete table of GO terms is provided in the supplementary file. There were 1442 transcripts up-regulated by both flg22 and nlp20 after 1-hour treatment, the largest portion of them were reported to response to stimulus (391/4057, number in

input/number in background) including innate immune response (81/347). Early response transcripts, such as transcripts participating in ET mediated signal transduction, were up-regulated only in 1 hour (11/74). In contrast, late response transcripts, for example transcripts related to SAR, were only induced in 6 hours (7/54). The transcripts specifically up-regulated by flg22 in 1 hour were diverse; for example, some of them related to regulation of signal transduction (16/128), stimulus response (176/4057), or phosphate metabolic process (53/1178).

Many transcripts related to metabolic processes were regulated after MAMP treatment, especially flg22 treatment. For instance, transcripts which play roles in regulation of metabolic processes were up-regulated 1 hour after flg22 treatment (136/2210). After 6 hours, many transcripts participating in cellular metabolic processes were down-regulated in flg22-treated samples (640/8742, FDR=0.015). Certain types of metabolic processes had transcripts down-regulated by flg22 and nlp20, like starch metabolic process (10/41) and cellular glucan metabolic process (10/87).

Table 3.1 shows some GO terms of up-regulated transcripts; "number in input/number in background" is shown as percentages. For example, around 60% of the genes with GO term "callose deposition in cell wall during defense response" were up-regulated by flg22 and nlp20 after 1 hour and 6 hour treatment. A group of immune response genes only responded to flg22. The up-regulation of ROS response genes after 6-hour nlp20 treatment but not flg22-treatment indicates that the oxidative status may be different between long-term flg22 and nlp20 treatment.

No GO term was identified for the small groups of transcripts which specifically respond to nlp20. However, there are some transcripts worth notice. AT1G33960, also known as *AVRRPT2-INDUCED GENE 1 (AIG1)*, was up-regulated 1 hour and 6

hours after nlp20 treatment, but not flg22 treatment. Another transcript increased in both time points was AT3G44830, encoding a lecithin:cholesterol acyltransferase family protein.

The small number of transcripts regulated after 24 hours of treatment also has candidates directly relating to immune response. AT2G26010 encodes PLANT DEFENSIN 1.3 (PDF1.3); it was up-regulated after 6 hour flg22 and nlp20 treatment and remains highly expressed after 24 hours of flg22 treatment. It is not proper to take all these transcripts as background noise, but some expressional changes may cause no physiological difference.

The RNA-seq results indicate that a core set of defense-related genes can be activated through perception of different MAMPs. However, there are also notable differences in the transcriptional changes in response to the various elicitors; flg22 causes broader transcriptome changes than nlp20 and C6, and C6 does not cause late transcriptome changes.
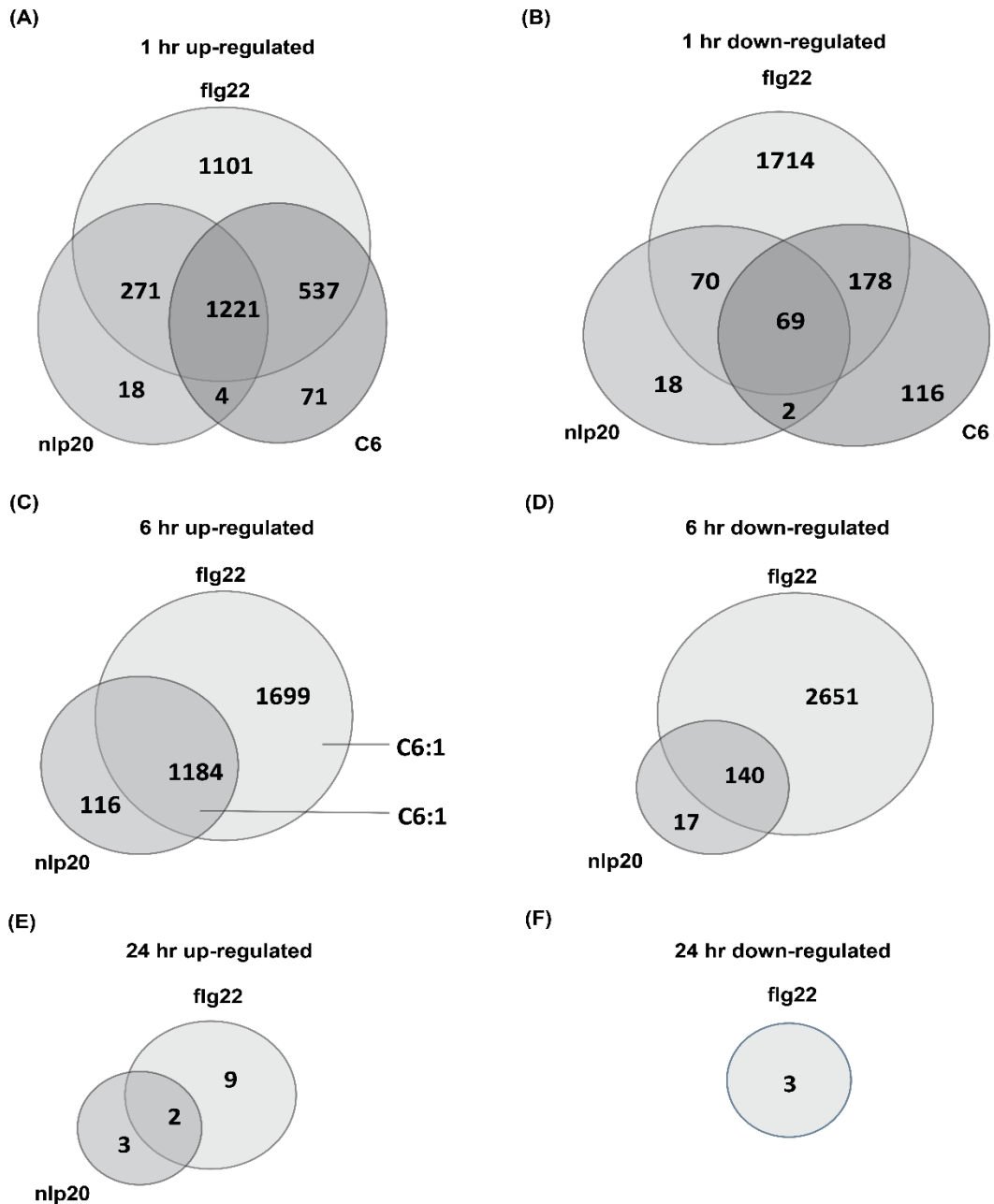
Figure 3-4. Genes differentially expressed between elicitors and mock treatment. 10-day-old Arabidopsis Col-0 seedlings were treated with H_2O, 10 µM C6, 0.5 µM nlp20 and 0.5 µM flg22. Up-regulated transcripts in 1 hour (A). Down-regulated transcripts in 1 hour (B). Up-regulated transcripts in 6 hours (C) down-regulated transcripts in 6 hours (D). Up-regulated transcripts in 24 hours (E). Down-regulated transcripts in 24 hours (F). False discovery rate [FDR] ≤0.01 and fold change≥2.

GO term	1 hr flg22	1hr flg22, nlp20	6 hr flg22	6 hr flg22, nlp20	6 hr nlp20
defense response	8.5%	19.2%	10.8%	15.5%	-
immune response	9%	23.4%	13.1%	16.1%	-
regulation of signal transduction	15.6%	-	11.7%	-	-
response to salicylic acid stimulus	-	11.5%	-	13.5%	-
response to ethylene stimulus	-	11.6%	-	10.1%	-
response to jasmonic acid stimulus	-	11.6%	-	12.6%	-
salicylic acid mediated signaling pathway	-	17.8%	-	13.3%	-
response to reactive oxygen species	-	14%	-	-	10.6%
systemic acquired resistance	-	-	-	13%	-
cellular catabolic process	-	-	11.1%	5.1%	-
protein modification process	8.4%	10.1%	8.5%	6.2%	-
callose deposition in cell wall during defense response	-	58.9%	-	64.7%	-

Table 3-1. Selected GO terms of up-regulated transcripts. The percentages indicate the number up-regulated genes with the GO term that were identified in the sample relative to the total number of genes with the GO term. No percentage shown indicates the false discovery rate [FDR] >0.01.

3.1.4 Late defense responses of MAMPs signaling

One of the last steps of defense responses is production of chemical compounds which deter pathogens. Here we checked callose deposition and camalexin production, two well-known plant defense mechanisms [204, 205]. Callose is a (1,3)-glucan cell wall polymer with some (1,6)-branches. Upon pathogen attack, callose is deposited between the plasma membrane and the pre-existing cell wall at sites of pathogen attack [206]. Camalexin (3-thiazol-2'-yl-indole) is an indole alkaloid phytoalexin which is toxic, and it is synthesized upon pathogen infection [205]. Both flg22 and nlp20 caused callose deposition (Figure 3-5B), but only nlp20 caused camalexin accumulation (Figure 3-5A). C6 was not able to trigger synthesis of callose or camalexin. As with the accumulation of SA, the accumulation of camalexin triggered by nlp20 also increased with time and with elicitor concentration (Figure 3-5A).

The cytochrome P450 enzyme CYP71B15 (PHYTOALEXIN DEFICIENT 3, PAD3) specifically participates in the camalexin biosynthesis pathway [207]. In our RNA-seq data, *PAD3* was induced by flg22 and C6 and increased 4-8 fold, but nlp20 treatment caused a 16-fold increase in 1 hour and more than 128-fold in 6 hours. This result is consistent with the high amount of camalexin accumulation observed in nlp20-treated Col-0. Increased expression of *PAD3* induced by flg22 and C6 did not result in a significant increase of camalexin.

Arabidopsis produces callose in response to flg22 perception, but produces both callose and camalexin in response to nlp20 perception. This finding further indicates that different immune receptors lead to distinct immune outputs, which could allow for varied responses when facing particular pathogen threats.

(A)

(B)
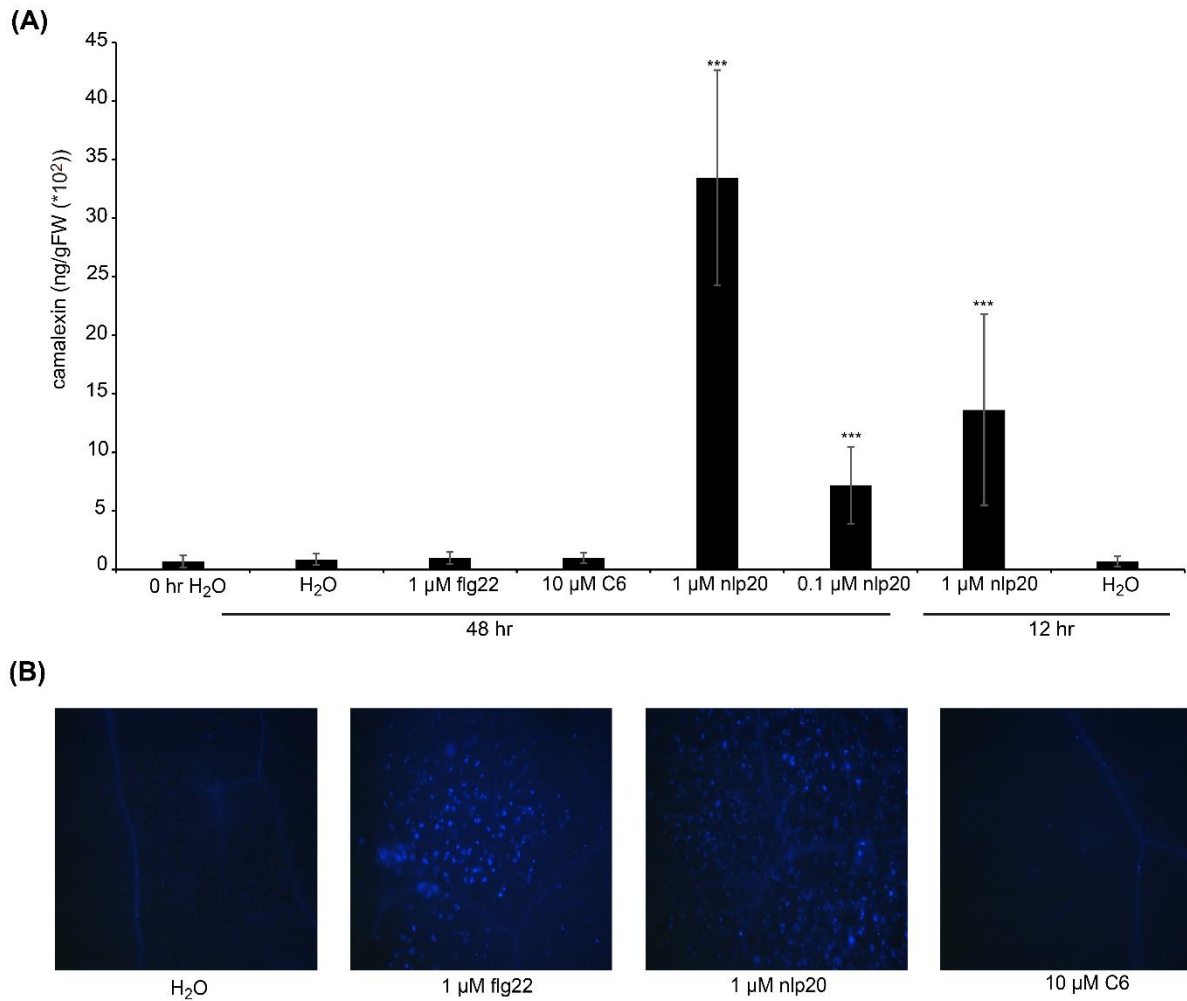
Figure 3-5. Effect of MAMPs on camalexin levels and callose deposition. Camalexin levels were measured in Col-0 leaves infiltrated with 1 µM flg22, 1 µM nlp20 (also 0.1 µM for 48 hours), 10 µM C6 or H_2O and harvested for 12 and 48 hours (A). FW = Fresh weight, bars present means ±s.d. of 4 replicates. Asterisks mark significant differences to H_2O control treatment as determined by Student's t test (** $P<0.01$, *** $P<0.001$). Microscopic representations of callose deposition by aniline blue staining (B). Col-0 leaves were infiltrated with 0.5 µM flg22, 0.5 µM nlp20, 10 µM C6 or H_2O for 16 hours. 10-times magnified leaf tissue under UV light are shown. The blue dots indicate callose deposition.

3.2 Screening for regulators of LRR-RK and LRR-RP signaling

LRR-RP constitutively associates with SOBIR1 or SOBIR1-like LRR-RKs to form a bimolecular equivalent of an authentic receptor kinase in a ligand-independent manner [36]. It seems that the signals from different LRR-RK and LRR-RP converge to SERKs as both LRR-RK and LRR-RP require SERKs to transduce signals after ligand perception [208]. However, the differential responses to nlp20 and flg22 described above suggest that these two classes of receptors have different signaling pathways or regulatory mechanisms. We applied luminol-based ROS burst assay to screen mutant lines to identify genes that have differential roles in response to flg22 and nlp20.

3.2.1 BAK1 participates in nlp20-triggered ROS burst

Previous studies have shown that the co-receptor BAK1 interacts with FLS2 and RLP23 in a stimulus-dependent manner [37, 42]. ROS assays were performed using BAK1 mutants, *bak1-4* and *bak1-5*, and with complementation lines with or without site-specific substitutions in phosphorylation sites. Site-specific substitution lines were *bak1-4/BAK1_Y403F*, *bak1-4/BAK1_S602/3/4_AAA* and *bak1-4/BAK1_S612A*. After flg22 treatment, both *bak1-4* and *bak1-5* showed significant reduction of ROS burst compared with Col-0. Furthermore, reduced ROS burst in site-specific substitution variants indicated that BAK1^{Y403F}, BAK1$^{S602/3/4\_AAA}$ and BAK1^{S612A} are not functional in flg22-induced signaling. On the other hand, ROS burst induced by nlp20 was not affected in *bak1-4*, but the point mutation line *bak1-5,* and all the complementation lines with replaced phosphorylation sites showed less

ROS production. This result indicates that BAK1 is crucial for FLS2 complex, but for RLP23-SOBIR1 complex, BAK1 plays a less important role. Other SERKs with functional redundancy may maintain the signaling pathway when BAK1 is absent, and the presence of BAK1^{Y403F}, BAK1$^{S602/3/4AAA}$ and BAK1^{S612A} interferes with signal transduction following RLP23-SOBIR1 complex, and mutated BAK1 has reduced ability to transduce signal from FLS2 and RLP23-SOBIR1 complex.
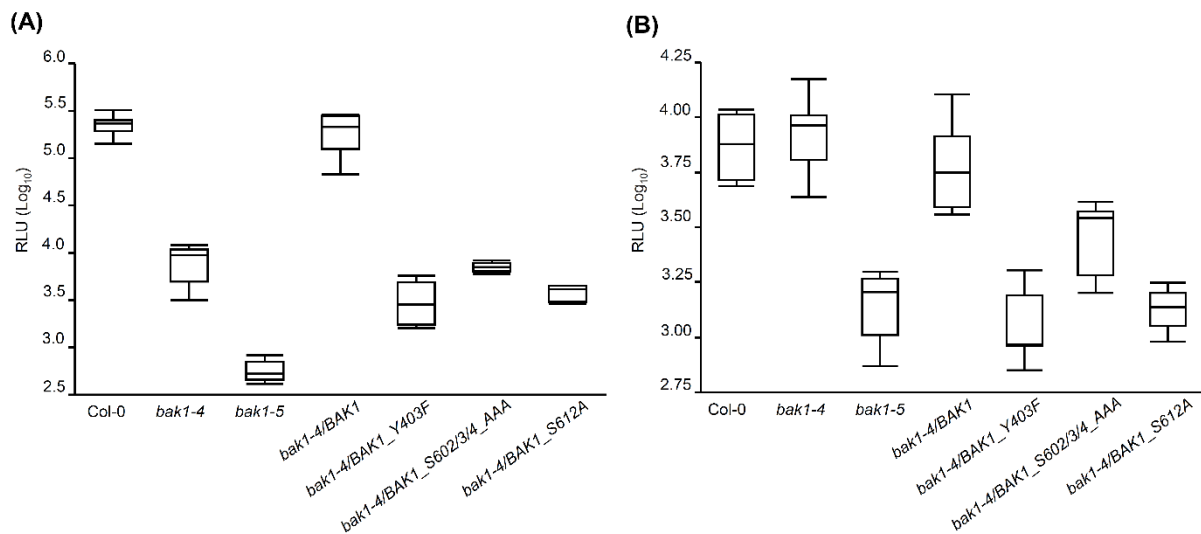
Figure 3-6. ROS burst of different BAK1 mutant lines triggered by flg22 or nlp20. Leaf discs of Col-0, *bak1-4*, *bak1-5*, bak1-4/BAK1, *bak1-4/BAK1_Y403F, bak1-4/BAK1_S602/3/4_AAA* and *bak1-4/BAK1_S612A* were treated with 0.5 μM flg22 (A) or 0.5 μM nlp20 (B). Boxplots are shown with median and quartiles of peak value minus background value, H$_2$O-treated samples had no peak value, therefore they are not in the figures. Bars represent mean min-max ranges (n≥6). The experiments were performed three times with similar results.

3.2.2 Some negative regulators in flg22 signaling also participate in nlp20 signaling

Immune responses in plants are strictly controlled because excessive or untimely activation of immune responses negatively influence plant development. Different strategies are applied to control the amplitude and duration of MTI. In Arabidopsis, many proteins have been found negatively regulating immune responses triggered by flg22. We wanted to know whether these proteins also play roles in regulating nlp20-triggered immune responses.

BIR2 is a pseudokinase regulating PRR complex formation. BIR2 interacts constitutively with BAK1, thereby preventing interaction with FLS2. [84]. As BAK1 is also involved in nlp20-induced immunity, we tested whether BIR2 is also a negative regulator for nlp20-induced immunity. Artificial microRNA (amiRNA) line amiR-*BIR2-1* and T-DNA insertion line *bir2-1* were treated with nlp20, and ROS production was monitored. Both amiR-*BIR2-1* and *bir2-1* showed significantly higher ROS burst than Col-0 wild type (WT) after nlp20 treatment. The ROS peak was 10-fold higher and reached the level of flg22-induced ROS burst (Figure 3-7A). This result fits the model that BIR2 regulates MAMP-triggered immunity by controlling BAK1 complex formation.

The phosphorylation status of PRR complexes must be kept under controlled because improper phosphorylation may lead to unintended signaling. Phosphatase like PP2A modulates signaling amplitude and fine-tunes immune responses by dephosphorylating PRR complex [87]. PP2A constitutively associates with and negatively regulates BAK1 activity. ROS production in response to flg22 in specific PP2A subunit A1 and C4 mutant lines, *pp2a-a1* and *pp2a-c4*, was higher than Col-0

WT [87]. After treating with nlp20, higher ROS production was also observed in *pp2a-a1* and *pp2a-c4* (Figure 3-7B), indicating that PP2A regulates BAK1 phosphorylation status not only in LRR-RK PRR complexes but also in LRR-RP PRR complexes.

Proteasomal degradation is an effective way to control the levels of signaling components in the cell. Selected proteins are marked by E3 ubiquitin ligase for degradation. This mechanism modulates immune signaling in both animals and plants [209, 210]. CALCIUM-DEPENDENT PROTEIN KINASE 28 (CPK28) facilitates BIK turnover and negatively regulates BIK1-mediated immune responses triggered by MAMPs like flg22 [178]. T-DNA insertion line *cpk28-1* produced significantly more ROS than Col-0 after flg22 treatment, whereas CPK28-OE showed reduced ROS burst [178]. In our study, *cpk28-1* also had a significantly higher ROS peak compared with Col-0 after nlp20 treatment (Figure 3-7C). It is likely that CPK28 regulates BIK1 in nlp20-triggered signaling.

A hetero trimeric G protein complex comprising EXTRA-LARGE GUANINE NUCLEOTIDE-BINDING PROTEIN 2 (XLG2), GUANINE NUCLEOTIDE-BINDING PROTEIN SUBUNIT-β (AGB1) and GUANINE NUCLEOTIDE-BINDING PROTEIN SUBUNIT-γ1 (AGG1) or AGG2 was shown to attenuate BIK1 proteasomal degradation and thereby modulate MTI activation [183]. In ROS assays, mutant lines for genes encoding these proteins showed similar response to flg22 and nlp20 treatment; no consistent results in *xlg2*, significant reduction of ROS burst in *agb1-2* and minor reduction in *agg1 agg2* (Figure 3-8). The results indicate that the regulation by G proteins also influences nlp20-triggerd ROS burst.

In conclusion, the negative regulatory mechanisms governing BAK1 and BIK1 function are similar for both LRR-RP and LRR-RK PRR complexes. BIR2, CPK28,

PP2A-A1, PP2A-C4 and G proteins are not the key regulator(s) for the differences observed for RK and RP signaling.
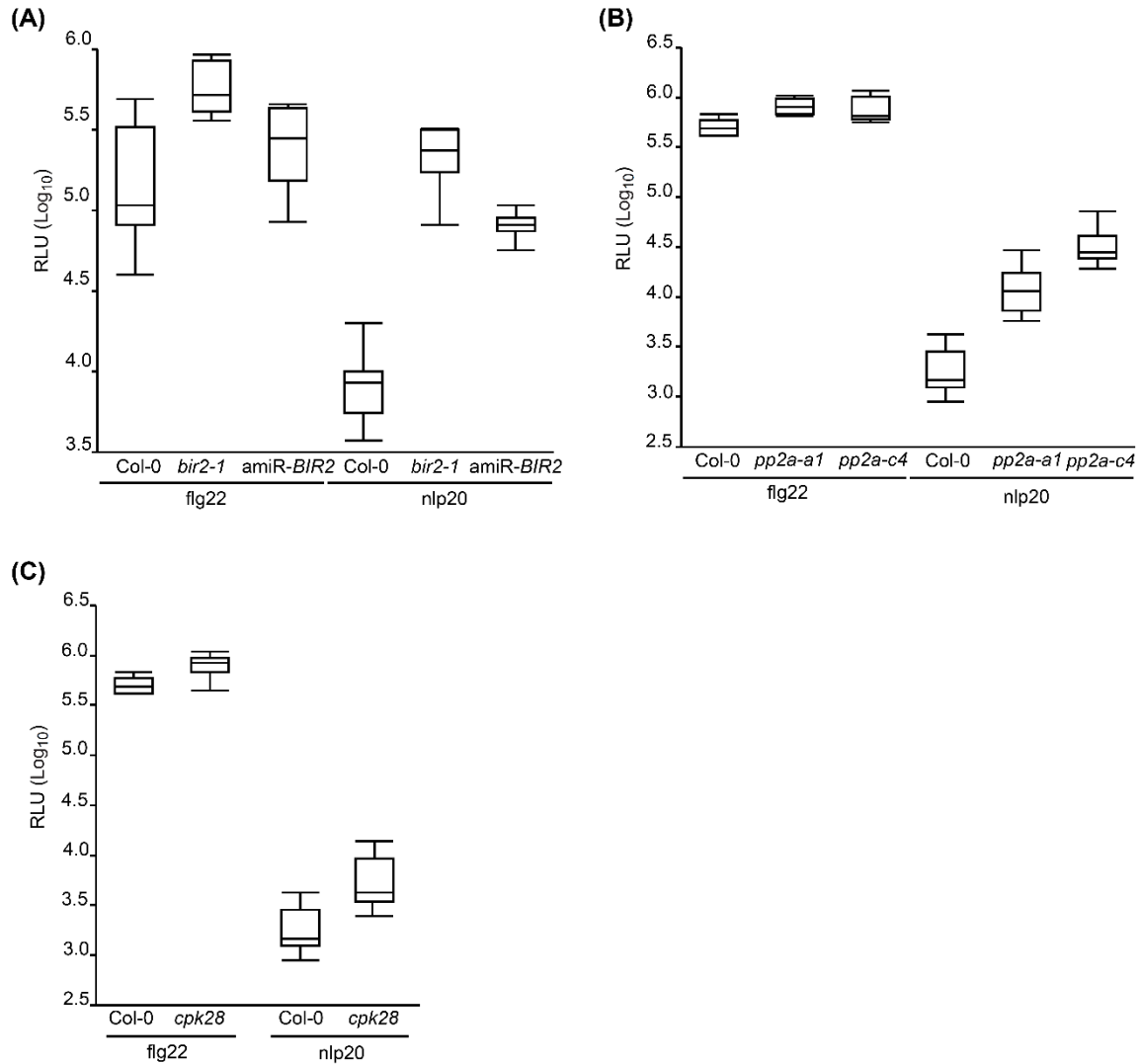
Figure 3-7. ROS burst of different regulator mutants triggered by flg22 or nlp20. Leaf discs of Col-0, *bir2-1* and amiR-*BIR2-1,* were treated with 0.5 µM flg22 or 0.5 µM nlp20 (A). Leaf discs of Col-0, *pp2a-a1* and *pp2a-c4,* were treated with 0.5 µM flg22 or 0.5 µM nlp20 (B). Leaf discs of Col-0 and *cpk28* were treated with 0.5 µM flg22 or 0.5 µM nlp20 (C). Boxplots are shown with median and quartiles of peak value minus background value, H_2O-treated samples had no peak value, therefore they are not in the figures. Bars represent mean min-max range. (n≥6). The experiments were performed three times with similar results.
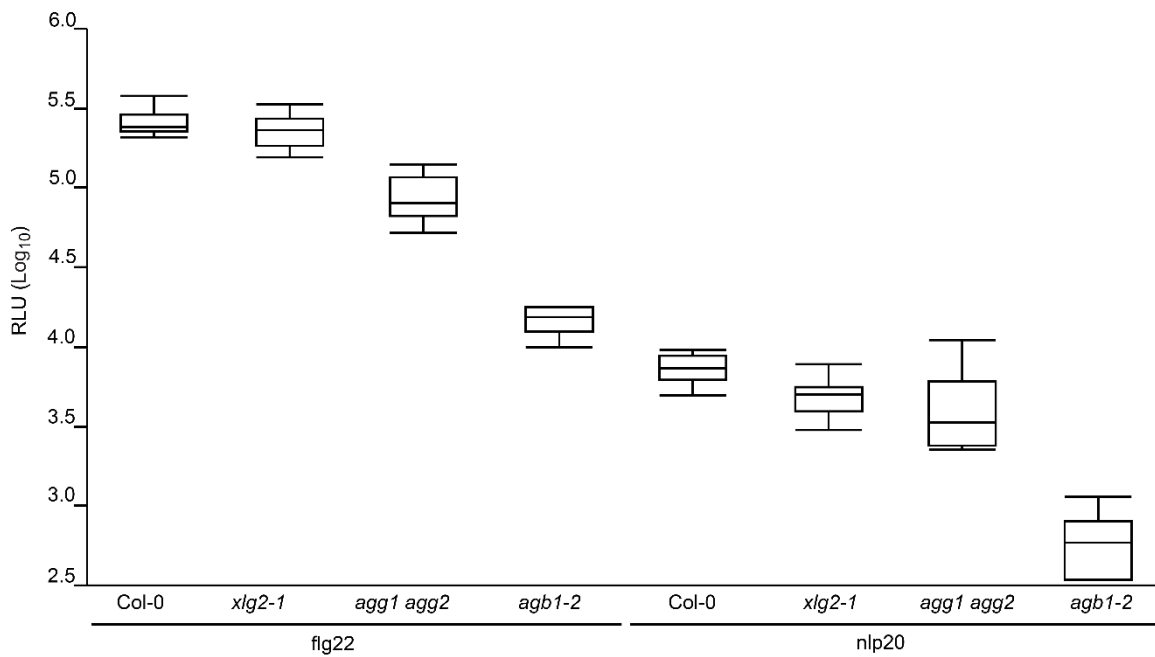
Figure 3-8. ROS burst of different G protein mutants triggered by flg22 or nlp20. Leaf discs of Col-0, *xlg2-1, agg1 agg2 and agb1-2* were treated with 0.5 μM flg22 or 0.5 μM nlp20. Boxplots are shown with median and quartiles of peak value minus background value, H_2O-treated samples had no peak value, therefore they are not in the figures. Bars represent mean min-max range (n≥6). The experiments were performed three times with similar results.

3.2.3 BIK1, PBL2 and PBL28 are candidate key regulators differentiating LRR-RP and LRR-RK signaling

The Arabidopsis genome encodes over 160 RLCKs [211], some of which have been proven to participate in immune response activation [212]. A tree based on protein sequence was constructed using the neighbor-joining method (Figure 3-9). In collaboration with Prof. Jian-Min Zhou's lab, we obtained and screened 37 *pbl* single mutant lines for ROS burst following nlp20 and flg22 treatment. For most of the mutants, significant differences were not observed or consistent results could not be obtained. Even for higher-order mutant lines *pbs1 pbl5 pbl7 pbl27*, *pbl31 pbl32*, and *pcrk1-2 pcrk2-1*, there was no significant difference in ROS burst after flg22 or nlp20 treatment (Figure 3-10 C). Two candidates, *pbl2* and *pbl28*, showed higher ROS burst after nlp20 treatment but not after flg22 treatment (Figure 3-10 A, B). PBL2 is a substrate of the AvrPphB protease, and it interacts with FLS2 in the absence of flg22 [49]. PBL28 has less homology to other PBL proteins, and its function is unknown.

BIK1 is the best-studied example in Arabidopsis RLCK subfamily VII. BIK1 associates with FLS2 and is likely to associate with BAK1 under resting state conditions [50]. Upon flg22 elicitation, BAK1 associates with FLS2 and phosphorylates BIK1. BIK1 phosphorylates both BAK1 and FLS2 and then dissociates from the PRR complex to activate downstream signaling components [49, 203]. Mutants lacking BIK1, or BIK1 and its homolog PBL1, display reduced ROS burst when treated with flg22. To our surprise, nlp20-treated *bik1* and *bik1pbl1* showed significantly higher ROS burst than Col-0 (Figure 3-11A), which indicates that BIK1 may function as a negative regulator in the signaling pathway following RLP23-SOBIR1 complex. The results of our *pbl* mutant screening suggest that, BIK1, PBL2

and PBL28 might be key determinants in the differential defense responses triggered by flg22 and nlp20.

Figure 3-9. Homology analysis of PBL family
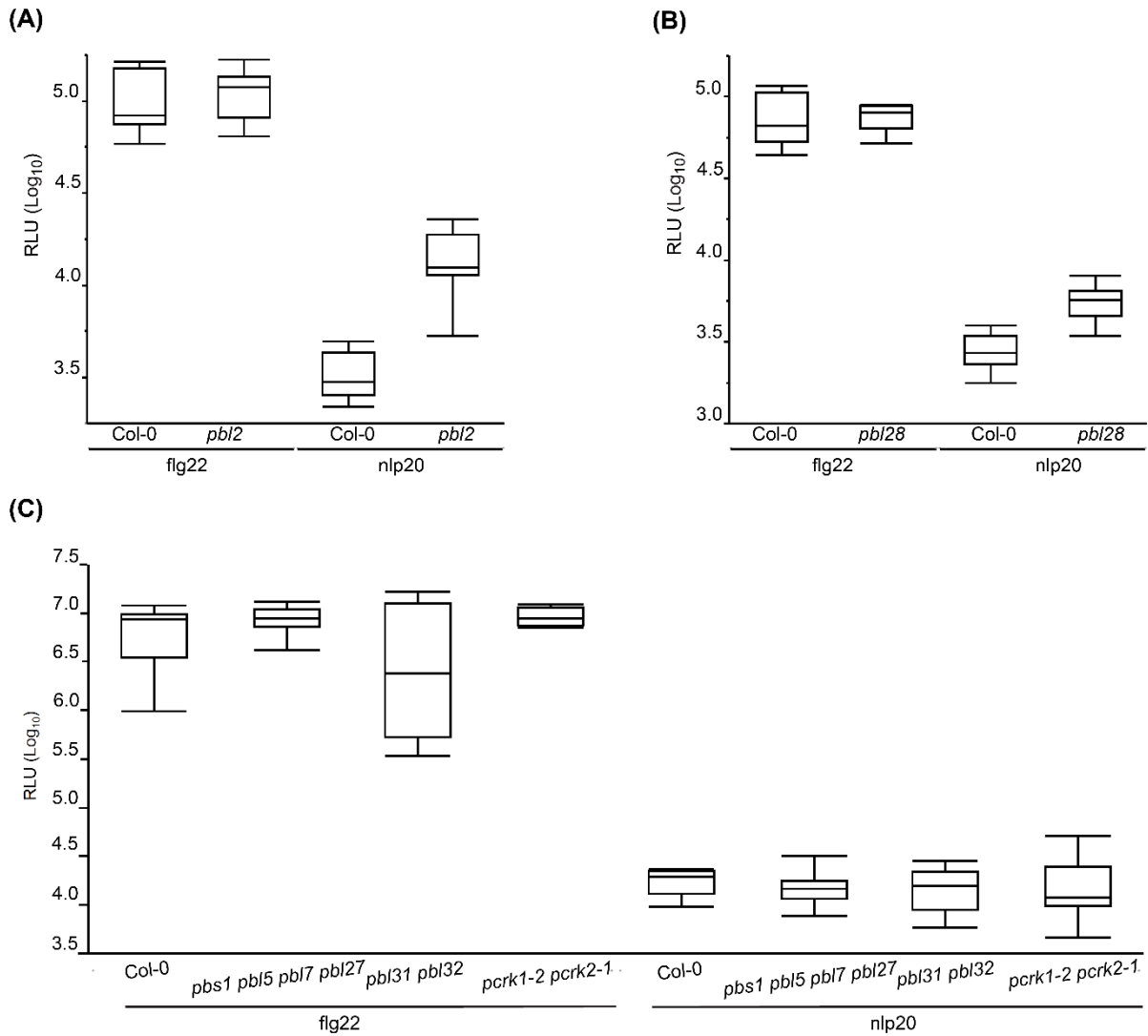
Figure 3-10. Screening of *pbl* mutants by ROS burst assay. Leaf discs of Col-0 and *pbl* mutants were treated with 0.5 µM flg22 or 0.5 µM nlp20. Results of pbl2 (A), pbl28 (B) and multi-mutant lines (C) are shown. Boxplots are shown with median and quartiles of peak value minus background value, H_2O-treated samples had no peak value, therefore they are not in the figures. Bar present means min-max range (n≥6). The experiments were performed three times with similar results.

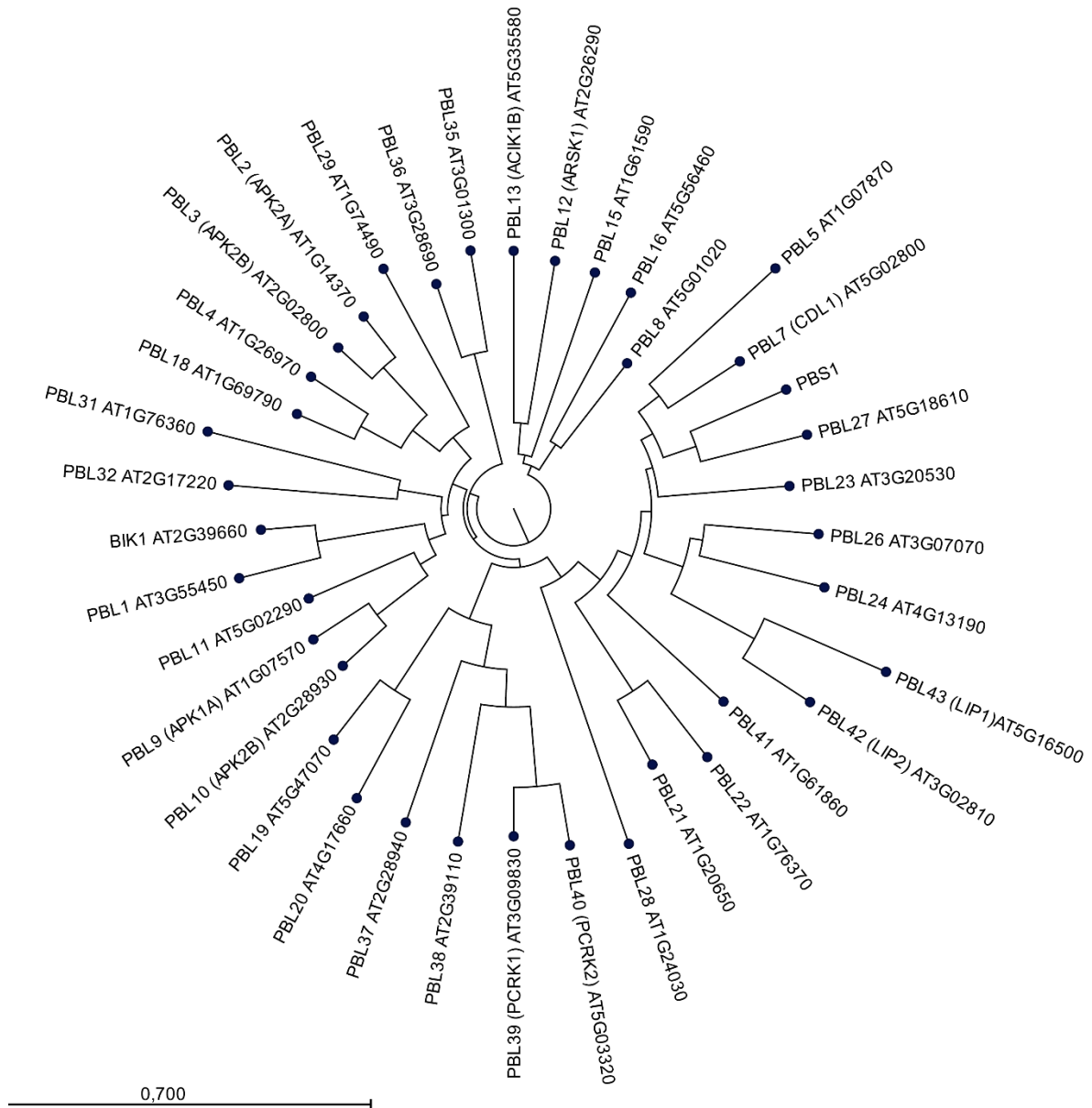# 3.3 Analyses of *bik1* mutants

From the screening results, BIK1 was identified as a key regulator that may play different roles in signaling pathways following activation of the FLS2 and the RLP23-SOBIR1 complexes. To further investigate the role of BIK1 in FL2 and RLP23 mediated signaling, we checked other immune responses in *bik1* and *bik1 pbl1*. BIK1 is required for ethylene signaling during immune activation. Conversely, ethylene perception regulates BIK1 phosphorylation in response to flg22 [213]. Ethylene was measured 6 hours after treatment of Col-0 and mutant leaves with 0.5 μM flg22 or 0.5 μM nlp20. Although *bik1* and *bik1 pbl1* showed significantly more ethylene than Col-0 after flg22 treatment, nlp20 induced more than 6-fold more ethylene in *bik1* and *bik1 pbl1* than Col-0 (Figure 3-11A). The results support the previous finding that nlp20 has higher ability to induce ethylene production. It also strengthens the hypothesis that the regulation of BIK1 and ethylene highly affect nlp20-triggered immune response.

SA was highly accumulated in *bik1* [214], and that may be the reason why *bik1* is more resistant to *Pseudomonas syringae* [49]. To better understand the relationship between BIK1 and SA, we treated *bik1* and *bik1 pbl1* leaves with water, nlp20 or flg22 for 24 hours. Our results also showed high levels of SA in *bik1* and *bik1pbl1* with mock or no treatment. With high basal level of SA, flg22 did not trigger more SA production, but nlp20 caused significantly more SA production in *bik1* and *bik1 pbl1* (Figure 3-11B).

Camalexin accumulation was the most substantial difference we observed between flg22 and nlp20 treatment in Col-0. High levels of camalexin was found in *bik1* and *bik1 pbl1* (Figure 3-11D). After 24-hours treatment, nlp20 triggered

significantly higher camalexin accumulation in these mutants than in Col-0. As with

Col-0, *bik1* and *bik1 pbl1* did not accumulate camalexin upon flg22 treatment.

Collectively, these results lead to the conclusion that BIK1 is a negative regulator

of nlp20-triggered response.
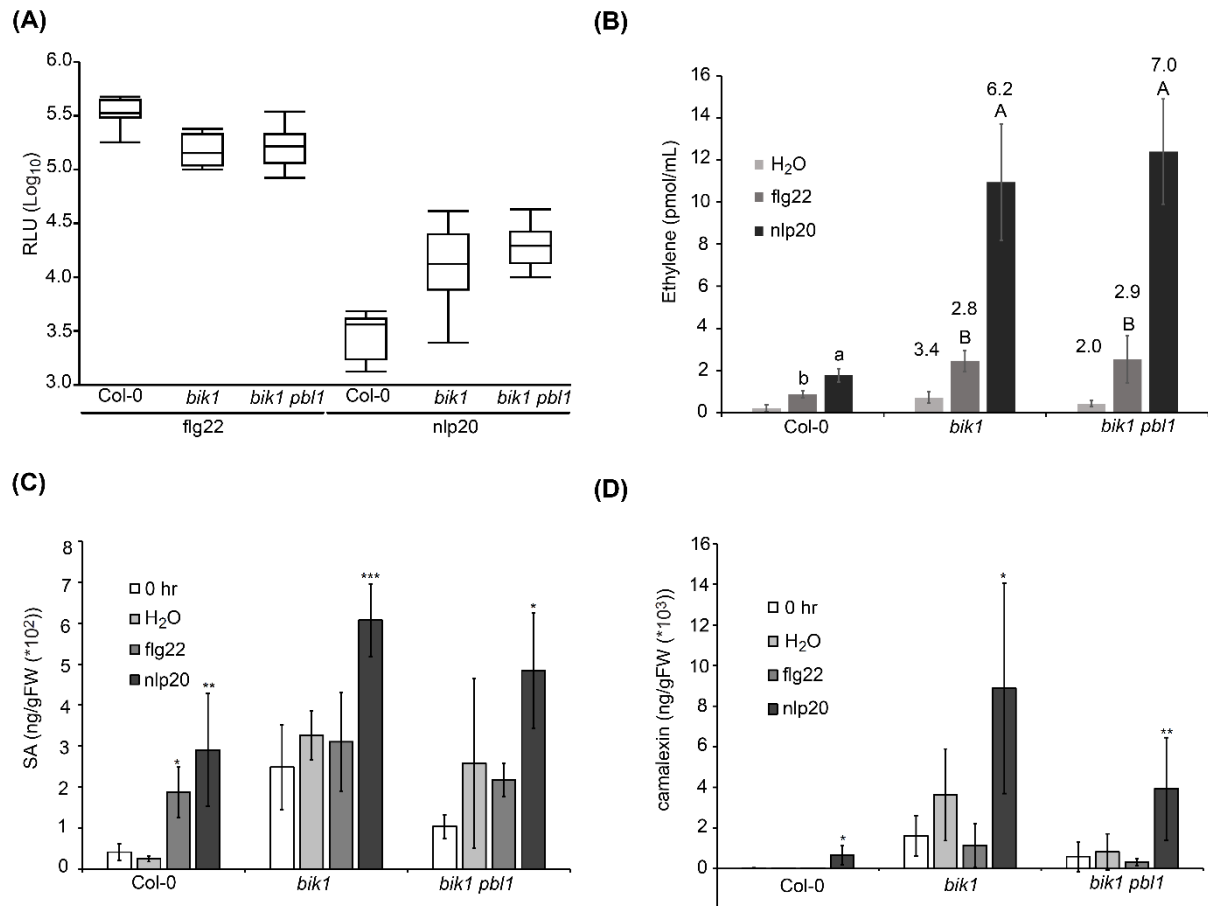
Figure 3-11. Analyses of *bik1* mutants. Leaf discs of Col-0 and *bik1* mutants were treated with 0.5 µM flg22 or 0.5 µM nlp20 for ROS assay (A) and ethylene production (B). For ROS burst assay, boxplot are shown with median and quartiles of increased value of ROS burst H_2O-treated samples had no peak value, bar present means min-max range (n≥6). For ethylene production, bars present mean ethylene production ±s.d. of 4 replicates after 6 hours of treatment; capital letter means significant difference (*P*<0.001), numbers mean fold change between mutants and Col-0 under the same treatment. The experiments were performed three times with similar results. Col-0 and *bik1* mutants were infiltrated with 0.5 µM flg22, 0.5 µM nlp20 or H_2O for SA accumulation (C) and camalexin accumulation (D). FW = Fresh weight, bars present means ±s.d. of 3 replicates. Asterisks mark significant differences to

H$_2$O control treatment as determined by Student's t test (** $P<0.01$, **$P<0.05$, *** $P<0.001$).

4. Discussion

4.1 Comparative analyses of signaling pathways following different receptor-types

SOBIR1 constitutively interacts with MAMP-perceiving RPs in the absence of ligands. A hypothesis has been proposed that LRR-RP/SOBIR1 complexes are equivalent to bi-molecular or bipartite LRR-RKs [36]. Both receptor-types require the recruitment of SERK proteins, such as BAK1, to transduce signals after MAMP perception. The subsequent responses include ROS and ethylene production, MAPK activation, and defense gene expression; these responses sometimes result in conferring immunity to pathogen infection. However, the molecular mechanisms underlying PRR complex assembly, signal transduction and response output of either immune pathway need further investigation. Inspired by the hypothesis that LRR-RP/SOBIR1 complexes are equivalent to bi-molecular or bipartite LRR-RKs, we would like to figure out to which extent signaling pathways activated through LRR-RK and LRR-RP-type PRRs differ.

Many studies have been published describing aspects of individual LRR-RK and LRR-RP-mediated signaling pathways. Although studies focusing on specific immune pathways provide clues to the differential functions of the receptors, it is difficult to compare the results of different studies directly. A collaborative study of 10 laboratories points out the difficulty of comparing results from different laboratories or in different experiments. The main reason for the observed differences was attributed to small variations in growth conditions and plant handling procedures [173]. We

conducted a comprehensive side-by-side analysis of signaling networks and immune outputs mediated through activation of LRR-RK, LRR-RP and LYM-RK.

Our work suggests substantial differences among Arabidopsis LRR-RK FLS2, LRR-RP RLP23, and LYM-RK CERK1-mediated cellular responses. Compared to nlp20, flg22 triggered fast and strong early responses, like ROS burst, MAPK activation, and Ca^{2+} burst (Brugman, unpublished data); flg22 also causes more extensive transcriptome reprogramming than nlp20. On the other hand, nlp20 triggered more prolonged ethylene and SA production than flg22. Furthermore, nlp20 triggered camalexin production which was not observed following flg22 treatment. C6 cannot trigger late defense responses. The in-depth comparative analysis of signaling networks and physiological outputs mediated through activation of different receptor-types challenge the hypothesis that LRR-RP/SOBIR1 complexes are the equivalent of a bi-molecular LRR-RK. Elucidation of the differences in these two related, but distinct signaling pathways requires further search of regulators participating in different pathways.

4.2 Genes responding differently to different MAMPs

Transcriptome reprogramming induced by pathogen infection is central for launching effective defense responses [11]. We used seedlings for our RNA-seq experiments to get an overview of transcriptome reprogramming in both leaves and roots. Our results showed that flg22 induced broad transcriptome reprogramming, which included most of the expressional changes caused by nlp20 and C6. However, there was a large group of genes that responded specifically to flg22. These genes not only related to defense response, but also to metabolism. Comparing different

microarray datasets also shows the highly similar but distinct transcriptome profiling of flg22, elf26, harpin, chitin and NPP1 [215].

A further look into the RNA-seq data provides hints of different late responses triggered by different MAMPs. In our RNA-seq data, the camalexin biosynthesis related gene *PAD3* is induced by flg22, nlp20 and C6. However, nlp20 induced much higher expression of *PAD3,* and nlp20 was the only elicitor tested which caused measurable camalexin accumulation. This result indicates that some information can be missed if we only check whether genes are regulated; we should further consider the magnitude of the transcriptional changes between different MAMP treatments.

Several genes displayed large differences in expression following MAMP treatment and may provide hints of the different responses upon different MAMP treatments. NAC domain containing protein 90 (NAC090) and ATERF019 are transcription factors [216] which are induced by flg22 after 1-hour treatment (79 and 724 fold change, respectively). ATERF019 is a member of the DREB subfamily A-5 of the ERF/AP2 transcription factor family. Previous studies found that overexpression of *ATERF019* delays flowering time and senescence, and also improves tolerance to water deprivation [217]. As transcription factors, NAC090 and ATERF019, could play a major role in flg22-mediated transcriptional reprogramming. ATERF019 is a particularly interesting candidate mediator of flg22-mediated responses because it has already been shown to regulate cell wall synthesis and metabolism [217], both of which are highly affected during pathogen invasion.

Another gene highly and specifically induced by flg22 is *BON ASSOCIATION PROTEIN 2 (BAP2)* (45 fold change after 1-hour flg22 treatment). BAP2 is a general inhibitor of programmed cell death and overexpression of BAP2 in yeast can inhibit

programmed cell death in yeast [218]. In Arabidopsis, biotic and abiotic stress can induce ROS burst; *BAP2* is up-regulated under stressful conditions, probably to inhibit ROS-induced cell death. The high expression of *BAP2* after flg22 treatment may be mediated by the high ROS burst induced by flg22. BAP1 is a homologous programmed cell death inhibitor [218]; unlike *BAP2, BAP1* is induced after all tested MAMP treatments.

NIM1-INTERACTING 1 (NIMIN1) forms a ternary complex with NONEXPRESSER OF PR GENES 1 (NPR1) and TGA factors upon SAR induction. It then binds to a positive regulatory cis-element of the PR-1 promoter, termed LS7, leading to PR-1 gene induction [219]. NIMIN1 is highly induced by flg22 after 1-hour treatment (36 fold change). TERPENE SYNTHASE 04 (TPS04), another gene highly induced by flg22 (42 fold change after 1-hour treatment, 116 fold change after 6-hour treatment), is a geranyl linalool synthase that produces a precursor to TMTT, a volatile plant defense C16-homoterpene. *TPS04* can also be induced by a fungal peptide mixture, larval infestation, and *Pseudomonas syringae* [220, 221]. Transcription of *TPS04* is blocked in JA biosynthetic and JA signaling mutants but not in SA and ET biosynthetic and/or signaling defective lines [220].

There are also late immune response genes which are specifically regulated upon flg22-treatment but not nlp20 or C6 treatment. AT5G46874, a gene up–regulated after 6-hour treatment (59 fold change), encodes a defensin-like family protein which is toxic to cells of other organisms. MYB87 (44 fold change) may function as a regulator of genes affecting cell wall organization and remodeling [222]. PEROXIDASE 52 (PRX52) is also up-regulated 6 hours after flg22 exposure (237

fold change); PRX52 involved in lignin biosynthesis and response to *Verticillium longisporum* infection [223].

There is a smaller group of genes that is specifically upregulated by nlp20, but not by flg22 or C6. In addition to *PAD3* which was discussed earlier, GDSL LIPASE 1 (GLIP1) and PLANT DEFENSIN 1.1 (PDF1.1) are also highly up-regulated (832 and 60 fold change, respectively). GLIP1 possesses antimicrobial activity which deters fungal infection, possibly by disruption of fungal cell walls [224]. In addition, GLIP1 elicits both local and systemic resistance in plants in an ET dependent manner [225]. PDF1.1 is a PR protein which renders Arabidopsis resistant to non-host *Cercospora beticola* [226].

4.3 BIK1 plays different roles in flg22-triggered and nlp20-triggered responses

We have established a negative regulatory role of the cytoplasmic protein kinases BIK1 and PBL1 in nlp20-mediated immune. This is in contrast to the positive regulatory role of these proteins in flg22 signaling [49, 50] revealing a differential role of the proteins in the respective signaling networks. BIK1 physically associates with FLS2 and BAK1 [49]; upon flg22 and elf18 perception, BIK1 interacts with and phosphorylates RbohD [227, 228]. An important question for future research is how BIK1 engenders its negative regulatory role in RP-mediated immune activation. The first step to answering this question is to determine if the inhibitory activity of BIK1 in nlp20 signaling requires BIK1 protein kinase activity. We are testing transgenic *bik1* plants expressing BIK1 kinase inactive mutant protein (mutated in the putative ATP binding site). Preliminary data shows that the BIK1 kinase inactive mutant protein

cannot complement the altered nlp20-induced ROS phenotype of *bik1*, suggesting that kinase activity is essential for the negative regulatory role of BIK1. Further studies are needed to check whether BIK1 also interacts with SOBIR1 in ligand (in)dependent fashion.

It is important to determine whether BIK1 has a different phosphorylation status after flg22 or nlp20 treatment. BIK1 is phosphorylated at multiple serine, threonine, and tyrosine sites by BAK1 upon flg22 treatment. Some of these residues are required for plant defense responses [50, 229]. BIK1 also regulates BR signaling via association with the BRI1/BAK1 complex [230]. It has been suggested that the distinct functions of BIK1 in immunity and BR signaling might be due to the differential phosphorylation of BIK1 by BAK1 and BRI1 [230]. Different role of BIK1 in MAMP triggered immunity might also be the outcome of different phosphorylation events. It has been shown that *bik1* is more susceptible to *Pst hrcC⁻* and *B. cinerea*, and BIK1^{T94A} and BIK1^{T242A} complement the resistance to *Pst hrcC⁻* but not to *B. cinerea* [213]*,* suggesting that the differential phosphorylation status of BIK1 has varied effects on immune signaling outputs.

BIK1 phosphorylated substrates (such as RbohD) are also targets of further investigation. Key questions include whether the same proteins are targeted upon nlp20 treatment, whether the phosphorylation patterns are the same, and what novel BIK1-interacting partners (substrates) are phosphorylated upon nlp20 treatment. These results might explain the differential involvement of BIK1 in flg22/FLS2 and nlp20/RLP23-mediated immune signaling.

Another approach will make use of chimeric PRRs to test whether protein kinase domains of the PRR FLS2 and RLP23/SOBIR1 heterodimers are solely

responsible for the differences in signal outputs (ROS burst, ethylene production, camalexin production) that have been observed for nlp20/RLP23/SOBIR1 and flg22/FLS2 PRR systems. In other words, would chimeric receptors in which kinase domains of FLS2 and SOBIR1 were replaced with one another result in flg22 perception with an nlp20 output response and vice versa? If so, this would suggest a strictly modular composition of these receptor-types.

4.4 PRR signaling specificity may be determined by RLCKs

In this study, we compared flg22/FLS2 and nlp20/RLP23-mediated immune signaling, however, it is still unknown whether there are differences in signaling networks and signal outputs mediated by the same receptor types. It was recently found that BIK1 has a negative regulatory role in BcPG3/RLP42 (Zhang, unpublished data) signaling similar to what is observed for nlp20/RLP23 signaling. This suggests that the phenomenon is likely RLP-specific and not a peculiar feature of RLP23 alone. Furthermore, high expression of *PAD3* and ethylene production was found as a response following RLP30 activation [112].

The large numbers of RLCKs in plants are evolutionarily related to RKs but lack a transmembrane domain [24, 212]. More and more studies suggest that RLCKs participate in immunity. PBS1 is a member of subfamily VII RLCKs, and it is monitored by the Arabidopsis NLR RESISTANCE TO PSEUDOMONAS SYRINGAE 5 (RPS5) [231]. Cleavage of Arabidopsis PBS1 by AvrPphB activates RPS5-mediated immune responses [232]. In addition to PBS1, a group of RLCKs were shown to be the substrates for the AvrPphB protease, including BIK1, PBL1, PBL2, PBL5, PBL7, PBL9, PBL11 [49, 232]. PBL27 was shown to connect CERK complex and MAPK cascade and regulate chitin-induced immunity in Arabidopsis [160].

Receptor-like Cytoplasmic Kinase 1 (PCRK1) and PCRK2 participate in plant immunity by regulating activation of SA biosynthesis [180]. It has been shown that BRASSINOSTEROID-SIGNALLING KINASE 1 (BSK1), a RLCK associated with growth signaling [233], associates with FLS2 to regulate flg22-induced immune responses, but not elf18-induced immune responses [234]. On the other hand, PBL13 has been reported to exert negative regulatory functions in both flg22 and elf18 signaling [179]. These observations raise the possibility that the large repertoire of RLCKs may contribute to the robustness and flexibility of plant immune system. These RLCKs vary in their affinity for different PRRs, which makes them possible to activate or restraint distinct branches of MTI signaling [235].

Although we expect PBLs to be involved in transmitting RLP23/SOBIR signaling, no *pbl* mutant showed strongly attenuated ROS burst in response to nlp20 treatment. This is likely due to the redundant function of PBLs. PBL28 is one of several *pbl* mutants which showed higher ROS burst specifically after nlp20 treatment but not flg22 treatment. Interestingly, it is the most non-homologous member in PBL family, indicating the possibility that it has a unique function among PBLs. The lack of a functionally redundant protein could explain why an nlp20-response phenotype can be observed in single mutant. Other *pbl28* mutant lines, complementation lines and higher-order knockout lines are needed to confirm the phenotype.

4.5 Other possible regulation

4.5.1 Apoplastic alkalinization

Unlike flg22, nlp20 fails to trigger extracellular alkalization in Arabidopsis cell suspensions [109]. Extracellular alkalization could facilitate the oxidative modification of redox-sensitive proteins. Alkalinization promotes dissociation of thiols, make them susceptible to interaction with reactive oxygen species. Research has shown pH-dependence of the reaction rates between hydrogen peroxide and free cysteine [236], glutathione [237], and thiols in proteins [238]. The observation that FLS2 activation causes alkalinization and strong ROS burst, whereas RLP23 activation produces no measureable alkalinization and only weak ROS burst suggests that these two receptors mobilize different mechanisms for pathogen control.

4.5.2 Participation of different SERKs

Genetic data indicate that BAK1/SERK3 is a major player transmitting signals from FLS2 and EFR [239]. All SERKs are capable of forming a complex with FLS2 and EFR, but SERK1 and SERK2 confer negligible functions in plant immunity [39, 240]. BAK1-LIKE1 (BKK1)/SERK4 can mediate FLS and EFR signaling, but it does so only in the absence of the preferred co-receptor BAK1. We found that *bak1-4* showed significantly decreased ROS burst than Col-0 when treated with flg22, but nlp20-induced ROS burst was not affected. RLP23 also interacts with SERK1, SERK2, BAK1 and BKK1 in a ligand-dependent manner; *bak1-5 bkk1* showed reduced ethylene production and ROS burst upon nlp20 treatment [42]. However, the roles of SERK1 and SERK2 in RLP23 signaling pathway still need to be clarified. It is likely that other SERKs compensate for the loss of BAK1 in nlp20 signaling.

Participation of different SERKs may partially account for different outputs of flg22 and nlp20.

Previous studies have shown that SERK members participate in different signaling, including BR signaling, immune signaling and cell death signaling. Single mutants of *serk1*, *bak1*, or *bkk1* have relatively weak BR responses, whereas the *serk1 bak1 bkk1* triple mutant is completely insensitive to BR treatment, suggesting a redundant role of these three SERKs in BR signaling [241]. It appears that SERK2 is not involved in BR signaling [241]. A recent report indicated that SERK5 in the Ler-0 ecotype also associates with BRI1 and has an important role in BR signaling [242].

AtPep1-triggered ROS production and ET accumulation are abolished in the *bak1 bkk1* double mutant but not in the individual single mutants, indicating BAK1 and BKK1 redundantly regulate AtPep1 signaling [39, 239, 243]. In addition to the critical roles in plant development and immunity, BAK1 and BKK1 redundantly and negatively regulate plant cell death. The *bak1-4 bkk1* double mutant is seedling lethal with spontaneous cell death and constitutive ROS production, but respective single mutants do not show the phenotype [244]. Upon pathogen infection, *bak1* mutants also exhibit spreading necrosis [245].

4.5.3 Phosphorylation sites of BAK1

The *bak1-5* mutant, which encodes a mutation in the BAK1 kinase domain, shows reduced kinase activity and largely compromised FLS2- and EFR-mediated plant immunity [51]. Intriguingly, the *bak1-5* mutant is not impaired in BRI1-mediated BR signaling and cell death control, suggesting that specific phosphorylation events contribute to specific signaling. All the BAK1 phosphorylation site mutant lines that

we tested (*bak1-4/BAK1_Y403F*, *bak1-4/BAK1_S602/3/4_AAA* and *bak1-4/BAK1_S612A*) show decreased ROS burst whether treated with flg22 or nlp20. Thus, these phosphorylation sites are important for both flg22- and nlp20-induced signaling. It is possible that other phosphorylation sites of BAK1 differentially determine signal outputs.

5. Summary

Plant cell surface receptors sense microbial pathogens by recognizing microbial structures called pathogen or microbe-associated molecular patterns (PAMPs/MAMPs). There are two major types of plant pattern recognition receptors: 1. Leucine-rich repeat receptor proteins (LRR-RP) and LRR receptor kinases (LRR-RK) and 2. Plant receptor proteins and receptor kinases carrying ectopic lysin motifs (LysM-RP and LysM-RK). Although many studies focused on the signal pathways triggered by these receptors individually, the exact overlap and the differences, respectively, between these pathways remain largely unknown.

In this study, *Arabidopsis thaliana* responses to three different MAMPs, flg22, nlp20, chitin (C6), via their corresponding receptor types, FLS2 (LRR-RK), RLP23 (LRR-RP), CERK1 (LysM-RK) were compared. Systematic analyses of various plant immune responses revealed that nlp20 triggers only slow and weak early responses such as ROS accumulation and MAPK activation. However, compared to flg22, nlp20 is capable of inducing higher levels of the phytohormones ethylene and salicylic acid. In contrast, flg22 triggers early responses (ROS, MAPKs) faster and stronger, and also causes more extensive transcriptome reprogramming. Both flg22 and nlp20 cause callose deposition, but only treatment with nlp20 results in the accumulation of the phytohormone camalexin. Additionally, the LysM-RK-ligand C6 can trigger strong early responses, but fails to induce late responses.

The two peptides nlp20 and flg22 are recognized by the LRR-RP RLP23 (together with its adaptor kinase SOBIR1) and the LRR-RK FLS2, respectively, and both receptor complexes recruit the co-receptor LRR-RLK BAK1 after ligand

perception. However, whereas BAK1 is indispensable for FLS2 function, it can be partially replaced by other BAK1 family members in RLP23-mediated nlp20 signaling. Analysis of further mutant lines indicated that the regulatory proteins BIR2, CPK28, PP2A, and G proteins impinge on both flg22- and nlp20-triggered signaling in a similar way.

Surprisingly, BIK1, which is a positive regulator in flg22-triggered signaling pathway, was shown here to negatively regulate nlp20-induced immune responses. Thus, higher levels of ROS, ethylene, SA and camalexin were measured in the *bik1* and *bik1 pbl1* mutants after nlp20 treatment than in the wild type control. However, the molecular mechanism of how BIK1 differently regulates flg22- and nlp20-triggered signaling pathways still remains to be clarified.

6. Zusammenfassung

Pflanzliche Zelloberflächenrezeptoren detektieren mikrobielle Pathogene durch Erkennen von mikrobiellen Strukturen, die auch als Pathogen- oder Mikroben-assoziierte molekulare Muster (PAMPs / MAMPs) bezeichnet werden. Es gibt zwei Haupttypen von Mustererkennungsrezeptoren: 1. Leucin-reiche Wiederholung-enthaltende Rezeptorproteine (LRR-RP) und LRR-Rezeptorkinasen (LRR-RK) und 2. Rezeptorproteine und Rezeptorkinasen, die ektopische Lysin-Motive tragen (LysM-RP und LysM-RK). Obwohl sich viele Studien mit einzelnen dieser Rezeptoren nachgeschalteten Signalwegen beschäftige haben, blieben bisher die genaue Überschneidung und die Unterschiede zwischen diesen Wegen unbekannt.

In dieser Studie wurden Signalwege in *Arabidopsis thaliana*-Pflanzen verglichen, die durch die drei verschiedenen MAMPs, flg22, nlp20, Chitin (C6), und ihre entsprechenden Rezeptortypen FLS2 (LRR-RK), RLP23 (LRR-RP), und CERK1 (LYM-RK) ausgelöst wurden. Systematische Analysen zeigten, dass nlp20 frühe Immunantworten wie ROS-Akkumulation und MAPK-Aktivierung nur recht langsam und schwach auslöst. Allerdings ist nlp20 in der Lage, im Vergleich zu flg22 größere Mengen der Phytohormone Ethylen und Salicylsäure zu induzieren. Im Gegensatz dazu löst Flg22 schnelle und starke frühe Immunantworten aus und verursacht auch eine umfangreiche Re-Programmierung des Transkriptoms. Sowohl flg22 als auch nlp20 verursachen eine Ablagerung von Callose, aber nur eine nlp20-Behandlung resultiert in einer Akkumulation des Phytoalexins Camalexin. Zusätzlich untersucht wurde der LysM-RK-Ligand C6, der zwar frühe Immunantworten stark auszulösen vermochte, nicht aber späte Immunantworten.

Die beiden Peptide nlp20 und flg22 werden vom LRR-RP RLP23 (zusammen mit seiner Adaptorkinase SOBIR1) bzw. der LRR-RK FLS2 erkannt und beide Rezeptorkomplexe rekrutieren die Co-Rezeptor LRR-RLK BAK1 nach der Ligandenwahrnehmung. Während BAK1 für die FLS2-Funktion unentbehrlich ist, kann es teilweise durch andere BAK1-Familienmitglieder in der RLP23-vermittelten nlp20-Signalisierung ersetzt werden. Die Untersuchung von weiteren Mutantenlinien zeigte, dass die regulatorischen Proteine BIR2, CPK28, PP2A und G Proteine eine ähnliche Funktion in der flg22- und nlp20-induzierten Signalweiterleitung haben.

Überraschenderweise zeigte sich BIK1, welches ein positiver Reglulator der flg22-getriggerten Signalwege ist, als ein negativer Regulator der nlp20-ausgelösten Immunantworten. Dies zeigte sich in erhöhten Mengen an ROS, Ethylen, SA und Camalexin in *bik1* und *bik1 pbl1* Mutanten nach nlp20 Behandlung im Vergleich zur Wildtyp-Kontrolle. Der molekulare Mechanismus wie BIK1 die flg22- und nlp20-ausgelösten Signalwege differentiell reguliert, muss allerdings noch geklärt werden.

7. References

1. Kemen, E. and J.D. Jones, *Obligate biotroph parasitism: can we link genomes to lifestyles?* Trends Plant Sci, 2012. **17**(8): p. 448-57.

2. Yeats, T.H. and J.K. Rose, *The formation and function of plant cuticles.* Plant Physiol, 2013. **163**(1): p. 5-20.

3. Mendgen, K., M. Hahn, and H. Deising, *Morphogenesis and mechanisms of penetration by plant pathogenic fungi.* Annu Rev Phytopathol, 1996. **34**: p. 367-86.

4. Longhi, S. and C. Cambillau, *Structure-activity of cutinase, a small lipolytic enzyme.* Biochim Biophys Acta, 1999. **1441**(2-3): p. 185-96.

5. Somerville, C., et al., *Toward a systems approach to understanding plant cell walls.* Science, 2004. **306**(5705): p. 2206-11.

6. Hamann, T., *Plant cell wall integrity maintenance as an essential component of biotic stress response mechanisms.* Front Plant Sci, 2012. **3**: p. 77.

7. Melotto, M., W. Underwood, and S.Y. He, *Role of stomata in plant innate immunity and foliar bacterial diseases.* Annu Rev Phytopathol, 2008. **46**: p. 101-22.

8. Osbourn, A.E., *Preformed Antimicrobial Compounds and Plant Defense against Fungal Attack.* Plant Cell, 1996. **8**(10): p. 1821-1831.

9. Nicaise, V., M. Roux, and C. Zipfel, *Recent Advances in PAMP-Triggered Immunity against Bacteria: Pattern Recognition Receptors Watch over and Raise the Alarm.* Plant Physiology, 2009. **150**(4): p. 1638-1647.

10. Tena, G., M. Boudsocq, and J. Sheen, *Protein kinase signaling networks in plant innate immunity.* Current Opinion in Plant Biology, 2011. **14**(5): p. 519-529.

11. Tsuda, K. and I.E. Somssich, *Transcriptional networks in plant immunity.* New Phytol, 2015. **206**(3): p. 932-47.

12. Boller, T. and G. Felix, *A Renaissance of Elicitors: Perception of Microbe-Associated Molecular Patterns and Danger Signals by Pattern-Recognition Receptors.* Annual Review of Plant Biology, 2009. **60**(1): p. 379-406.

13. Yamaguchi, Y. and A. Huffaker, *Endogenous peptide elicitors in higher plants.* Curr Opin Plant Biol, 2011. **14**(4): p. 351-7.

14. Dangl, J.L., D.M. Horvath, and B.J. Staskawicz, *Pivoting the plant immune system from dissection to deployment.* Science, 2013. **341**(6147): p. 746-51.

15. Cui, H., K. Tsuda, and J.E. Parker, *Effector-triggered immunity: from pathogen perception to robust defense.* Annu Rev Plant Biol, 2015. **66**: p. 487-511.

16. Van der Biezen, E.A. and J.D. Jones, *Plant disease-resistance proteins and the gene-for-gene concept.* Trends Biochem Sci, 1998. **23**(12): p. 454-6.

17. van der Hoorn, R.A. and S. Kamoun, *From Guard to Decoy: a new model for perception of plant pathogen effectors.* Plant Cell, 2008. **20**(8): p. 2009-17.

18. Cesari, S., et al., *A novel conserved mechanism for plant NLR protein pairs: the "integrated decoy" hypothesis.* Front Plant Sci, 2014. **5**: p. 606.

19. Wu, C.H., et al., *The "sensor domains" of plant NLR proteins: more than decoys?* Front Plant Sci, 2015. **6**: p. 134.

20. Sarris, P.F., et al., *Comparative analysis of plant immune receptor architectures uncovers host proteins likely targeted by pathogens.* BMC Biol, 2016. **14**: p. 8.

21. Kroj, T., et al., *Integration of decoy domains derived from protein targets of pathogen effectors into plant immune receptors is widespread.* New Phytol, 2016. **210**(2): p. 618-26.

22. Jones, J.D.G. and J.L. Dangl, *The plant immune system.* Nature, 2006. **444**(7117): p. 323-329.

23. Belkhadir, Y., et al., *The growth-defense pivot: crisis management in plants mediated by LRR-RK surface receptors.* Trends Biochem Sci, 2014. **39**(10): p. 447-56.

24. Shiu, S.H. and A.B. Bleecker, *Expansion of the receptor-like kinase/Pelle gene family and receptor-like proteins in Arabidopsis.* Plant Physiol, 2003. **132**(2): p. 530-43.

25. Wang, G., et al., *A genome-wide functional investigation into the roles of receptor-like proteins in Arabidopsis.* Plant Physiol, 2008. **147**(2): p. 503-17.

26. Gomez-Gomez, L. and T. Boller, *FLS2: an LRR receptor-like kinase involved in the perception of the bacterial elicitor flagellin in Arabidopsis.* Mol Cell, 2000. **5**(6): p. 1003-11.

27. Ranf, S., et al., *A lectin S-domain receptor kinase mediates lipopolysaccharide sensing in Arabidopsis thaliana.* Nat Immunol, 2015. **16**(4): p. 426-33.

28. Brutus, A., et al., *A domain swap approach reveals a role of the plant wall-associated kinase 1 (WAK1) as a receptor of oligogalacturonides.* Proc Natl Acad Sci U S A, 2010. **107**(20): p. 9452-7.

29. Zipfel, C., et al., *Perception of the bacterial PAMP EF-Tu by the receptor EFR restricts Agrobacterium-mediated transformation.* Cell, 2006. **125**(4): p. 749-60.

30. Li, J. and J. Chory, *A putative leucine-rich repeat receptor kinase involved in brassinosteroid signal transduction.* Cell, 1997. **90**(5): p. 929-38.

31. Zhu, J.Y., J. Sae-Seaw, and Z.Y. Wang, *Brassinosteroid signalling.* Development, 2013. **140**(8): p. 1615-20.

32. Belkhadir, Y. and Y. Jaillais, *The molecular circuitry of brassinosteroid signaling.* New Phytol, 2015. **206**(2): p. 522-40.

33. Wang, W., M.Y. Bai, and Z.Y. Wang, *The brassinosteroid signaling network-a paradigm of signal integration.* Curr Opin Plant Biol, 2014. **21**: p. 147-53.

34. Karlova, R., et al., *The Arabidopsis SOMATIC EMBRYOGENESIS RECEPTOR-LIKE KINASE1 protein complex includes BRASSINOSTEROID-INSENSITIVE1.* Plant Cell, 2006. **18**(3): p. 626-38.

35. Ou, Y., et al., *RGF1 INSENSITIVE 1 to 5, a group of LRR receptor-like kinases, are essential for*

the perception of root meristem growth factor 1 in Arabidopsis thaliana. Cell Res, 2016. **26**(6): p. 686-98.

36.   Gust, A.A. and G. Felix, *Receptor like proteins associate with SOBIR1-type of adaptors to form bimolecular receptor kinases.* Curr Opin Plant Biol, 2014. **21**: p. 104-11.

37.   Chinchilla, D., et al., *A flagellin-induced complex of the receptor FLS2 and BAK1 initiates plant defence.* Nature, 2007. **448**(7152): p. 497-500.

38.   Heese, A., et al., *The receptor-like kinase SERK3/BAK1 is a central regulator of innate immunity in plants.* Proc Natl Acad Sci U S A, 2007. **104**(29): p. 12217-22.

39.   Roux, M., et al., *The Arabidopsis leucine-rich repeat receptor-like kinases BAK1/SERK3 and BKK1/SERK4 are required for innate immunity to hemibiotrophic and biotrophic pathogens.* Plant Cell, 2011. **23**(6): p. 2440-55.

40.   Li, J., et al., *BAK1, an Arabidopsis LRR receptor-like protein kinase, interacts with BRI1 and modulates brassinosteroid signaling.* Cell, 2002. **110**(2): p. 213-22.

41.   Nam, K.H. and J. Li, *BRI1/BAK1, a receptor kinase pair mediating brassinosteroid signaling.* Cell, 2002. **110**(2): p. 203-12.

42.   Albert, I., et al., *An RLP23-SOBIR1-BAK1 complex mediates NLP-triggered immunity.* 2015. **1**: p. 15140.

43.   Postma, J., et al., *Avr4 promotes Cf-4 receptor-like protein association with the BAK1/SERK3 receptor-like kinase to initiate receptor endocytosis and plant immunity.* New Phytol, 2016. **210**(2): p. 627-42.

44.   Du, J., et al., *Elicitin recognition confers enhanced resistance to Phytophthora infestans in potato.* Nat Plants, 2015. **1**(4): p. 15034.

45.   Saur, I.M., et al., *NbCSPR underlies age-dependent immune responses to bacterial cold shock protein in Nicotiana benthamiana.* Proc Natl Acad Sci U S A, 2016. **113**(12): p. 3389-94.

46.   Chinchilla, D., et al., *One for all: the receptor-associated kinase BAK1.* Trends Plant Sci, 2009. **14**(10): p. 535-41.

47.   Liebrand, T.W., H.A. van den Burg, and M.H. Joosten, *Two for all: receptor-associated kinases SOBIR1 and BAK1.* Trends Plant Sci, 2014. **19**(2): p. 123-32.

48.   Li, J., *Multi-tasking of somatic embryogenesis receptor-like protein kinases.* Curr Opin Plant Biol, 2010. **13**(5): p. 509-14.

49.   Zhang, J., et al., *Receptor-like cytoplasmic kinases integrate signaling from multiple plant immune receptors and are targeted by a Pseudomonas syringae effector.* Cell Host Microbe, 2010. **7**(4): p. 290-301.

50.   Lu, D., et al., *A receptor-like cytoplasmic kinase, BIK1, associates with a flagellin receptor complex to initiate plant innate immunity.* Proc Natl Acad Sci U S A, 2010. **107**(1): p. 496-501.

51.   Liu, Z., et al., *BIK1 interacts with PEPRs to mediate ethylene-induced immunity.* Proc Natl Acad Sci U S A, 2013. **110**(15): p. 6205-10.

52. Samakovlis, C., et al., *In vitro induction of cecropin genes--an immune response in a Drosophila blood cell line.* Biochem Biophys Res Commun, 1992. **188**(3): p. 1169-75.

53. Wyant, T.L., M.K. Tanner, and M.B. Sztein, *Potent immunoregulatory effects of Salmonella typhi flagella on antigenic stimulation of human peripheral blood mononuclear cells.* Infect Immun, 1999. **67**(3): p. 1338-46.

54. Wyant, T.L., M.K. Tanner, and M.B. Sztein, *Salmonella typhi flagella are potent inducers of proinflammatory cytokine secretion by human monocytes.* Infect Immun, 1999. **67**(7): p. 3619-24.

55. Steiner, T.S., et al., *Enteroaggregative Escherichia coli expresses a novel flagellin that causes IL-8 release from intestinal epithelial cells.* J Clin Invest, 2000. **105**(12): p. 1769-77.

56. McDermott, P.F., et al., *High-affinity interaction between gram-negative flagellin and a cell surface polypeptide results in human monocyte activation.* Infect Immun, 2000. **68**(10): p. 5525-9.

57. Ciacci-Woolwine, F., P.F. McDermott, and S.B. Mizel, *Induction of cytokine synthesis by flagella from gram-negative bacteria may be dependent on the activation or differentiation state of human monocytes.* Infect Immun, 1999. **67**(10): p. 5176-85.

58. Felix, G., et al., *Plants have a sensitive perception system for the most conserved domain of bacterial flagellin.* Plant J, 1999. **18**(3): p. 265-76.

59. Gomez-Gomez, L. and T. Boller, *FLS2: An LRR Receptor-like Kinase Involved in the Perception of the Bacterial Elicitor Flagellin in Arabidopsis.* Molecular Cell, 2000. **5**(6): p. 1003-1011.

60. Gust, A.A., et al., *Bacteria-derived peptidoglycans constitute pathogen-associated molecular patterns triggering innate immunity in Arabidopsis.* Journal of Biological Chemistry, 2007. **282**(44): p. 32338-48.

61. Zipfel, C., et al., *Bacterial disease resistance in Arabidopsis through flagellin perception.* Nature, 2004. **428**(6984): p. 764-7.

62. Asai, T., et al., *MAP kinase signalling cascade in Arabidopsis innate immunity.* Nature, 2002. **415**(6875): p. 977-983.

63. Zhang, J., et al., *A Pseudomonas syringae effector inactivates MAPKs to suppress PAMP-induced immunity in plants.* Cell Host Microbe, 2007. **1**(3): p. 175-85.

64. Boutrot, F., et al., *Direct transcriptional control of the Arabidopsis immune receptor FLS2 by the ethylene-dependent transcription factors EIN3 and EIL1.* Proceedings of the National Academy of Sciences, 2010. **107**(32): p. 14502-14507.

65. Melotto, M., et al., *Plant Stomata Function in Innate Immunity against Bacterial Invasion.* Cell, 2006. **126**(5): p. 969-980.

66. Hann, D.R. and J.P. Rathjen, *Early events in the pathogenicity of Pseudomonas syringae on Nicotiana benthamiana.* The Plant Journal, 2007. **49**(4): p. 607-618.

67. Robatzek, S., et al., *Molecular identification and characterization of the tomato flagellin*

receptor LeFLS2, an orthologue of Arabidopsis FLS2 exhibiting characteristically different perception specificities. Plant Molecular Biology, 2007. **64**(5): p. 539-547.

68.   Takai, R., et al., *Analysis of Flagellin Perception Mediated by flg22 Receptor OsFLS2 in Rice.* Molecular Plant-Microbe Interactions, 2008. **21**(12): p. 1635-1642.

69.   de Torres, M., et al., *Pseudomonas syringae effector AvrPtoB suppresses basal defence in Arabidopsis.* Plant J, 2006. **47**(3): p. 368-82.

70.   Hann, D.R. and J.P. Rathjen, *Early events in the pathogenicity of Pseudomonas syringae on Nicotiana benthamiana.* Plant J, 2007. **49**(4): p. 607-18.

71.   Dunning, F.M., et al., *Identification and Mutational Analysis of Arabidopsis FLS2 Leucine-Rich Repeat Domain Residues That Contribute to Flagellin Perception.* The Plant Cell, 2007. **19**(10): p. 3297-3313.

72.   Mueller, K., et al., *Chimeric FLS2 Receptors Reveal the Basis for Differential Flagellin Perception in Arabidopsis and Tomato.* The Plant Cell, 2012. **24**(5): p. 2213-2224.

73.   Sun, Y., et al., *Structural basis for flg22-induced activation of the Arabidopsis FLS2-BAK1 immune complex.* Science, 2013. **342**(6158): p. 624-8.

74.   Schulze, B., et al., *Rapid heteromerization and phosphorylation of ligand-activated plant transmembrane receptors and their associated kinase BAK1.* Journal of Biological Chemistry, 2010.

75.   Somssich, M., et al., *Real-time dynamics of peptide ligand-dependent receptor complex formation in planta.* Sci Signal, 2015. **8**(388): p. ra76.

76.   Sun, W., et al., *Probing the Arabidopsis flagellin receptor: FLS2-FLS2 association and the contributions of specific domains to signaling function.* Plant Cell, 2012. **24**(3): p. 1096-113.

77.   Lang, T. and A. Mansell, *The negative regulation of Toll-like receptor and associated pathways.* Immunol Cell Biol, 2007. **85**(6): p. 425-434.

78.   Irani, N.G. and E. Russinova, *Receptor endocytosis and signaling in plants.* Current Opinion in Plant Biology, 2009. **12**(6): p. 653-659.

79.   Robatzek, S., D. Chinchilla, and T. Boller, *Ligand-induced endocytosis of the pattern recognition receptor FLS2 in Arabidopsis.* Genes & Development, 2006. **20**(5): p. 537-542.

80.   Lu, D., et al., *Direct Ubiquitination of Pattern Recognition Receptor FLS2 Attenuates Plant Innate Immunity.* Science, 2011. **332**(6036): p. 1439-1442.

81.   Lee, H.Y., et al., *Arabidopsis RTNLB1 and RTNLB2 Reticulon-Like Proteins Regulate Intracellular Trafficking and Activity of the FLS2 Immune Receptor.* The Plant Cell, 2011. **23**(9): p. 3374-3391.

82.   Maruta, N., et al., *Membrane-localized extra-large G proteins and Gbg of the heterotrimeric G proteins form functional complexes engaged in plant immunity in Arabidopsis.* Plant Physiol, 2015. **167**(3): p. 1004-16.

83.   Halter, T., et al., *BIR2 affects complex formation of BAK1 with ligand binding receptors in plant*

defense. Plant Signal Behav, 2014. **9**.

84. Halter, T., et al., *The leucine-rich repeat receptor kinase BIR2 is a negative regulator of BAK1 in plant immunity.* Curr Biol, 2014. **24**(2): p. 134-43.

85. Gomez-Gomez, L., Z. Bauer, and T. Boller, *Both the extracellular leucine-rich repeat domain and the kinase activity of FSL2 are required for flagellin binding and signaling in Arabidopsis.* Plant Cell, 2001. **13**(5): p. 1155-63.

86. Ding, Z., et al., *Phosphoprotein and phosphopeptide interactions with the FHA domain from Arabidopsis kinase-associated protein phosphatase.* Biochemistry, 2007. **46**(10): p. 2684-96.

87. Segonzac, C., et al., *Negative control of BAK1 by protein phosphatase 2A during plant innate immunity.* Embo j, 2014. **33**(18): p. 2069-79.

88. Kunze, G., et al., *The N terminus of bacterial elongation factor Tu elicits innate immunity in Arabidopsis plants.* The Plant Cell, 2004. **16**(12): p. 3496-507.

89. Zipfel, C., et al., *Perception of the Bacterial PAMP EF-Tu by the Receptor EFR Restricts Agrobacterium-Mediated Transformation.* Cell, 2006. **125**(4): p. 749-760.

90. Kunze, G., et al., *The N terminus of bacterial elongation factor Tu elicits innate immunity in Arabidopsis plants.* Plant Cell, 2004. **16**(12): p. 3496-507.

91. Albert, M., et al., *Arabidopsis thaliana Pattern Recognition Receptors for Bacterial Elongation Factor Tu and Flagellin Can Be Combined to Form Functional Chimeric Receptors.* Journal of Biological Chemistry, 2010. **285**(25): p. 19035-19042.

92. Albert, M. and G. Felix, *Chimeric receptors of the Arabidopsis thaliana pattern recognition receptors EFR and FLS2.* Plant Signaling & Behavior, 2010. **5**(11): p. 1430-1432.

93. Saijo, Y., et al., *Receptor quality control in the endoplasmic reticulum for plant innate immunity.* EMBO J, 2009. **28**(21): p. 3439-3449.

94. Nekrasov, V., et al., *Control of the pattern-recognition receptor EFR by an ER protein complex in plant immunity.* EMBO J, 2009. **28**(21): p. 3428-3438.

95. Ottmann, C., et al., *A common toxin fold mediates microbial attack and plant defense.* Proceedings of the National Academy of Sciences of the United States of America, 2009. **106**(25): p. 10359-10364.

96. Li, J., et al., *Specific ER quality control components required for biogenesis of the plant innate immune receptor EFR.* Proceedings of the National Academy of Sciences, 2009. **106**(37): p. 15973-15978.

97. Felix, G. and T. Boller, *Molecular sensing of bacteria in plants. The highly conserved RNA-binding motif RNP-1 of bacterial cold shock proteins is recognized as an elicitor signal in tobacco.* J Biol Chem, 2003. **278**(8): p. 6201-8.

98. Wang, L., et al., *The pattern-recognition receptor CORE of Solanaceae detects bacterial cold-shock protein.* Nat Plants, 2016. **2**: p. 16185.

99. Song, W.Y., et al., *A receptor kinase-like protein encoded by the rice disease resistance gene,*

Xa21. Science, 1995. **270**(5243): p. 1804-6.

100.   Park, C.J. and P.C. Ronald, *Cleavage and nuclear localization of the rice XA21 immune receptor.* Nat Commun, 2012. **3**: p. 920.

101.   Wei, T., et al., *Mutation of the rice XA21 predicted nuclear localization sequence does not affect resistance to Xanthomonas oryzae pv. oryzae.* PeerJ, 2016. **4**: p. e2507.

102.   Pruitt, R.N., et al., *The rice immune receptor XA21 recognizes a tyrosine-sulfated protein from a Gram-negative bacterium.* Sci Adv, 2015. **1**(6): p. e1500245.

103.   Chen, X., et al., *An XA21-associated kinase (OsSERK2) regulates immunity mediated by the XA21 and XA3 immune receptors.* Mol Plant, 2014. **7**(5): p. 874-92.

104.   Park, C.J., et al., *Rice XB15, a protein phosphatase 2C, negatively regulates cell death and XA21-mediated innate immunity.* PLoS Biol, 2008. **6**(9): p. e231.

105.   Chen, X., et al., *An ATPase promotes autophosphorylation of the pattern recognition receptor XA21 and inhibits XA21-mediated immunity.* Proc Natl Acad Sci U S A, 2010. **107**(17): p. 8029-34.

106.   Dong, S., et al., *The NLP toxin family in Phytophthora sojae includes rapidly evolving groups that lack necrosis-inducing activity.* Mol Plant Microbe Interact, 2012. **25**(7): p. 896-909.

107.   Oome, S. and G. Van den Ackerveken, *Comparative and functional analysis of the widely occurring family of Nep1-like proteins.* Mol Plant Microbe Interact, 2014. **27**(10): p. 1081-94.

108.   Qutob, D., et al., *Phytotoxicity and innate immune responses induced by Nep1-like proteins.* Plant Cell, 2006. **18**(12): p. 3721-44.

109.   Bohm, H., et al., *A conserved peptide pattern from a widespread microbial virulence factor triggers pattern-induced immunity in Arabidopsis.* PLoS Pathog, 2014. **10**(11): p. e1004491.

110.   Bi, G., et al., *Arabidopsis thaliana receptor-like protein AtRLP23 associates with the receptor-like kinase AtSOBIR1.* Plant Signal Behav, 2014. **9**(1).

111.   Zhang, L., et al., *Fungal endopolygalacturonases are recognized as microbe-associated molecular patterns by the arabidopsis receptor-like protein RESPONSIVENESS TO BOTRYTIS POLYGALACTURONASES1.* Plant Physiol, 2014. **164**(1): p. 352-64.

112.   Zhang, W., et al., *Arabidopsis receptor-like protein30 and receptor-like kinase suppressor of BIR1-1/EVERSHED mediate innate immunity to necrotrophic fungi.* Plant Cell, 2013. **25**(10): p. 4227-41.

113.   Jehle, A.K., et al., *The receptor-like protein ReMAX of Arabidopsis detects the microbe-associated molecular pattern eMax from Xanthomonas.* Plant Cell, 2013. **25**(6): p. 2330-40.

114.   Jehle, A.K., et al., *Perception of the novel MAMP eMax from different Xanthomonas species requires the Arabidopsis receptor-like protein ReMAX and the receptor kinase SOBIR.* Plant Signal Behav, 2013. **8**(12): p. e27408.

115.   Fradin, E.F. and B.P. Thomma, *Physiology and molecular aspects of Verticillium wilt diseases caused by V. dahliae and V. albo-atrum.* Mol Plant Pathol, 2006. **7**(2): p. 71-86.

116. de Jonge, R., et al., *Tomato immune receptor Ve1 recognizes effector of multiple fungal pathogens uncovered by genome and RNA sequencing.* Proc Natl Acad Sci U S A, 2012. **109**(13): p. 5110-5.

117. Fradin, E.F., et al., *Interfamily Transfer of Tomato Ve1 Mediates Verticillium Resistance in Arabidopsis.* Plant Physiology, 2011. **156**(4): p. 2255-2265.

118. Fradin, E.F., et al., *Genetic Dissection of Verticillium Wilt Resistance Mediated by Tomato Ve1.* Plant Physiology, 2009. **150**(1): p. 320-332.

119. de Jonge, R., et al., *Tomato immune receptor Ve1 recognizes effector of multiple fungal pathogens uncovered by genome and RNA sequencing.* Proceedings of the National Academy of Sciences, 2012. **109**(13): p. 5110-5115.

120. Fuchs, Y., et al., *Ethylene Biosynthesis-Inducing Protein from Cellulysin Is an Endoxylanase.* Plant Physiology, 1989. **89**(1): p. 138-143.

121. Hanania, U. and A. Avni, *High-affinity binding site for ethylene-inducing xylanase elicitor on Nicotiana tabacum membranes.* The Plant Journal, 1997. **12**(1): p. 113-120.

122. Bar, M., et al., *BAK1 is required for the attenuation of ethylene-inducing xylanase (Eix)-induced defense responses by the decoy receptor LeEix1.* Plant J, 2010. **63**(5): p. 791-800.

123. Rotblat, B., et al., *Identification of an essential component of the elicitation active site of the EIX protein elicitor.* The Plant Journal, 2002. **32**(6): p. 1049-1055.

124. Thomma, B.P., T. Nurnberger, and M.H. Joosten, *Of PAMPs and effectors: the blurred PTI-ETI dichotomy.* Plant Cell, 2011. **23**(1): p. 4-15.

125. Jones, D.A., et al., *Isolation of the tomato Cf-9 gene for resistance to Cladosporium fulvum by transposon tagging.* Science, 1994. **266**(5186): p. 789-93.

126. Rivas, S., et al., *CITRX thioredoxin interacts with the tomato Cf-9 resistance protein and negatively regulates defence.* Embo j, 2004. **23**(10): p. 2156-65.

127. Laurent, F., G. Labesse, and P. de Wit, *Molecular cloning and partial characterization of a plant VAP33 homologue with a major sperm protein domain.* Biochem Biophys Res Commun, 2000. **270**(1): p. 286-92.

128. Nekrasov, V., A.A. Ludwig, and J.D. Jones, *CITRX thioredoxin is a putative adaptor protein connecting Cf-9 and the ACIK1 protein kinase during the Cf-9/Avr9- induced defence response.* FEBS Lett, 2006. **580**(17): p. 4236-41.

129. Liebrand, T.W., et al., *Endoplasmic reticulum-quality control chaperones facilitate the biogenesis of Cf receptor-like proteins involved in pathogen resistance of tomato.* Plant Physiol, 2012. **159**(4): p. 1819-33.

130. Leslie, M.E., et al., *The EVERSHED receptor-like kinase modulates floral organ shedding in Arabidopsis.* Development, 2010. **137**(3): p. 467-76.

131. Gao, M., et al., *Regulation of cell death and innate immunity by two receptor-like kinases in Arabidopsis.* Cell Host Microbe, 2009. **6**(1): p. 34-44.

132. Meroueh, S.O., et al., *Three-dimensional structure of the bacterial cell wall peptidoglycan.* Proceedings of the National Academy of Sciences of the United States of America, 2006. **103**(12): p. 4404-4409.

133. Schleifer, K.H. and O. Kandler, *Peptidoglycan types of bacterial cell walls and their taxonomic implications.* Bacteriological Reviews, 1972. **36**(4): p. 407-477.

134. Gust, A.A., et al., *Bacteria-derived peptidoglycans constitute pathogen-associated molecular patterns triggering innate immunity in Arabidopsis.* J Biol Chem, 2007. **282**(44): p. 32338-48.

135. Ao, Y., et al., *OsCERK1 and OsRLCK176 play important roles in peptidoglycan and chitin signaling in rice innate immunity.* Plant J, 2014. **80**(6): p. 1072-84.

136. Willmann, R., et al., *Arabidopsis lysin-motif proteins LYM1 LYM3 CERK1 mediate bacterial peptidoglycan sensing and immunity to bacterial infection.* Proceedings of the National Academy of Sciences of the United States of America, 2011. **108**(49): p. 19824-9.

137. Gimenez-Ibanez, S., et al., *AvrPtoB Targets the LysM Receptor Kinase CERK1 to Promote Bacterial Virulence on Plants.* Current biology, 2009. **19**(5): p. 423-429.

138. Willmann, R., et al., *Arabidopsis lysin-motif proteins LYM1 LYM3 CERK1 mediate bacterial peptidoglycan sensing and immunity to bacterial infection.* Proc Natl Acad Sci U S A, 2011. **108**(49): p. 19824-9.

139. Faulkner, C., et al., *LYM2-dependent chitin perception limits molecular flux via plasmodesmata.* Proc Natl Acad Sci U S A, 2013. **110**(22): p. 9166-70.

140. Cao, Y., Y. Liang, and K. Tanaka, *The kinase LYK5 is a major chitin receptor in Arabidopsis and forms a chitin-induced complex with related kinase CERK1.* 2014. **3**.

141. Kouzai, Y., et al., *Targeted Gene Disruption of OsCERK1 Reveals Its Indispensable Role in Chitin Perception and Involvement in the Peptidoglycan Response and Immunity in Rice.* Mol Plant Microbe Interact, 2014. **27**(9): p. 975-82.

142. Liu, B., et al., *Lysin motif-containing proteins LYP4 and LYP6 play dual roles in peptidoglycan and chitin perception in rice innate immunity.* Plant Cell, 2012. **24**(8): p. 3406-19.

143. Miya, A., et al., *CERK1, a LysM receptor kinase, is essential for chitin elicitor signaling in Arabidopsis.* Proceedings of the National Academy of Sciences, 2007. **104**(49): p. 19613-19618.

144. Kaku, H., et al., *Plant cells recognize chitin fragments for defense signaling through a plasma membrane receptor.* Proceedings of the National Academy of Sciences, 2006. **103**(29): p. 11086-11091.

145. Okada, M., et al., *High-Affinity Binding Proteins for N-Acetylchitooligosaccharide Elicitor in the Plasma Membranes from Wheat, Barley and Carrot Cells: Conserved Presence and Correlation with the Responsiveness to the Elicitor.* Plant and Cell Physiology, 2002. **43**(5): p. 505-512.

146. Felix, G., M. Regenass, and T. Boller, *Specific perception of subnanomolar concentrations of chitin fragments by tomato cells: induction of extracellular alkalinization, changes in protein*

phosphorylation, and establishment of a refractory state. The Plant Journal, 1993. **4**(2): p. 307-316.

147. Wan, J., et al., *A LysM Receptor-Like Kinase Plays a Critical Role in Chitin Signaling and Fungal Resistance in Arabidopsis.* The Plant Cell, 2008. **20**(2): p. 471-481.

148. Shibuya, N. and E. Minami, *Oligosaccharide signalling for defence responses in plant.* Physiological and Molecular Plant Pathology, 2001. **59**(5): p. 223-233.

149. Kaku, H., et al., *Plant cells recognize chitin fragments for defense signaling through a plasma membrane receptor.* Proceedings of the National Academy of Sciences of the United States of America, 2006. **103**(29): p. 11086-11091.

150. Shimizu, T., et al., *Two LysM receptor molecules, CEBiP and OsCERK1, cooperatively regulate chitin elicitor signaling in rice.* The Plant Journal, 2010. **64**(2): p. 204-214.

151. Wan, J., et al., *A LysM Receptor-Like Kinase Plays a Critical Role in Chitin Signaling and Fungal Resistance in Arabidopsis.* Plant Cell, 2008. **20**(2): p. 471-481.

152. Liu, T., et al., *Chitin-Induced Dimerization Activates a Plant Immune Receptor.* Science, 2012. **336**(6085): p. 1160-1164.

153. Willmann, R. and T. Nurnberger, *How Plant Lysin Motif Receptors Get Activated: Lessons Learned from Structural Biology.* Sci. Signal., 2012. **5**(230): p. pe28-.

154. Liu, T., et al., *Chitin-induced dimerization activates a plant immune receptor.* Science, 2012. **336**(6085): p. 1160-4.

155. Petutschnig, E.K., et al., *The lysin motif receptor-like kinase (LysM-RLK) CERK1 is a major chitin-binding protein in Arabidopsis thaliana and subject to chitin-induced phosphorylation.* J Biol Chem, 2010. **285**(37): p. 28902-11.

156. Miya, A., et al., *CERK1, a LysM receptor kinase, is essential for chitin elicitor signaling in Arabidopsis.* Proc Natl Acad Sci U S A, 2007. **104**(49): p. 19613-8.

157. Wan, J., et al., *LYK4, a lysin motif receptor-like kinase, is important for chitin signaling and plant innate immunity in Arabidopsis.* Plant Physiol, 2012. **160**(1): p. 396-406.

158. Shinya, T., et al., *Functional characterization of CEBiP and CERK1 homologs in Arabidopsis and rice reveals the presence of different chitin receptor systems in plants.* Plant and Cell Physiology, 2012.

159. Le, M.H., et al., *LIK1, a CERK1-interacting kinase, regulates plant immune responses in Arabidopsis.* PLoS One, 2014. **9**(7): p. e102245.

160. Shinya, T., et al., *Selective regulation of the chitin-induced defense response by the Arabidopsis receptor-like cytoplasmic kinase PBL27.* Plant J, 2014. **79**(1): p. 56-66.

161. Huffaker, A., G. Pearce, and C.A. Ryan, *An endogenous peptide signal in Arabidopsis activates components of the innate immune response.* Proc Natl Acad Sci U S A, 2006. **103**(26): p. 10098-103.

162. Yamaguchi, Y., G. Pearce, and C.A. Ryan, *The cell surface leucine-rich repeat receptor for*

AtPep1, an endogenous peptide elicitor in Arabidopsis, is functional in transgenic tobacco cells. Proc Natl Acad Sci U S A, 2006. **103**(26): p. 10104-9.

163. Yamaguchi, Y., et al., *PEPR2 is a second receptor for the Pep1 and Pep2 peptides and contributes to defense responses in Arabidopsis.* Plant Cell, 2010. **22**(2): p. 508-22.

164. Krol, E., et al., *Perception of the Arabidopsis danger signal peptide 1 involves the pattern recognition receptor AtPEPR1 and its close homologue AtPEPR2.* J Biol Chem, 2010. **285**(18): p. 13471-9.

165. Ryan, C.A., A. Huffaker, and Y. Yamaguchi, *New insights into innate immunity in Arabidopsis.* Cell Microbiol, 2007. **9**(8): p. 1902-8.

166. Tintor, N., et al., *Layered pattern receptor signaling via ethylene and endogenous elicitor peptides during Arabidopsis immunity to bacterial infection.* Proc Natl Acad Sci U S A, 2013. **110**(15): p. 6211-6.

167. Ross, A., et al., *The Arabidopsis PEPR pathway couples local and systemic plant immunity.* Embo j, 2014. **33**(1): p. 62-75.

168. Ma, Y., et al., *Linking ligand perception by PEPR pattern recognition receptors to cytosolic Ca2+ elevation and downstream immune signaling in plants.* Proc Natl Acad Sci U S A, 2012. **109**(48): p. 19852-7.

169. Zipfel, C., *Combined roles of ethylene and endogenous peptides in regulating plant immunity and growth.* Proc Natl Acad Sci U S A, 2013. **110**(15): p. 5748-9.

170. Yamada, K., et al., *Danger peptide receptor signaling in plants ensures basal immunity upon pathogen-induced depletion of BAK1.* Embo j, 2016. **35**(1): p. 46-61.

171. Hou, S., et al., *The secreted peptide PIP1 amplifies immunity through receptor-like kinase 7.* PLoS Pathog, 2014. **10**(9): p. e1004331.

172. Choi, J., et al., *Identification of a plant receptor for extracellular ATP.* Science, 2014. **343**(6168): p. 290-4.

173. Massonnet, C., et al., *Probing the reproducibility of leaf growth and molecular phenotypes: a comparison of three Arabidopsis accessions cultivated in ten laboratories.* Plant Physiol, 2010. **152**(4): p. 2142-57.

174. Nakagawa, T., et al., *Development of series of gateway binary vectors, pGWBs, for realizing efficient construction of fusion genes for plant transformation.* J Biosci Bioeng, 2007. **104**(1): p. 34-41.

175. Gimenez-Ibanez, S., et al., *AvrPtoB targets the LysM receptor kinase CERK1 to promote bacterial virulence on plants.* Curr Biol, 2009. **19**(5): p. 423-9.

176. Nekrasov, V., et al., *Control of the pattern-recognition receptor EFR by an ER protein complex in plant immunity.* Embo j, 2009. **28**(21): p. 3428-38.

177. Albrecht, C., et al., *Arabidopsis SOMATIC EMBRYOGENESIS RECEPTOR KINASE proteins serve brassinosteroid-dependent and -independent signaling pathways.* Plant Physiol, 2008. **148**(1):

p. 611-9.

178. Monaghan, J., et al., *The calcium-dependent protein kinase CPK28 buffers plant immunity and regulates BIK1 turnover.* Cell Host Microbe, 2014. **16**(5): p. 605-15.

179. Lin, Z.J., et al., *PBL13 Is a Serine/Threonine Protein Kinase That Negatively Regulates Arabidopsis Immune Responses.* Plant Physiol, 2015. **169**(4): p. 2950-62.

180. Kong, Q., et al., *Two Redundant Receptor-Like Cytoplasmic Kinases Function Downstream of Pattern Recognition Receptors to Regulate Activation of SA Biosynthesis.* Plant Physiol, 2016. **171**(2): p. 1344-54.

181. Liu, J., et al., *Membrane-bound RLCKs LIP1 and LIP2 are essential male factors controlling male-female attraction in Arabidopsis.* Curr Biol, 2013. **23**(11): p. 993-8.

182. Ding, L., S. Pandey, and S.M. Assmann, *Arabidopsis extra-large G proteins (XLGs) regulate root morphogenesis.* Plant J, 2008. **53**(2): p. 248-63.

183. Liang, X. and P. Ding, *Arabidopsis heterotrimeric G proteins regulate immunity by directly coupling to the FLS2 receptor.* 2016. **5**: p. e13568.

184. Ullah, H., et al., *The beta-subunit of the Arabidopsis G protein negatively regulates auxin-induced cell division and affects multiple developmental processes.* Plant Cell, 2003. **15**(2): p. 393-409.

185. Trusov, Y., et al., *Heterotrimeric G protein gamma subunits provide functional selectivity in Gbetagamma dimer signaling in Arabidopsis.* Plant Cell, 2007. **19**(4): p. 1235-50.

186. Ashby, A.M., et al., *Ti plasmid-specified chemotaxis of Agrobacterium tumefaciens C58C1 toward vir-inducing phenolic compounds and soluble factors from monocotyledonous and dicotyledonous plants.* J Bacteriol, 1988. **170**(9): p. 4181-7.

187. Green, M.R. and J. Sambrook, *Molecular Cloning: A Laboratory Manual (Fourth Edition).* 2012: Cold Spring Harbor Labotory Press.

188. Speth, C. and S. Laubinger, *Rapid and parallel quantification of small and large RNA species.* Methods Mol Biol, 2014. **1158**: p. 93-106.

189. Livak, K.J. and T.D. Schmittgen, *Analysis of relative gene expression data using real-time quantitative PCR and the 2(-Delta Delta C(T)) Method.* Methods, 2001. **25**(4): p. 402-8.

190. Bradford, M.M., *A rapid and sensitive method for the quantitation of microgram quantities of protein utilizing the principle of protein-dye binding.* Anal Biochem, 1976. **72**: p. 248-54.

191. Laemmli, U.K., *Cleavage of structural proteins during the assembly of the head of bacteriophage T4.* Nature, 1970. **227**(5259): p. 680-5.

192. Langmead, B., et al., *Ultrafast and memory-efficient alignment of short DNA sequences to the human genome.* Genome Biol, 2009. **10**(3): p. R25.

193. Li, H. and R. Durbin, *Fast and accurate long-read alignment with Burrows-Wheeler transform.* Bioinformatics, 2010. **26**(5): p. 589-95.

194. Robinson, M.D., D.J. McCarthy, and G.K. Smyth, *edgeR: a Bioconductor package for*

differential expression analysis of digital gene expression data. Bioinformatics, 2010. **26**(1): p. 139-40.

195.   McCarthy, D.J., Y. Chen, and G.K. Smyth, *Differential expression analysis of multifactor RNA-Seq experiments with respect to biological variation.* Nucleic Acids Res, 2012. **40**(10): p. 4288-97.

196.   Iizasa, E., M. Mitsutomi, and Y. Nagano, *Direct binding of a plant LysM receptor-like kinase, LysM RLK1/CERK1, to chitin in vitro.* J Biol Chem, 2010. **285**(5): p. 2996-3004.

197.   Wojtaszek, P., *Oxidative burst: an early plant response to pathogen infection.* Biochem J, 1997. **322 (Pt 3)**: p. 681-92.

198.   Willmann, R. and T. Nurnberger, *How plant lysin motif receptors get activated: lessons learned from structural biology.* Sci Signal, 2012. **5**(230): p. pe28.

199.   Rasmussen, M.W., et al., *MAP Kinase Cascades in Arabidopsis Innate Immunity.* Front Plant Sci, 2012. **3**: p. 169.

200.   Bari, R. and J.D. Jones, *Role of plant hormones in plant defence responses.* Plant Mol Biol, 2009. **69**(4): p. 473-88.

201.   Grant, M. and C. Lamb, *Systemic immunity.* Curr Opin Plant Biol, 2006. **9**(4): p. 414-20.

202.   Mishina, T.E. and J. Zeier, *Pathogen-associated molecular pattern recognition rather than development of tissue necrosis contributes to bacterial induction of systemic acquired resistance in Arabidopsis.* Plant J, 2007. **50**(3): p. 500-13.

203.   Du, Z., et al., *agriGO: a GO analysis toolkit for the agricultural community.* Nucleic Acids Res, 2010. **38**(Web Server issue): p. W64-70.

204.   Ellinger, D. and C.A. Voigt, *Callose biosynthesis in Arabidopsis with a focus on pathogen response: what we have learned within the last decade.* Ann Bot, 2014. **114**(6): p. 1349-58.

205.   Glawischnig, E., *Camalexin.* Phytochemistry, 2007. **68**(4): p. 401-6.

206.   Nishimura, M.T., et al., *Loss of a callose synthase results in salicylic acid-dependent disease resistance.* Science, 2003. **301**(5635): p. 969-72.

207.   Zhou, N., T.L. Tootle, and J. Glazebrook, *Arabidopsis PAD3, a gene required for camalexin biosynthesis, encodes a putative cytochrome P450 monooxygenase.* Plant Cell, 1999. **11**(12): p. 2419-28.

208.   Ma, X., et al., *SERKing Coreceptors for Receptors.* Trends Plant Sci, 2016. **21**(12): p. 1017-1033.

209.   Trujillo, M., et al., *Negative regulation of PAMP-triggered immunity by an E3 ubiquitin ligase triplet in Arabidopsis.* Curr Biol, 2008. **18**(18): p. 1396-401.

210.   Kondo, T., T. Kawai, and S. Akira, *Dissecting negative regulation of Toll-like receptor signaling.* Trends Immunol, 2012. **33**(9): p. 449-58.

211.   Lehti-Shiu, M.D., et al., *Evolutionary history and stress regulation of plant receptor-like kinase/pelle genes.* Plant Physiol, 2009. **150**(1): p. 12-26.

212.   Lin, W., et al., *Big roles of small kinases: the complex functions of receptor-like cytoplasmic*

kinases in plant immunity and development. J Integr Plant Biol, 2013. **55**(12): p. 1188-97.

213. Laluk, K., et al., *Biochemical and genetic requirements for function of the immune response regulator BOTRYTIS-INDUCED KINASE1 in plant growth, ethylene signaling, and PAMP-triggered immunity in Arabidopsis.* Plant Cell, 2011. **23**(8): p. 2831-49.

214. Veronese, P., et al., *The membrane-anchored BOTRYTIS-INDUCED KINASE1 plays distinct roles in Arabidopsis resistance to necrotrophic and biotrophic pathogens.* Plant Cell, 2006. **18**(1): p. 257-73.

215. Boudsocq, M., et al., *Differential innate immune signalling via Ca(2+) sensor protein kinases.* Nature, 2010. **464**(7287): p. 418-22.

216. Riechmann, J.L., et al., *Arabidopsis transcription factors: genome-wide comparative analysis among eukaryotes.* Science, 2000. **290**(5499): p. 2105-10.

217. Scarpeci, T.E., et al., *Overexpression of AtERF019 delays plant growth and senescence and improves drought tolerance in Arabidopsis.* J Exp Bot, 2016.

218. Yang, H., et al., *The Arabidopsis BAP1 and BAP2 genes are general inhibitors of programmed cell death.* Plant Physiol, 2007. **145**(1): p. 135-46.

219. Weigel, R.R., et al., *NIMIN-1, NIMIN-2 and NIMIN-3, members of a novel family of proteins from Arabidopsis that interact with NPR1/NIM1, a key regulator of systemic acquired resistance in plants.* Plant Mol Biol, 2001. **46**(2): p. 143-60.

220. Attaran, E., M. Rostas, and J. Zeier, *Pseudomonas syringae elicits emission of the terpenoid (E,E)-4,8,12-trimethyl-1,3,7,11-tridecatetraene in Arabidopsis leaves via jasmonate signaling and expression of the terpene synthase TPS4.* Mol Plant Microbe Interact, 2008. **21**(11): p. 1482-97.

221. Herde, M., et al., *Identification and regulation of TPS04/GES, an Arabidopsis geranyllinalool synthase catalyzing the first step in the formation of the insect-induced volatile C16-homoterpene TMTT.* Plant Cell, 2008. **20**(4): p. 1152-68.

222. Fujiwara, S., et al., *Chimeric repressor analysis identifies MYB87 as a possible regulator of morphogenesis via cell wall organization and remodeling in Arabidopsis.* Biotechnol Lett, 2014. **36**(5): p. 1049-57.

223. Fernandez-Perez, F., et al., *The suppression of AtPrx52 affects fibers but not xylem lignification in Arabidopsis by altering the proportion of syringyl units.* Physiol Plant, 2015. **154**(3): p. 395-406.

224. Oh, I.S., et al., *Secretome analysis reveals an Arabidopsis lipase involved in defense against Alternaria brassicicola.* Plant Cell, 2005. **17**(10): p. 2832-47.

225. Kwon, S.J., et al., *GDSL lipase-like 1 regulates systemic resistance associated with ethylene signaling in Arabidopsis.* Plant J, 2009. **58**(2): p. 235-45.

226. De Coninck, B.M., et al., *Arabidopsis thaliana plant defensin AtPDF1.1 is involved in the plant response to biotic stress.* New Phytol, 2010. **187**(4): p. 1075-88.

227. Kadota, Y., et al., *Direct regulation of the NADPH oxidase RBOHD by the PRR-associated kinase BIK1 during plant immunity.* Mol Cell, 2014. **54**(1): p. 43-55.

228. Li, L., et al., *The FLS2-associated kinase BIK1 directly phosphorylates the NADPH oxidase RbohD to control plant immunity.* Cell Host Microbe, 2014. **15**(3): p. 329-38.

229. Lin, W., et al., *Tyrosine phosphorylation of protein kinase complex BAK1/BIK1 mediates Arabidopsis innate immunity.* Proc Natl Acad Sci U S A, 2014. **111**(9): p. 3632-7.

230. Lin, W., et al., *Inverse modulation of plant immune and brassinosteroid signaling pathways by the receptor-like cytoplasmic kinase BIK1.* Proc Natl Acad Sci U S A, 2013. **110**(29): p. 12114-9.

231. Ade, J., et al., *Indirect activation of a plant nucleotide binding site-leucine-rich repeat protein by a bacterial protease.* Proc Natl Acad Sci U S A, 2007. **104**(7): p. 2531-6.

232. Shao, F., et al., *Cleavage of Arabidopsis PBS1 by a bacterial type III effector.* Science, 2003. **301**(5637): p. 1230-3.

233. Tang, W., et al., *BSKs mediate signal transduction from the receptor kinase BRI1 in Arabidopsis.* Science, 2008. **321**(5888): p. 557-60.

234. Shi, H., et al., *BR-SIGNALING KINASE1 physically associates with FLAGELLIN SENSING2 and regulates plant innate immunity in Arabidopsis.* Plant Cell, 2013. **25**(3): p. 1143-57.

235. Couto, D. and C. Zipfel, *Regulation of pattern recognition receptor signalling in plants.* Nat Rev Immunol, 2016. **16**(9): p. 537-52.

236. Luo, D., S.W. Smith, and B.D. Anderson, *Kinetics and mechanism of the reaction of cysteine and hydrogen peroxide in aqueous solution.* J Pharm Sci, 2005. **94**(2): p. 304-16.

237. Finley, J.W., E.L. Wheeler, and S.C. Witt, *Oxidation of glutathione by hydrogen peroxide and other oxidizing agents.* J Agric Food Chem, 1981. **29**(2): p. 404-7.

238. Griffiths, S.W., J. King, and C.L. Cooney, *The reactivity and oxidation pathway of cysteine 232 in recombinant human alpha 1-antitrypsin.* J Biol Chem, 2002. **277**(28): p. 25486-92.

239. Schulze, B., et al., *Rapid heteromerization and phosphorylation of ligand-activated plant transmembrane receptors and their associated kinase BAK1.* J Biol Chem, 2010. **285**(13): p. 9444-51.

240. Schwessinger, B., et al., *Phosphorylation-dependent differential regulation of plant growth, cell death, and innate immunity by the regulatory receptor-like kinase BAK1.* PLoS Genet, 2011. **7**(4): p. e1002046.

241. Gou, X., et al., *Genetic evidence for an indispensable role of somatic embryogenesis receptor kinases in brassinosteroid signaling.* PLoS Genet, 2012. **8**(1): p. e1002452.

242. Wu, W., et al., *Somatic embryogenesis receptor-like kinase 5 in the ecotype Landsberg erecta of Arabidopsis is a functional RD LRR-RLK in regulating brassinosteroid signaling and cell death control.* Front Plant Sci, 2015. **6**: p. 852.

243. Postel, S., et al., *The multifunctional leucine-rich repeat receptor kinase BAK1 is implicated in Arabidopsis development and immunity.* Eur J Cell Biol, 2010. **89**(2-3): p. 169-74.

244. He, K., et al., *BAK1 and BKK1 regulate brassinosteroid-dependent growth and brassinosteroid-independent cell-death pathways.* Curr Biol, 2007. **17**(13): p. 1109-15.

245. Kemmerling, B., et al., *The BRI1-associated kinase 1, BAK1, has a brassinolide-independent role in plant cell-death control.* Curr Biol, 2007. **17**(13): p. 1116-22.

8. Appendix

Abbreviations

amiRNA   artificial microRNA

At   *Arabidopsis thaliana*

Avr   avirulence

BAK1   BRI1-ASSOCIATED RECEPTOR KINASE 1

BAP2   BON ASSOCIATION PROTEIN 2

BIK1   BOTRYTIS-INDUCED KINASE 1

BIR2   BAK1-interacting RLK 2

BR   brassinosteroid

BRI1   BRASSINOSTEROID INSENSITIVE 1

BSK1   BRASSINOSTEROID-SIGNALLING KINASE 1

C6   chitinhexamer

C7   chitinheptamer

C8   chitinoctamer

CDPK   calcium-dependent protein kinase

CEBiP   CHITIN ELICITOR-BINDING PROTEIN

Cf   *Cladisporium fulvum*

CLV2   CLAVATA 2

CORE   Cold shock protein receptor

CPK28   CALCIUM-DEPENDENT PROTEIN KINASE 28

CSP   COLD SHOCK PROTEIN

CSPR   CSP RECEPTOR

DAMP   damage-associated molecular patterns

DORN1   Does not Respond to Nucleotides 1

eATP   extracellular ATP

EFR   ELONGATION FACTOR-TU RECEPTOR

EF-Tu   ELONGATION FACTOR-TU

EGF   epidermal growth factor

EIX   ETHYLENE-INDUCING XYLANASE

ELR   ELICITIN RESPONSE

eMax   enigmatic MAMP of *Xanthomonas*

ER   Endoplasmic Reticulum

ET   ethylene

ETI   effector-triggered immunity

FLS2   FLAGELLIN-SENSING 2

GLIP1   GDSL LIPASE 1

GO   Gene Ontology

HR   hypersensitive response

JA   jasmonic acid

KAPP   KINASE-ASSOCIATED PROTEIN PHOSPHATASE

Le   *Lycopersicon esculentum*

LecRK-I.9   lectin receptor kinase-I.9

LORE   LIPOOLIGOSACCHARIDE-SPECIFIC REDUCED ELICITATION

LPS   lipopolysaccharides

LRR   leucine-rich repeat

LYK5   LysM-CONTAINING RECEPTOR-LIKE KINASE 5

LYM1   LysM DOMAIN CONTAINING GPI-ANCHORED PROTEIN 1

LysM   lysine motifs

MAMP   microbe-associated molecular patterns

MAPK   mitogen-associated protein kinase

MTI   MAMP-triggered immunity

NAC090   NAC domain containing protein 90

Nb   *Nicotiana benthamina*

NBS-LRR   nucleotide-binding site leucine-rich repeat

NEP1   NECROSIS- AND ETHYLENE-INDUCING PEPTIDE 1

NIMIN1   NIM1-INTERACTING 1

NLP   NEP1-LIKE PROTEIN

NLR   nucleotide-binding domain leucine-rich repeat-containing receptor

NPR1   NONEXPRESSER OF PR GENES 1

OG   oligogalacturonide

Os   *Oryza sativa*

PAD3   PHYTOALEXIN DEFICIENT 3

PAMP   pathogen-associated molecular pattern

PBL   PBS1‑LIKE KINASE

PBS1   AVRPPHB SUSCEPTIBLE 1

PDF1.1   PLANTDEFENSIN 1.1

PEPR1   PEP RECEPTOR 1

PGN   Peptidoglycan

Pi   *Phytophthora infestans*

PP2A   PROTEIN PHOSPHATASE 2A

PP2C   PROTEIN PHOSPHATASE 2C

Pp   *Phytopthora parasitica*

Pph　　　　　*P. syringae* pv. *Phaseolicola*

PROPEPs　　　PRECURSOR OF PEPTIDEs

Pta　　　　　*P. syringae* pv. *Tabaci*

Pto DC3000　　*Pseudomonas syringae* pv. tomato DC3000

PUB12　　　　PLANT U-BOX 12

RLCK　　　　　RECEPTOR-LIKE CYTOPLASMIC KINASE

ReMAX　　　　RECEPTOR OF eMax

RPS5　　　　　RESISTANCE TO PSEUDOMONAS SYRINGAE 5

PIP1　　　　　PAMP-induced peptide 1

PG　　　　　　endopolygalacturonase

PRR　　　　　pattern recognition receptor

PRX52　　　　PEROXIDASE 52

PTI　　　　　　PAMP-triggered immunity

RbohD　　　　NADPH/respiratory burst oxidase D

RBPG1　　　　RESPONSIVENESS TO BOTRYTIS POLYGALACTURONASES 1

RK　　　　　　receptor kinase

RLK　　　　　receptor-like kinase

RLP　　　　　receptor-like protein

RNA-Seq　　　Next-generation RNA-sequencing

ROS　　　　　reactive oxygen species

RP　　　　　　receptor protein

RTNLB1　　　Reticulon-like protein B1

SA　　　　　　salicylic acid

SAR　　　　　systemic acquired resistance

SCFE1　　　　sclerotinia culture filtrate elicitor 1

SERK3   SOMATIC EMBRYOGENESIS RECEPTOR KINASE 3

Sl   *Solanum lycopersicum*

SOBIR1   SUPPRESSOR OF BIR1‑1

TMM   TOO MANY MOUTHS

TPS04   TERPENE SYNTHASE 04

WAK1   WALL-ASSOCIATED KINASE 1

WT   wild type

XB15   XA21-BINDING PROTEIN 15

Acknowledgements

First of all, I would like to tender my sincere gratitude to Prof. Dr. Thorsten Nürnberger, who provided this fascinating project and the resource I need to complete this work. It is my honor to take his supervision and I see a world I have never imagined.

I would like to thank Dr. Andrea Gust, the second referee of my dissertation, who was so supportive that she not only gave advice on my work, but also helped me to deal with other problems I had in the lab.

I would like to thank my examiners Prof. Dr. Georg Felix, Prof. Dr. Klaus Harter and my PhD committee member Prof. Dr. Sascha Laubinger for critical discussions and constructive suggestions. Special thanks to Dr. Rory Pruitt, who helped a lot in my writing and contributed to the following work of this project.

Thanks to the Plant Cultivation team and Analytics team of the Central Facility, the genomic center of Max Planck Institute for Developmental Biology, and all the collaborative labs; this work cannot be done without their support.

I would like to thank Liane Schön for her friendly help regarding administrative issues. I am also grateful to have good colleagues and friends in the Department of Plant Biochemistry. I learned a lot from them; from work to living, from different cultures to different life experience.

Last but not least I would like to thank my parents. They support me in pursuing my dream and they are always there when I need assistance. Thanks to my friends who are not only in Tübingen, but also in Taiwan or other place in the world. They made my life plentiful.

Curriculum Vitae

Wan, Wei-Lin

Education

- Ph.D., Zentrum für Molekularbiologie der Pflanzen (ZMBP), University of Tübingen, Germany, 2017

- M.S., Institute of Plant Biology, National Taiwan University, Taiwan, 2010

- B.S., Department of Life Science, National Taiwan University, Taiwan, 2008

Experimental Experience

- Ph.D. Dissertation, 08/2013-12/2017

  Title: Comparative Analysis of Signaling Pathways Triggered by Different Pattern-recognition Receptor-types

  Supervisor: Prof. Dr. Thorsten Nürnberger, Zentrum für Molekularbiologie der Pflanzen (ZMBP), University of Tübingen, Germany

- Master thesis, 07/2008-07/2010

  Title: Functional Study of the Peptide Hormone *Ib*HypSys in Signal Transduction

  Supervisor: Prof. Dr. Shih-Tong Jeng, Institute of Plant Biology, National Taiwan University, Taiwan

- Summer Research Program at North Carolina State University, 07/01-08/07, 2009

  Title: Expression of *Populus trichocarpa* peroxidase (PO3)

- Supervisor: Prof. Dr. Vincent Chiang, Department of Forestry and Environmental Resources, North Carolina State University, U.S.A.

- National Science Council Research Plan on College Students, 07/2007-02/2008

  Title: Analyzing cis-elements of a H_2O_2-inducible promoter, *GSTF8* promoter, in Arabidopsis

  Supervisor: Prof. Dr. Shih-Tong Jeng, Institute of Plant Biology, National Taiwan University, Taiwan

Working Experience

- Research assistant in Institute of Plant and Microbial Biology, Academia Sinica, Taiwan, 01/2012-08/2012

  Supervisor: Dr. Na-Sheng Lin

- Military service: Political warfare officer in The 1st Regional Support Command 08/2010-07/2011

Awards

- Award of exhibiting an excellent poster at the annual contest of the Institute, Institute of Plant Biology, National Taiwan University, Taiwan, 2010

International Conferences and Presentations

- The 5th International Conference on Biotic Plant Interactions (ICBPI), Xiamen, China, 08/2017

Title: Differential signaling networks triggered by LRR-RK and LRR-RP-type receptors (Talk)

- International Society for Molecular Plant-Microbe Interaction (MPMI) 17th Congress, Portland, U.S.A., 07/2016

  Title: Comparative Analysis of Signaling Pathways Triggered by Different Pattern-recognition Receptor-types (Poster)

- 11th International Congress of Plant Molecular Biology (IPMB), Foz do Iguacu, Brazil, 10/2015

  Title: Comparative Analysis of Signaling Pathways Triggered by Different Pattern-recognition Receptor-types (Poster)

- International Society for Molecular Plant-Microbe Interaction (MPMI) 16th Congress, Rhodes, Greece, 07/2014

  Title: Lysin-motif-proteins Mediate Peptidoglycan-perception In *Arabidopsis Thaliana* (Poster)

- Annual Meeting of American Society of Plant Biology, Minneapolis, 08/2011

  Title: Functional Study of the Peptide Hormone *Ib*HypSys in Signal Transduction (Poster)

Publications

- Li. et.al. (2016) Signal transduction and regulation of *Ib*preproHypSys in sweet potato. *Plant Cell Environment*